

UC San Diego

UC San Diego Electronic Theses and Dissertations

Title

Development of acid-sensitive N-ethoxybenzylimidazoles for use as linkers in drug delivery systems

Permalink

<https://escholarship.org/uc/item/6th9r5v5>

Author

Luong, Alice

Publication Date

2011

Peer reviewed|Thesis/dissertation

UNIVERSITY OF CALIFORNIA, SAN DIEGO

Development of acid-sensitive *N*-ethoxybenzylimidazoles for use as linkers in drug delivery systems

A dissertation submitted in partial satisfaction of the requirements for the degree
Doctor in Philosophy

in

Chemistry

by

Alice Luong

Committee in charge:

Professor Jerry Yang, Chair
Professor Thomas Hermann
Professor Stephen Howell
Professor Elizabeth Komives
Professor J. Andrew McCammon

2011

Copyright

Alice Luong, 2011

All rights reserved.

This Dissertation of Alice Luong is approved, and it is acceptable in quality and form
for publication on microfilm and electronically:

Chair

University of California, San Diego

2011

DEDICATION

This work is dedicated to my family: to my mother, a three time cancer survivor, who has fought so hard against this disease; to my father, who is always there to support my mother; and to my three sisters, who I hope will never have to fight a battle with cancer.

I also dedicate this thesis to William, who has always believed in me, and has supported me in every way through this process.

TABLE OF CONTENTS

SIGNATURE PAGE	iii
DEDICATION.....	iv
TABLE OF CONTENTS.....	v
LIST OF FIGURES	viii
LIST OF ABBREVIATIONS.....	xiv
ACKNOWLEDGEMENTS	xv
VITA	xvii
ABSTRACT OF THE DISSERTATION.....	xviii
Chapter 1 Introduction: Acid-sensitive linkers in cancer drug delivery systems (DDSs)	1
1.1 Introduction	1
1.2 Hydrazone linkers.....	4
1.3 Acetal linkers.....	7
1.4 Amidomalonate linkers	9
1.5 Cis-aconityl linkers	11
1.6 Imine linkers	14
1.7 Trityl Groups.....	15
1.7 Diaryltriazolyl linkers.....	16
1.8 Conclusions.....	18
Chapter 2 The development of <i>N</i> -ethoxybenzylimidazoles (NEBIs) as an acid- sensitive hydrolyzable group	20
2.1 Introduction	20
2.2 Kinetic analysis of the NEBI	23
2.3 Electronic effects on NEBI hydrolysis	23
2.4 NEBI stability studies.....	27
2.5 Temperature dependence of NEBI hydrolysis	28
2.6 Conclusions.....	29
2.7 Experimentals	31
Chapter 3 Hydrolysis and Cytotoxicity Studies of a doxorubicin-linked NEBI.....	40
3.1 Introduction	40

3.2	Conjugation of doxorubicin to the NEBI platform	41
3.3	Hydrolysis of a doxorubicin-linked NEBI	43
3.4	Cytotoxicity studies of 3.6 and 3.7	44
3.5	Conclusions.....	45
3.6	Experimentals	46
Chapter 4	Development of a bifunctional NEBI crosslinker for use in a model drug delivery system	53
4.1	Introduction	53
4.2	Synthesis of bifunctional crosslinkers	55
4.3	Conjugation of doxorubicin to HSA.....	57
4.4	Characterization of doxorubicin conjugates 4.7 and 4.9	60
4.5	Colocalization studies of 4.7 in cells	61
4.6	Cytotoxicity studies of 4.7	63
4.7	Cellular uptake studies of 4.7 vs 3.7	65
4.8	Metabolism of 4.7	67
4.9	Conclusions.....	69
4.10	Experimentals	70
Chapter 5	<i>Ortho-N</i> -ethoxybenzylimidazoles (<i>o</i> -NEBI): a two step hydrolysis for release of alcohol containing drugs	85
5.1	Introduction	85
5.2	<i>o</i> -NEBI-methyl ester: proof-of-concept	88
5.3	Synthesis of an <i>o</i> -NEBI-alcohol containing drug conjugate.....	91
5.4	Synthesis and characterization of an <i>o</i> -NEBI conjugated to 5-fluoro-2'-deoxyuridine.....	92
5.5	Increasing the rates of hydrolysis of <i>o</i> -NEBI	96
5.6	Synthesis and characterization of chloro- <i>o</i> -NEBI-5-FU conjugate	99
5.7	Summary of data	103
5.8	Conclusions.....	104
5.9	Experimentals	105
Chapter 6	Studies towards the release of an amine containing drug from an <i>ortho-N</i> -ethoxybenzylimidazole platform.....	116
6.1	Introduction	116

6.2	Electronic effects of substitution on the rate <i>ortho</i> -formylbenzoyl ester hydrolysis	117
6.3	The presence of a nucleophile on the rate <i>ortho</i> -formylbenzoyl ester hydrolysis	119
6.4	Hydrolysis studies of substituted <i>N</i> -(2-formylbenzoyl)doxorubicin	120
6.5	Cytotoxicity studies of substituted <i>N</i> -(2-formylbenzoyl)doxorubicin.....	121
6.6	Additional electronic effects on <i>o</i> -NEBI hydrolysis	122
6.7	Conclusions.....	123
6.8	Experimentals	124
Chapter 7	Towards the development of methods to site-specifically conjugate chemotherapeutic agents to trastuzumab via <i>o</i> -NEBI linkers	134
7.1	Introduction	134
7.2	Co-localization studies	137
7.3	Modification of trastuzumab.....	138
7.4	Verification of <i>N</i> -terminal transamination of trastuzumab	139
7.5	Cytotoxicity Studies	145
7.6	Conclusions.....	146
7.7	Experimentals	148
REFERENCES	151

LIST OF FIGURES

Figure 1.1	Tuning the rates of hydrazone hydrolysis.	5
Figure 1.2	Gemtuzumab ozogamicin, trade named Mylotarg®	6
Figure 1.3	Hydrolysis of poly(ethylene oxide) conjugated to 5-fluoro-2'-deoxyuridine at pH 5.0 and 7.4.....	8
Figure 1.4	A) An acid-labile HMPA co-polymer conjugated to a diamminocyclohexyl Pt moiety via amidomalonate linkers (AP5346). B) Hydrolysis studies of AP5346 shows increased rates of release of platinum at pH 5.4 (●) compared to pH 7.4 (■). 59, 62 The acid-sensitive amidomalonate group is circled in red.....	11
Figure 1.5	A) Conjugation of daunomycin to cis-Aconitic anhydride. B) Mechanism of amide hydrolysis from the cis-aconityl linker in acidic environments. ⁶⁸	12
Figure 1.6	Yields and half lives of model compounds in buffer at pH 5.0 and 7.4 at 37 °C	15
Figure 1.7	The IC ₅₀ of substituted trityl linked difluoronucleosides and its half-lives of hydrolysis (t _{1/2}) at pH 5.4, 6.4 and 7.4. The acid-sensitive trityl group is circled in red	16
Figure 1.8	The hydrolysis of a triazole acid-sensitive linker for proof-of-concept. Structures for drug delivery applications. The acid-sensitive diaryltriazole group is circled in red.....	17
Figure 2.1	A) Acidic hydrolysis of protected imidazoles. B) The pka of known protonated-imidazoles.	21
Figure 2.2	The proposed deprotection mechanism of N-linked imidazoles.....	22
Figure 2.3	Hydrolysis of the NEBI gives benzaldehyde, imidazole and EtOH.....	22
Figure 2.4	The dependence of the concentration of 2-[N-morpholino]ethanesulfonic acid (MES) buffer on the rates of hydrolysis of N-ethoxybenzylimidazole 2.1.....	23
Figure 2.5	General procedure for the synthesis of N-ethoxybenzylimidazoles (NEBIs) 2.1-2.8 from the corresponding benzaldehydes.....	25
Figure 2.6	Half-lives (t _{1/2}) and rate constants (k) for the hydrolysis of NEBIs in D ₂ O at pD = 5.5 and pD = 7.4. ^a 0.5M MES buffer solution ^b 0.5M HEPES buffer ^c No hydrolysis detected after > 8 weeks.	25

Figure 2.7	Linear Hammett correlation for the hydrolysis of 2.1-2.4 in 0.5 M MES buffered D ₂ O (pD = 5.5) at 37 °C, where R = n-butyl (Bu), H, Br, and NO ₂ .	26
Figure 2.8	A comparison of hydrolysis rates of 2.1, 2.9 and 2.10.	27
Figure 2.9	Hydrolysis of NEBI groups in buffered solutions containing biologically-relevant Lewis Acids or FBS. ^a [FeCl ₃] used in these experiments was 0.01 mM due to solubility limitations of FeCl ₃ in buffer.	28
Figure 2.10	A) The rate of hydrolysis for 2.1 at pH 5.5 and varying temperatures. B) The Eyring Plot used to relate temperature and rate. The slope from this graph allowed for calculation of ΔH^\ddagger , while the y-intercept may be used to calculate ΔS^\ddagger .	29
Figure 3.1	Doxorubicin	41
Figure 3.2	Synthetic scheme for para-N-ethoxybenzylimidazole-doxorubicin conjugate 3.6. Reagents: a) SOCl ₂ , ethanol; b) triethyl orthoformate, HCl, ethanol, 78% yield for two steps; c) SOCl ₂ , acetyl chloride, neat; d) NaH, imidazole, THF, 33% yield for two steps; e) NaOH, THF/H ₂ O, 90% yield; f) doxorubicin, EDC, THF, 54% yield.	42
Figure 3.3	A) The schematic for hydrolysis of 3.6. B) Hydrolysis of 3.6 at 37 °C at pH 5.5 and pH 7.4, monitored at 470 nm using HPLC methods.	44
Figure 3.4	Cytotoxicity of 3.7 tested on 2008 human ovarian carcinoma cells using the SRB Assay.	45
Figure 4.1	The structure of two bifunctional NEBI crosslinkers developed.	54
Figure 4.2	Synthetic scheme for bifunctional crosslinker para-N-ethoxybenzylimidazole-azide-carboxylic acid 4.1. Reagents: a) sodium azide, DCM and water; b) potassium carbonate, copper sulfate, in DCM, MeOH, and water 53 % yield for two steps; c) acetyl chloride, thionyl chloride; d) A, NaH, in THF, 28% yield over two steps; e) lithium hydroxide, water and THF.	56
Figure 4.3	Synthetic scheme for bifunctional crosslinker para-N-ethoxybenzylimidazole-alkyne-carboxylic acid 4.2. Reagents: a) NHS, EDC, DCM; b) 0.1 M HEPES buffer 53 % yield; c) acetyl chloride, thionyl chloride; d) B, NaH, in THF, 21% yield over two steps; e) lithium hydroxide, water and THF.	57
Figure 4.4	Conjugation of doxorubicin to HSA via a NEBI linker using click chemistry. TCEP = tris(2-carboxyethyl)phosphine, TBTA = tris(benzyltriazolylmethyl)amine	58

- Figure 4.5 A) Synthetic scheme for azido-doxorubicin 4.8. Reagents: potassium carbonate, copper sulfate, in DCM, MeOH. B) Synthetic scheme for 4.9 59
- Figure 4.6. SDS-PAGE gel characterization of compounds 4.6, 4.7, 4.9. 4.6 is in lane 2. 4.5 is in lane 4. 4.9 is in lane 5. The gel was analyzed by Coomassie Blue staining (left) and fluorescence imaging (right). The legend indicates the components used to generate the protein species in each lane of the gel. 61
- Figure 4.7 Fluorescence imaging studies for the internalization and localization of 4.7 in human ovarian carcinoma 2008 cells. A) Differential interference contrast image of a human ovarian carcinoma 2008 cell. B) Fluorescence micrograph from a z-slice through the cell showing the location of 4.7 (red) inside the cell. The subcellular distribution of 4.7 was determined by monitoring the intrinsic fluorescence of doxorubicin C) Fluorescence micrograph from the same z-slice through the cells as shown in (B), except showing only the location of the lysosomes, which were stained with Lyotracker blue. D) A merged fluorescence micrograph of (B) and (C) indicating areas of co-localization of 4.7 and the Lyotracker Blue. Scale bar = 5 μm 63
- Figure 4.8 A) Cytotoxicity study of 4.7, 4.9 and 3.7, showed that conjugate 4.7 was the most cytotoxic of all the doxorubicin containing compounds. B) Control studies showed that HSA and HSA-alkyne (4.6) did not contribute towards the cytotoxicity found in compounds 4.7 and 4.9 in A. C) Comparison of the viability of human ovarian carcinoma 2008 cells with or without exposure to a 50 μM concentration of 4-carboxybenzaldehyde..... 65
- Figure 4.9 Analysis of the uptake of 4.7 and 3.7 by human ovarian carcinoma 2008 cells. A) and B) are micrographs of representative z-slices through cells that were incubated with molecule 4.7 (A) or molecule 3.7 (B) for 3 h. Here, the intrinsic fluorescence of doxorubicin is shown in red. Scale bar = 15 μm . C) The bar graph indicates that there is approximately 5.5 times the amount of doxorubicin in the cells incubated with molecule 4.7 compared to cells incubated with molecule 3.7. Average total fluorescence per cell was determined from analysis of 10 cells in each sample image. Analysis of the data in (C) revealed a p -value of 3.2×10^{-9} 66
- Figure 4.10 LC-MS analysis of the lysate of human ovarian carcinoma 2008 cells treated with 4.7. A) The LC trace of the flow through sample. B) The LC trace of the MeOH sample. The samples were monitored at 480 nm (the absorbance of doxorubicin) to highlight possible doxorubicin metabolites. ESI-Negative ion mode was used to determine the mass of the peaks observed at 480 nm.^{109, 110} 68

Figure 5.1	A) Assisted hydrolysis of o-formylbenzoates. B) The hypothesized hydrolysis of an o-NEBI methyl ester. C) Schematic of the goal for the new o-NEBI platform	87
Figure 5.2	The synthetic scheme for o-NEBI carrying a methyl ester 5.1. Reagents: a) MeI and potassium carbonate in DMF, 88% yield b) ethylorthoformate, EtOH, and TsOH, 76% yield c) acetyl chloride, thionyl chloride d) imidazole, NaH, in THF, 28% yield over two steps	88
Figure 5.3	A) A schematic of the hydrolysis of 5.1 into 5.2 in step one, followed by the hydrolysis of 5.2 in step two to give 5.3 . B) Hydrolysis of 5.1 at pH 5.5 and 7.4 while incubated at 37 °C. C) Hydrolysis of 5.2 , step two, measured independently at pH 5.5 and 7.4 while incubated at 37 °C. D) The concentrations of 5.1 , 5.2 and 5.3 at pH 5.5 monitored over time by HPLC.	90
Figure 5.4	Compound 5.4 showed no hydrolysis at pH 5.5 and 7.4 after 6 days while incubated at 37 °C.....	91
Figure 5.5	Synthesis of an o-NEBI with a carboxylic acid, 5.5 . Reagents: LiOH in THF/water.	91
Figure 5.6	Schematic for the synthesis of 5.7 . Reagents: 2M6NBA, DMAP, TEA, Microwave, 100 °C. 7% yield.....	94
Figure 5.7	A) Schematic of 5.7 hydrolysis B) Hydrolysis of 5.7 and pH 5.5 and 7.4. C) Concentration of 5.7 and 5.6 over time as 5.7 hydrolyzes at pH 5.5.	95
Figure 5.8	Cytotoxicity of 5.6 and 5.7 on 2008 and MCF-7 cells.....	96
Figure 5.9	Schematic of the synthesis of 5.8 . Reagents: a) n-BuLi, DMF, -78 °C, 51% yield, b) EtI and sodium carbonate in DMF, 52% yield, c) ethyl orthoformate, EtOH, TsOH, 88% yield, d) thionyl chloride, reflux, neat e) imidazole, NaH in THF, 30% yield over two steps.	97
Figure 5.10	Schematic for the synthesis of 5.9 . Reagents: a) EtI and potassium carbonate in DMF, 71% yield b) ethyl orthoformate, EtOH, TsOH, 67% yield, c) thionyl chloride, reflux neat d) 2-chloro-imidazole, NaH in THF, 60% yield over two steps.....	99
Figure 5.11	Schematic of the synthesis of 5.10 . Reagents: a) LiOH in THF/water b) 5.6 , 2M6NBA, DMAP, TEA, Microwave, 100 °C. 6% yield.	100
Figure 5.12	The hydrolysis of 5.10 at A) pH 5.5 and B) pH 7.4. C) Graph of 5.10 hydrolysis.	101
Figure 5.13	Cytotoxicity of studies 5.10 compared to 5.7 and 5.6 (native 5-FU)..	102

Figure 5.14	The half-life of both steps of hydrolysis for o-NEBI derivatives 5.1, 5.8 and 5.9.	103
Figure 5.15	A comparison of hydrolysis half-lives of 5.7 and 5.10, and cytotoxicity of 5.5, 5.7, and 5.10.	103
Figure 5.7	Cytotoxicity of 2-carboxybenzaldehyde and 2-chloro-imidazole.	115
Figure 6.1	Schematic of the synthesis of 6.1 , 6.2 and 6.3 . A) Synthesis of 6.1. Reagents: a) Zn, sodium hydroxide in water at 0 °C, 96% yield b) water and concentrated HCl, NaNO ₂ , MeOH c) potassium hydroxide, MeOH 60% yield, d) MeI, sodium carbonate, DMF, e) manganese oxide, THF, 55% yield. B) Synthesis of 6.2 f) LiOH, THF, water, 98% yield, g) manganese oxide, THF, reflux 32% yield, h) EtI, potassium carbonate, DMF, 92% yield. C) Synthesis of 6.3 i) 1,3-dibromo-5,5-dimethylhydantoin, DCM, j) LiOH, THF, water, 20% over two steps, k) manganese oxide, THF, 60 °C, 45% yield, l) MeI, potassium carbonate, DMF, 75% yield.	118
Figure 6.2	Hydrolysis of substituted orthoformylbenzoyl esters. ^a 50 mM MES buffer with 30% DMSO. ^b 50 mM MES buffer, with 2.5 mM glutathione and 30% DMSO. ^c 50 mM HEPES buffer with 30% DMSO	119
Figure 6.3	Synthesis of substituted N-(2-formylbenzoyl)doxorubicin. Reagents: EDC and DMAP.	120
Figure 6.4	Cytotoxicity of doxorubicin and its derivatives.	122
Figure 6.5	Synthetic scheme for 6.10. Reagents: a) ethylorthoformate, EtOH, and TsOH, 33% yield b) thionyl chloride c) imidazole, NaH, in THF, 64% yield over two steps.	123
Figure 7.1	Cytotoxicity of trastuzumab on BT-474, SK-BR-3 and MCF-7 cells. ..	136
Figure 7.2	Proposed schematic for conjugation of 5-fluoro-2-deoxyuridine to trastuzumab.	137
Figure 7.3	BT474 cells incubated with 7.2 and LysoTracker Blue. A) Fluorescence of 7.2. B) Fluorescence of LysoTracker Blue C) Colocalized image of A) and B) where there if fluorecence found from both channels. The correlation between fluorescein and lyotracker blue was found to be 0.6560 for this cell line.	138
Figure 7.4	SK-BR-3 cells incubated with 7.2 and LysoTracker Blue. A) Fluorescence of 7.2. B) Fluorescence of LysoTracker Blue C) Colocalized image of A) and B) where there if fluorecence found from both channels. The correlation between fluorescein and lyotracker blue was found to be 0.2599 for this cell line.	138

Figure 7.5	Schematic for modification of N-terminal amino acids with PLP, and formation of an oxime.	139
Figure 7.6	a) Schematic of labeling of 7.3 and 7.4 with AF-488 hydroxylamine. b) SDS-Page gel Coomassie Blue analysis of labeling of 7.1, 7.3 and 7.4 with AF-488. c) Fluorescent image of SDS-PAGE gel.	140
Figure 7.7	Proposed mechanism for decarboxylation.....	141
Figure 7.8	A) Sample 7.1, unmodified trastuzumab for control purposes. B) Sample 7.3, transaminated trastuzumab, with a increase peak at 1880.9 which correlates with a the $M+H^+$ modified heavy chain. C) Sample 7.3, transaminated trastuzumab with a new peak at 1833.9 which correlates for the $M+H^+$ of the modified light chain.	144
Figure 7.9	LC-MS data comparing the intensity of mass peaks correlating to the heavy and light chain of 7.1 to 7.4. The peaks were normalized by an internal control, and the ratio provided the amount of unmodified heavy and light chain of 7.4. Assuming the lower intensity is due to conversion by PLP, we were able to calculate the percent modified by PLP.....	145
Figure 7.10	Cytotoxicity studies of 7.1, 7.3 and 7.4 on SK-BR-3 cells. Modification of trastuzumab with PLP showed no changes in cytotoxicity of trastuzumab.	146

LIST OF ABBREVIATIONS

2M6NBA – 2-methyl-6-nitrobenzoic anhydride

cat. - catalytic

DDS – drug delivery system

DMF - dimethylformamide

DMSO – dimethylsulfoxide

EDG – electron donating group

EtOAc – ethyl acetate

EtOH – ethanol

EWG – electron withdrawing group

h – hours

HEPES - (4-(2-hydroxyethyl)-1-piperazineethanesulfonic acid)

MeOH - methanol

MES - 2-(*N*-morpholino)ethanesulfonic acid

NEBI – *N*-ethoxybenzylimidazole

THF – tetrahydrofuran

TsOH – tosylic acid

ACKNOWLEDGEMENTS

I would like to acknowledge Professor Jerry Yang for all of his support in the last few years. He introduced me to the world of organic chemistry, and I will be forever grateful.

I would also like to thank current and past members of the Yang Lab for all of their support in the past few years. I would like to thank Lila Habib and Christina Capule for being my friends and supporting me through the ups and downs of work and life. I would also like to thank Xiaobei Zhao for always being insightful. Although Lynn Tross was in the lab for only a short period of time, I was lucky to learn more about organic chemistry from her. With her help, my yields improved greatly. Tawny Issarapanichkit was the best undergraduate intern anyone could ask for. She helped prepare many starting materials and purified many columns. I would also like to thank the entire lab for their feedback during group meeting presentations, and offering advice on how to improve my work.

A special thanks to the Stephen Howell lab, especially Gerald Manorek, who taught me how to perform the SRB assay, and also provided me with 2008 cells over the years.

A large portion of Chapter 2 and 3 was taken from a published manuscript, Acidic Hydrolysis of N-ethoxybenzylimidazoles (NEBIs): Potential Applications as pH-Sensitive Linkers for Drug Delivery, that appears in Bioconjugate Chemistry, 2007. Seong Deok Kong, Alice Luong, Gerald Manorek, Stephen B. Howell, and Jerry Yang. Dr. Seong Deok Kong was the primary investigator and author of this

paper. He was responsible for most of the preliminary work in chapter 2 and developed the NEBI from scratch. Using the early data that he obtained, I was able to step in and take this project to where it is today. Reproduced with permission from S. D. Kong, A. Luong, G. Manorek, S. B. Howell and J. Yang, *Bioconjugate Chemistry*, 2007, **18**, 293-296. Copyright 2011 American Chemical Society. <http://pubs.acs.org/doi/abs/10.1021/bc060224s>

A large portion of Chapter 4 was taken from a published manuscript, pH-Sensitive, *N*-ethoxybenzylimidazole (NEBI) bifunctional crosslinkers enable triggered release of therapeutics from drug delivery carriers, that appears in *Organic and Biomolecular Chemistry* 2010. Alice Luong, Tawny Issarapanichkit, Seong Deok Kong, Rina Fong and Jerry Yang, Royal Publishing Society, 2010. The dissertation author was the primary investigator and author of this paper. Figures from this publication are reproduced by permission of The Royal Society of Chemistry. <http://pubs.rsc.org/en/Content/ArticleLanding/2010/OB/c0ob00228c>

VITA

- 2005 Bachelor of Science in Biochemistry, University of California, Davis
- 2007 Master of Science in Chemistry, University of California, San Diego
- 2011 Doctor of Philosophy in Chemistry, University of California, San Diego

PUBLICATIONS

“pH-Sensitive, *N*-ethoxybenzylimidazole (NEBI) bifunctional crosslinkers enable triggered release of therapeutics from drug delivery carriers” Luong, A., Issarapanichkit T., Kong, S.D., Fong, R., Yang, J., *Org. Biomol. Chem.*, 2010, 8, 5105-5109

“Acidic Hydrolysis of *N*-ethoxybenzylimidazoles (NEBIs): Potential Applications as pH-Sensitive Linkers for Drug Delivery” Kong, S.D., Luong, A., Manorek, G., Howell, S.B., Yang, J., *Bioconjugate Chem.*, 2007, 18, 293–296.

PRESENTATIONS

“Development of Improved Drug Delivery Methods for Treatment of Cancer” Luong, A., Issarapanichkit, T., Kong, S.D., Fong, R., Yang J., Graduate Education Day, Sacramento, CA., May 12, 2010.

“pH-Sensitive, *N*-ethoxybenzylimidazole (NEBI) bifunctional crosslinkers enable triggered release of therapeutics from drug delivery carriers”, Luong, A., Issarapanichkit, T., Velez K., Yang, J., 239th ACS National Meeting, San Francisco, CA, United States, March 21-25, 2010

“*N*-ethoxybenzylimidazoles: a novel acid-sensitive linker for controlled release of therapeutics from drug delivery systems”, Luong, A., Issarapanichkit, T., Velez K., Yang, J., 31st Annual San Antonio Breast Cancer Symposium, San Antonio, Texas, December 10 - 14, 2008

“*N*-ethoxybenzylimidazoles: pH Sensitive linkers for controlled release of cancer therapeutics”, Luong, A., Kong, S.D., Manorek, G., Howell, S.B., Yang, J., 234th ACS National Meeting, Boston, MA, United States, August 19-23, 2007

PATENT

“Acid-Sensitive Linkers for Drug Delivery,” Yang, J., Kong, S.D., Luong, A., and S. Howell
U.S. Patent Pending, publication: 20110053878, 03/03/2011

ABSTRACT OF THE DISSERTATION

Development of acid-sensitive *N*-ethoxybenzylimidazoles for use as linkers in drug delivery systems

by

Alice Luong

Doctor of Philosophy in Chemistry

University of California, San Diego, 2011

Professor Jerry Yang, Chair

This thesis describes the development of acid-sensitive *N*-ethoxybenzylimidazoles (NEBIs) for use as linkers in drug delivery systems (DDSs). A common characteristic of many DDSs is the rapid internalization and intracellular localization of the DDS into the acidic endosomes and lysosomes of cells upon arrival to the targeted tissue. NEBIs, like other acid-sensitive moieties, can serve as crosslinkers for DDSs to conjugate small molecule drugs to macromolecules. While these conjugates are stable at physiological conditions, they hydrolyze in mildly acidic environments for the triggered release of small molecule drugs. Chapter 2 describes the initial studies performed to characterize the NEBI platform. We found that hydrolysis of the NEBI at pH 5.5 exhibited a > 10-fold acceleration in rate of hydrolysis compared to in solutions at normal, physiological pH. Chapter 3 describes the incorporation of an amine containing chemotherapeutic, doxorubicin, to the NEBI, and its hydrolytic properties and cytotoxicity. Chapter 4 describes the

design of an acid-sensitive bifunctional NEBI cross-linker with a carboxylic acid functionality on one side and an azide functionality on the other side. This bifunctional crosslinker was used to construct a model DDS, by conjugating the anticancer drug doxorubicin to a human serum album model carrier. This model DDS was used to evaluate the utility of a NEBI as an acid-sensitive linker by analyzing the uptake and activity of the DDS on human ovarian cancer cells. Our most difficult challenge in Chapter 4, the inability to release native drug, was addressed in Chapter 5. An *ortho*-NEBI was designed to undergo two sequential hydrolysis steps, hydrolysis of the NEBI followed by the hydrolysis of an ester, to release native alcohol containing drugs. Studies with 5-fluoro-2'-deoxyuridine (5-FU) conjugated to the *ortho*-NEBI via an ester bond found that native 5-FU was released from this *ortho*-NEBI system. The cytotoxicity of the *ortho*-NEBI-5-FU exhibited IC₅₀ values equal in the same order of magnitude of native 5-FU. Chapters 6 and 7 describe attempts in releasing amine containing drugs from the *ortho*-NEBI platform and studies towards the development of methods for site selective conjugation of a drug to a breast cancer targeting antibody, trastuzumab.

Chapter 1

Introduction: Acid-sensitive linkers in cancer drug delivery systems (DDSs)

1.1 Introduction

Drug delivery systems (DDSs) have been extensively studied with the goal of improving chemotherapeutics. Although chemotherapeutics have helped many cancer patients, the non-specific nature of these chemotherapeutics have caused considerable side effects such as anemia, appetite changes, fatigue, alopecia, memory changes, nausea, vomiting, nerve changes etc.¹ In addition, many of these chemotherapeutics are not water soluble, and require the administration of solubilizing agents that may cause additional side effects. The ultimate goal of cancer DDSs is to specifically target cancer tumors cells, while leaving healthy cells

untouched.^{2, 3} Ideally, DDSs would also deliver a higher concentration of chemotherapeutics to the target site, increase the circulation time of the chemotherapeutic by escaping the reticuloendothelial system process,⁴ eliminate the requirement of solvents by increasing the water solubility of the chemotherapeutic,⁵ and promote endocytosis and enhance tumor uptake.⁶

An example of a successful DDS is Abraxane[®], a nanoparticle formulation of paclitaxel. Paclitaxel, a mitotic inhibitor, requires a 3 hour infusion, has a maximum dose of 175 mg/m² and has a circulation half-life of 20 h. There are many side effects associated with the use of paclitaxel such as anemia, edema, nausea, and sensory neuropathy. The administration of paclitaxel without a DDS also requires the use of a solubilizing agent, Cremophor[®] EL/Ethanol, which can cause hypersensitivity reactions and peripheral neuropathy. The use of Cremophor[®] EL/Ethanol, therefore, must be accompanied by the administration of antihistamines and corticosteroids. The development of Abraxane[®] has alleviated some of these side effects associated with paclitaxel, and has eliminated the need of Cremophor[®] EL/Ethanol, while increasing the maximum dose. The advantages of Abraxane[®] include the elimination of antihistamine and corticosteroids, decreasing the infusion time to 30 minutes, increasing the maximum dose to 260 mg/m², and improving the circulation half-life to 27 h.⁷

In order to specifically target cancer cells and tumors, some DDSs exploit the use of macromolecules or nanoparticles to passively target tumors through the enhanced permeation and retention (EPR) effect, or contain targeting moieties that bind specifically to tumors. The EPR effect occurs due to the poor vasculature around tumor cells which have been shown to be “leaky.” Nanoparticles designed

to be 40-200 nm in diameter, for instance, have been found to fit through these leaky vessels and accumulate around tumors.^{6, 8-10} DDSs can also selectively target cancer cells and tumors through conjugation to tumor targeting carriers such as proteins, antibodies, peptides, aptamers, ligands, or polyunsaturated fatty acids.¹¹⁻¹⁶ These tumor targeting carriers can specifically bind to proteins or receptors that are overexpressed on cancer cells surfaces.

Tumor targeting agents also act as drug delivery carriers, or can be conjugated to drug delivery carriers. Chemotherapeutics may be absorbed,⁷ encapsulated,¹⁷⁻²¹ or covalently linked²² to drug delivery carriers. Cationic polymers or lipids such as poly-L-lysine, polyethylenimine, and chitosan can form micelles²³⁻²⁵ and may be used to encapsulate chemotherapeutics. Chemotherapeutics may also be covalently linked to carriers via a variety of cleavable linkers such as acid-sensitive linkers,²⁶ disulfides linkers,^{27, 28} enzymatically cleaved linkers,²⁹ ultrasound cleaved linkers,³⁰ and photodynamic linkers.³⁰ The combination of these components leads to a DDS that can specifically target cancer tumors and release the drug in a cancerous environment.

This thesis will focus on the development of a novel acid-sensitive linker platform for conjugation of chemotherapeutics to DDSs. While acid-sensitive linkers may also be useful in applications outside of cancer drug delivery (such as the development of vaccines,³¹ the delivery of genes,³² the development of biocides³³, and the controlled release of fragrances,³⁴ they have attributed particular attention for the potential treatment of cancer. While physiological pH is 7.4, the pH of the environment surrounding tumors is ~ 6.8 (although this number can vary from one tumor type to the next as well as from one patient to the next).³⁵⁻³⁷ DDSs targeting

tumors via the EPR effect and carrying conjugated drugs via acid-labile linkers can accumulate around the tumor and trigger the release of chemotherapeutics. In addition, there are many targeting agents that may specifically undergo endocytosis and enter mildly acidic environment of endosomes and lysosomes of cancer cells (pH = 5.5-6.0 and 4.5-5.0 respectively),^{38, 39} which can also trigger the release of drugs from a DDS comprising acid-sensitive linkers.

An ideal acid-sensitive linker in a DDS would have an increased rate of hydrolysis at pH ~5.5, but be stable at physiological conditions (pH = 7.4, 37 °C). The half-life of hydrolysis should be rather short, preferably, less than 24 hours at pH 5.5. This takes into consideration that molecules localized in the endosomes and lysosomes persist for approximately for 1-5 hours. Acid-sensitive linkers should also be able to easily conjugate drugs to carriers, have tunable rates of hydrolysis, be synthetic accessible in useful quantities, and have the ability to conjugate a variety of chemotherapeutics. This chapter will briefly review some of the advantages and disadvantages of different types of acid-labile linkers that have been reported in the literature.

1.2 Hydrazone linkers

Hydrazones have been extensively studied as acid-labile linkers for DDSs.²⁷ Many macromolecules, such as poly-glutamic acid, dextran,⁴⁰ hydroxypropylmethacrylamide (HMPA), and antibodies^{11, 41} have been conjugated to ketone containing anthracyclines such as doxorubicin and daunorubicin via hydrazone linkers. Advantages of using hydrazone linkers include the ability to tune the rates of hydrolysis from a half-life of less than one hour to 45 h at pH 5.5 (Figure

1.1).^{26, 27} The half-life of hydrolysis at pH 5.0 range from 10-20 times faster than at physiological pH of 7.4. In addition, hydrazones can be easily prepared from aldehydes or ketones and hydrazides under very mild conditions, and also in aqueous solutions.⁴²

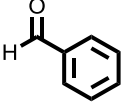
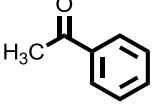
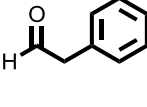
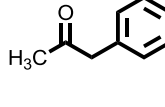
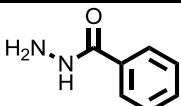
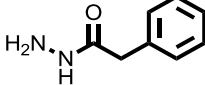
Hydrolysis half-life								
	pH 5.0	pH 7.4	pH 5.0	pH 7.4	pH 5.0	pH 7.4	pH 5.0	pH 7.4
	27h	>72h	3h	>72h	<1h	18h	<1h	15h
	45h	>72h	4.5h	59h	<2h	42h	<2h	23h

Figure 1.1 Tuning the rates of hydrazone hydrolysis.

In some studies, hydrazones have been found to be superior to other types of acid-sensitive linkers in DDSs. In 1991, Kaneko *et al.* compared the release profiles of doxorubicin conjugates that were made with hydrazones, hydrazine carboxylate, carbonic dihydrazine, semicarbazone, thiosemicarbazone and arylhydrazone. Hydrolysis and cytotoxicity studies showed that the hydrazone conjugate had the highest rate of doxorubicin release and, therefore, were the most cytotoxic when tested on Duadi cells.⁴³ In two studies, hydrazones were found to be more effective for doxorubicin release than acid-sensitive carbamates.^{44, 45} Additionally, hydrazones were found to be more effective in a DDS than an enzymatically cleavable linker.⁴⁶ Lee *et al.* also found that a dendrimer carrier conjugated to doxorubicin via a hydrazone was more effective in xenografted mice

tumors in mice when compared to commercially available Doxil, a liposomal formulation of doxorubicin.⁴⁴

Hydrazones have been the only acid-sensitive linker to achieve FDA approval in a DDS. Initial attempts of creating a DDS using a hydrazone linker in an antibody drug conjugate (ADC) with doxorubicin was not successful reportedly due to the lack of potency of doxorubicin. In addition, the half-life of hydrolysis was at pH 5.0 was 43 h, which is considered slow release rate.^{11, 41} Since these initial studies, a new ADC was developed, gemtuzumab ozogamicin (Figure 1.2, trade name Mylotarg[®]), for treatment of acute myeloid leukemia. Mylotarg[®] was the first, and so far the only FDA approved ADC using an acid-sensitive linker, which was a major milestone in the field of DDSs. This ADC consisted of a CD33 targeted antibody conjugated to calicheamicin via a hydrazone linker (2-3 drugs/antibody). Unfortunately, Mylotarg[®] failed as a drug post-FDA approval clinical trials, when there was no improvement in clinical benefit observed, and after a greater number of deaths occurred in the group of patients who received Mylotarg[®] compared with those receiving chemotherapy alone.^{11, 47} The failure of Mylotarg[®] was thought to be due to the poor specificity of the targeting moiety, the CD33 targeting antibody, and not due to the hydrazone linker.

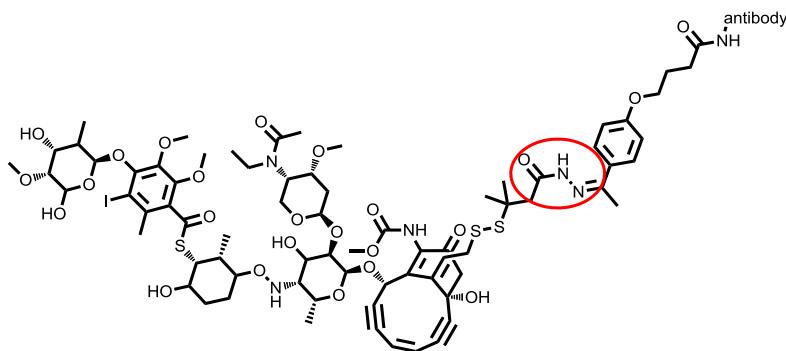


Figure 1.2 Gemtuzumab ozogamicin, trade named Mylotarg[®]

Of all the acid labile linkers available, hydrazones have received the most attention. While hydrazone linkers are limited by the requirement of the presence of a carbonyl and hydrazide functionality (both are common functionalities found in current drugs), they are still continually studied and have considerable potential in cancer DDSs due to their tunable hydrolytic properties.³

1.3 Acetal linkers

Acetals are known acid-sensitive moieties that were originally found to be useful as protecting groups for aldehydes. They can be synthesized from aldehyde and alcohols, which make them great candidates as acid-sensitive linkers for delivery of alcohol-containing drugs. The hydrolysis of acetals are specific acid-catalyzed reactions.⁴⁸ The mechanism involves a fast pre-equilibrium protonation of the acetal, followed by a unimolecular rate dependent decomposition of the protonated intermediate to an alcohol, and a resonance stabilized carbonium ion.⁴⁸ The rate of hydrolysis of simple substituted benzaldehyde acetals and their reaction kinetics are well known in the literature.⁴⁹⁻⁵¹

While acetals do have the potential to be great acid-sensitive linkers, there have not been many reports of acetals as acid-sensitive linker in DDSs.⁵² Gillies et al. made several conjugates of model drug molecules with poly(ethylene oxide), and demonstrated the potential of acetals for conjugation of primary and secondary alcohols, (as well as diols) in drug delivery. These conjugates were shown to undergo hydrolysis at a higher rate at pH 5.0 compared to 7.4 (Figure 1.3).⁵²

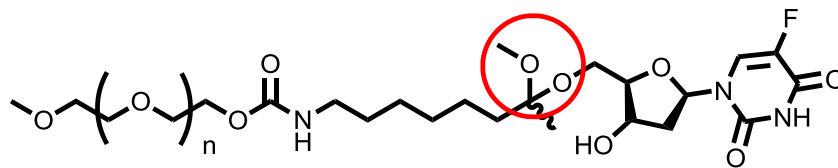
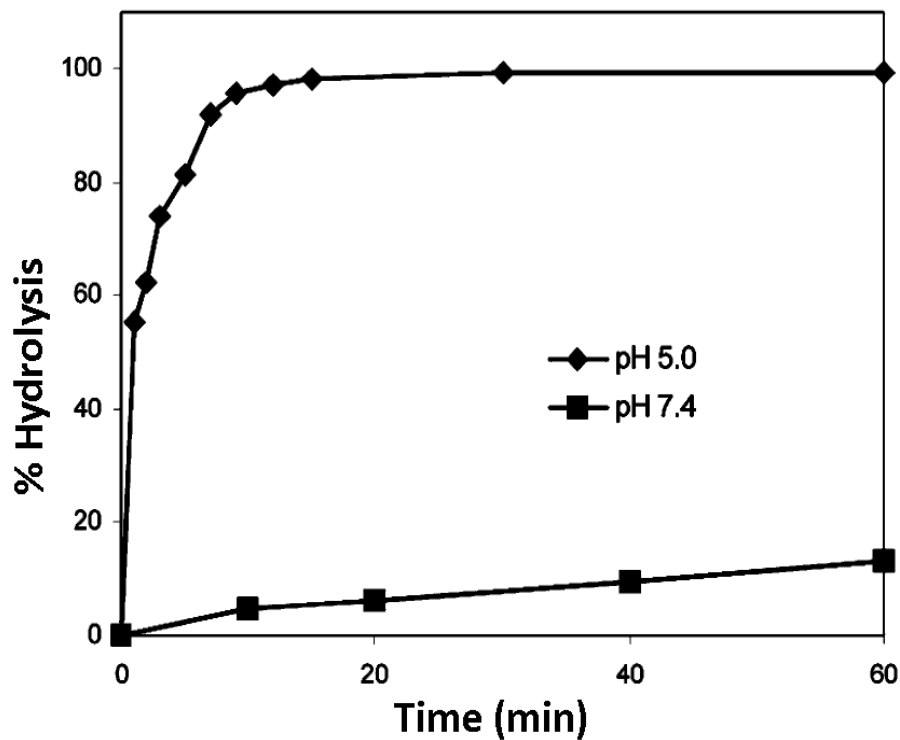


Figure 1.3 Hydrolysis of poly(ethylene oxide) conjugated to 5-fluoro-2'-deoxyuridine at pH 5.0 and 7.4.

While there have not been many studies on acetals as acid-sensitive linkers for conjugation of drugs to carriers, acetals are still prevalent in the drug delivery field. The attention has shifted to acid-sensitive polymers and materials that contain acetals for encapsulation of drugs in DDSs. Acetals for instance, have been incorporated with micelles that are stable at pH 7.4, but hydrolyze at pH 5.4 with a half-life of 6.5 h. This micelle was able to encapsulate paclitaxel and doxorubicin with a fairly high drug load (13.0 and 11.7 wt % respectively). In mildly acidic environments, the hydrolysis of the acetals causes the micelle to swell, leading to

release of drug load.⁵³ In another instance, acetals were used to render dextran polymers insoluble by masking the dextran hydroxyl groups. Using a double emulsion protocol, a model for a drug (pyrene) was encapsulated with 3.6% wt. In mildly acidic environments, the hydrolysis of the acetal moiety solubilizes the dextran, releasing the loaded drug. For proof-of-concept, fluorescein was also encapsulated by this dextran polymer. Hydrolysis studies showed a 10 h half-life at pH 5.5 and 15 day half-life at pH 7.4.^{31, 54} Polymeric hydrogel nanoparticles have also been engineered with acetals to undergo a transition from a hydrophobic material to a hydrophilic material at pH 5.0. This change in solubility causes the nanoparticles to swell to a volume 350-fold larger and release encapsulated drugs. In this instance, the nanoparticles was used to encapsulate paclitaxel and was found to have a dose dependent cytotoxic response *in vivo* against lung cancer.⁵⁵

The current literature shows a shift of acetals from acid-sensitive linkers in DDSs to using them as components in materials used for drug encapsulation. The advantages of using acetals in drug encapsulation method include the ability to load a larger variety drugs without alcohol functional groups and an increased loading capability while maintaining an easily tunable rate of hydrolysis.⁵⁴ These acetal containing polymers have great potential due to the highly tunable nature of acetal hydrolysis. These pH-responsive materials remain promising for targeted delivery of anticancer drugs.

1.4 Amidomalonate linkers

In recent years, there has been increasing interest in developing DDSs for platinum containing drugs such as cisplatin, carboplatin and oxaliplatin.⁵⁶ The first

platinum containing drug, Cisplatin, was FDA approved in 1978. These chemotherapeutic drugs induce apoptosis through the binding and crosslinking of DNA.⁵⁷ This class of platinum containing drugs is widely used for treatment of cancer, but they are limited by non specificity towards tumors, a narrow therapeutic index, and low water solubility. Attempts to improve the delivery of cisplatin through encapsulation in Stealth® liposomes advanced to phase II clinical studies. While this liposome, SPI-77, showed minimal toxicity, it also lacked a clinical response, and the clinical study was ended early.⁵⁸

Amidomalونات have been specifically developed as acid-labile linkers for delivery of platinum containing drugs through chelation, and have shown more promise than the Stealth liposomal formulations.^{59, 60} The effects of amidomalونات in platinum drug formulations has been previously reviewed.⁶¹ First attempts in delivering cisplatin type drugs used a peptide sequence carrier that was prone to cleavage by lysosomal enzymes.⁶² Continued developments have led to AP5346, a (HMPA-based) polymer derivatized with an amidomalonato chelating group (Figure 1.4). A diaminocyclohexyl-Pt moiety is chelated to the amidomalonato via an N,O linkage, and the final product contains ~ 10% Pt by weight. Figure 1.4 shows increased rates of release of platinum at pH 5.4, compared to pH 7.4.⁶³ *In vivo* studies showed that AP5346 was ~ 20 less toxic to normal tissues than oxaliplatin. AP5346 also resulted in a prolonged tumor growth delay. AP5346 has been developed into ProLindac, which has completed phase I/II clinical studies. A comprehensive review for the development of ProLindac has recently been reported.⁶²

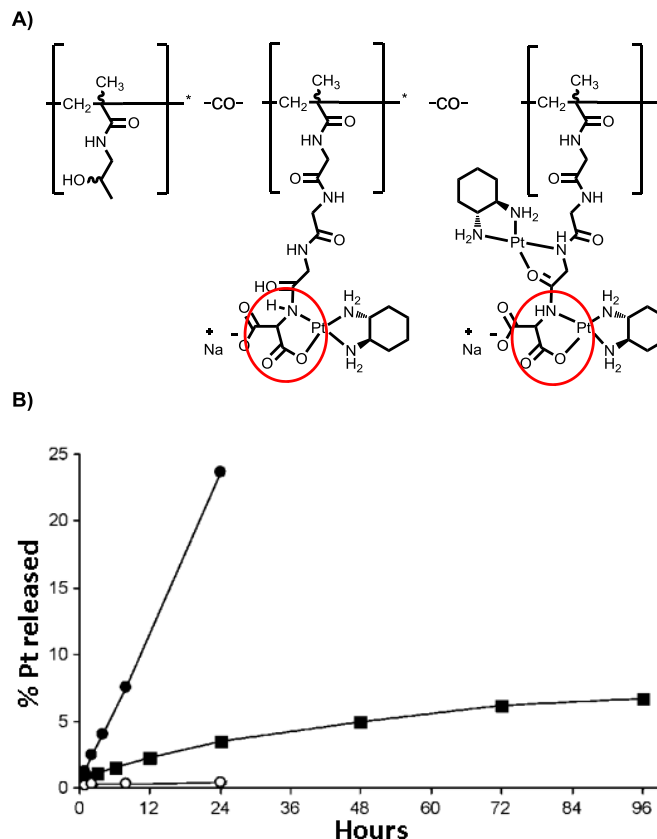


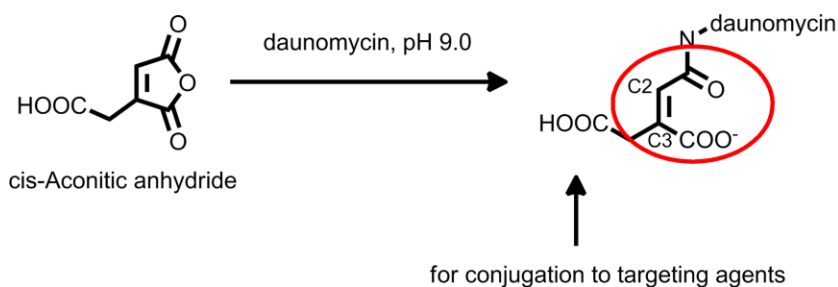
Figure 1.4 A) An acid-labile HMPA co-polymer conjugated to a diamminocyclohexyl Pt moiety via amidomalonnate linkers (AP5346). B) Hydrolysis studies of AP5346 shows increased rates of release of platinum at pH 5.4 (●) compared to pH 7.4 (■). 59, 62 The acid-sensitive amidomalonnate group is circled in red.

1.5 Cis-aconityl linkers

Cis-aconityl linkers are acid-sensitive moieties that are useful for release of amine-containing drugs such as anthracyclines. Shen and Ryser were the first to describe the synthesis of poly-D-lysine doxorubicin conjugates using a cis-aconityl spacer.⁶⁴ Since this initial report, cis-aconityl groups have been used to conjugate molecules to many macromolecules such as lectin,⁶⁵ alginate,⁶⁶ HMPA, polyvinyl alcohol, PLLA-PEG di-block copolymer etc.⁶⁷ Cis-aconityl linkers are synthesized

from cis-aconitic anhydride (Figure 1.5).⁶⁴ Reaction with an amine containing drug leads to a ring opening, which has a carboxylic functionality for conjugating to a drug delivery carrier (Figure 1.5A). In mildly acidic conditions, the amide bond undergoes an assisted hydrolysis (Figure 1.5B). Conjugates using cis-aconityl linkers with doxorubicin have been recently reviewed.²⁶

A



B

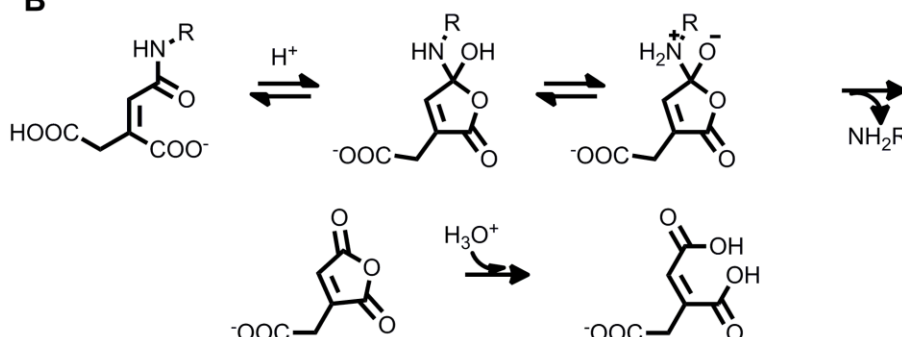


Figure 1.5 A) Conjugation of daunomycin to cis-Aconitic anhydride. B) Mechanism of amide hydrolysis from the cis-aconityl linker in acidic environments.⁶⁸

Recent studies have shown increases in drug loading in some systems using cis-aconityl linkers. Doxorubicin was conjugated to a polymer⁴⁵ and chitosan⁶⁹ in two different DDSs with relatively good drug loading (6-10%). In the case of the polymer conjugate, only about 15% of the doxorubicin was released after 96 hours at pH 5.5. In the case of the chitosan DDS, release of doxorubicin at 81 hours ranged from ~37-53% at pH 5.0. Various other studies of DDSs containing

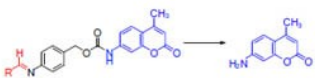
doxorubicin conjugated to a carrier via a cis-aconityl linker have shown doxorubicin release ranging from 22%-63%^{66, 70, 71} at pH 5.0 after 48 hours. These results were consistent with the hypothesis that the conjugates apparently enter the acidic compartment of cells, but due to the slow release of doxorubicin, the IC₅₀ of these conjugates, in relation to free doxorubicin, were 10-100 times less potent *in vitro*.^{66, 70, 71} While cis-aconityl linkers have been used to increase the drug loading of DDSs, they are ineffective due to their slow rate of drug release. Studies have shown that there is a correlation between the rate of drug release and potency of a DDS comprised of an acid-sensitive linker.⁴³ The low potency of DDS comprised of a cis-aconityl linker *in vitro* can be most likely attributed to the slow rates of cis-aconityl hydrolysis.

Increasing the rate of hydrolysis of cis-aconityl groups would most likely improve its potency in DDSs. Although rates of hydrolysis can be influenced by alkyl substitution at the C2 and C3 position (Figure 1.4A),⁷² there have not been many studies where there have been substitution on the C2 or C3 position to increase the rates of hydrolysis. One study showed that when R is H, Me, Et, Pr, Bt, the relative rates of hydrolysis is 1, 31.2, 32.8, 44.5, 68. Unfortunately, there are known competitive reactions such as decarboxylation, double-bond isomerization and hydrolysis reactions observed during coupling of the amine to cis-aconitic anhydride.^{73, 74} In addition, polymeric systems are known to not completely release conjugated drugs under acidic conditions due to the isomerization of the double bond leading to the trans isomer, which is incapable of intramolecular catalytic hydrolysis.⁷³ The poor capability to effectively release conjugated drugs, increase

the rate of hydrolysis from cis-aconityl linkers, and synthetic challenges may ultimately prevent the successful incorporation of cis-aconityl linkers in DDSs.

1.6 Imine linkers

Up until recently, imines were not widely employed in DDS due to their instability under physiological conditions.⁷⁵ Imines are currently gaining attention since it has been found that π - π interactions from benzyl substitution can improve the stability of imines in physiological conditions, but has relevant rates of hydrolysis in mildly acidic conditions.²³ More recently, Muller et. al. developed a more versatile method for a acid-sensitive prodrug that may be used to conjugate a large number of drugs to delivery carriers. By incorporating a self-immolative linker, drugs with nucleophilic functional groups such as OH, NH₂, or SH can be chemically bound via transiently stable carbonate, carbamate, or O,S-thiocarbonate bonds. Hydrolysis of the imine de-masks an amino group, which can trigger the release of the OH, SH, or NH₂ containing drug via a spontaneous benzyl elimination. The rates of hydrolysis for imines were tunable by adding various substituents on the benzaldehyde component. At pH 5.0, these imines have half-lives that ranged from 14 to over 120 times lower than at pH 7.4 (Figure 1.6). Although more work must be done to show if imines would be useful as acid-sensitive linkers *in vitro* and *in vivo*, an imine platform for drug delivery has potential due to the tunability of the rates of hydrolysis, synthetic accessibility, and the variety of drugs that can be conjugated to drug carriers.⁷⁶



R =	$t_{1/2}$ pH 5.0 ^a (h)	$t_{1/2}$ pH 7.4 ^b (h)
	0.28	26
	0.33	13
	0.57	8
	0.45	14
	0.62	36
	0.47	9
	1.02	36
	1.35	65
	0.83	50
	0.55	39
	0.57	89
	2.88	365

^a Acetate buffer, 20 mM.
^b Phosphate buffer, 20 mM.

Figure 1.6 Yields and half lives of model compounds in buffer at pH 5.0 and 7.4 at 37 °C

1.7 Trityl Groups

Trityl groups were first explored by Leznoff and Frechet in the 1970s for multistep synthesis on solid phase.⁷⁷ Trityl groups more recently were explored for use as linkers in drug delivery. On acidic treatment, trityl esters give trityl cations, which are stabilized by three aromatic rings. Substituents introduced on these aromatic rings can alter the rate of hydrolysis.^{26, 77} Patel et al. showed hydrolysis half-life ranged from 2.35 hours to over 33 days at pH 5.4 (Figure 1.7). At pH 7.4, the half-life of hydrolysis starts at 133.3 hours to over 33 days. Rates of release at pH 5.4 range from 39 to more than 55 times faster than pH 7.4. Trityl groups have not garnered much attention since trityl linked difluoronucleoside immunoconjugates, which showed good *in vitro* cytotoxicity correlating with the rates of drug release, exhibited disappointing results *in vivo*.⁷⁸

derivative	R	R'	$t_{1/2}$ (h) pH 5.4	$t_{1/2}$ (h) pH 6.4	$t_{1/2}$ (h) pH 7.4	IC ₅₀ μg/mL
1 (meta)	OMe	OMe	2.35	23.3	133	0.352
2 (para)	OMe	OMe	3.71	14.8	146	0.288
3 (para)	Me	OMe	2.40	43.0	229	2.71
4 (para)	H	OMe	16.7	243	800	0.966
5 (para)	H	Me	26.5	368	stable	6.04
6 (para)	H	H	stable	stable	stable	> 10

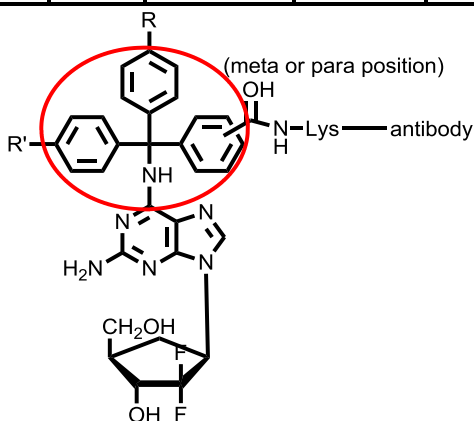


Figure 1.7 The IC₅₀ of substituted trityl linked difluoronucleosides and its half-lives of hydrolysis ($t_{1/2}$) at pH 5.4, 6.4 and 7.4. The acid-sensitive trityl group is circled in red

1.7 Diaryltriazolyl linkers

A new twist of the acid-labile trityl group has been recently reported. Since the synthesis of triazoles have been greatly improved by the concept of “click chemistry,” as shown by Sharpless and co-workers,⁷⁹ one of the aromatic rings in the trityl group was replaced with a triazole for ease of conjugation to drug delivery carriers to give diaryltriazolyl protecting groups. Cycloaddition of 1,1 disubstituted

propargyl alcohols and alkyl azides should lead to both conjugation to a DDS and the formation of acid-sensitive moiety that hydrolyzes to release an alcohol containing drug (Figure 1.8). Early investigations of diaryltriazolyl protecting groups show slow rates of hydrolysis, with a half-life of 60 h at pH 4.3, while stable at pH 7.4. Further investigations into this diaryltriazolyl platform must be completed to increase the rates of hydrolysis before it can be a viable acid-sensitive linker for DDSs. This diaryltriazolyl platform would be useful for the delivery of alcohol-containing drugs. This platform is promising due to the potential of ease of conjugation and synthetic accessibility through “click chemistry.”⁸⁰

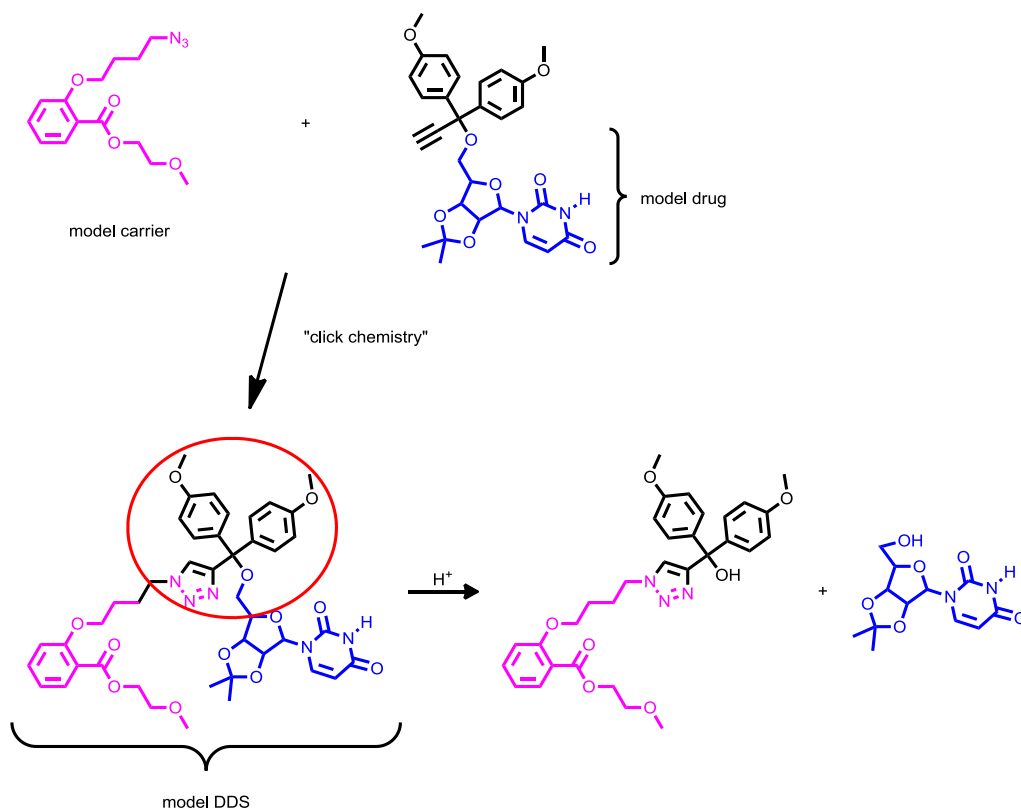


Figure 1.8 The hydrolysis of a triazole acid-sensitive linker for proof-of-concept. Structures for drug delivery applications. The acid-sensitive diaryltriazole group is circled in red.

1.8 Conclusions

Substantial research has gone into developing acid-sensitive linkers for drug delivery. Due to space constraints, some less well-explored acid-sensitive linkers were not described in detail. Some less explored acid-sensitive linkers include carbamates,^{81, 82} vinyl ether linkages⁸³ and silyl ether linkers.⁸⁴ Successful DDSs that have incorporated acid-sensitive linkers are usually those that possess rapid rates of hydrolysis in mildly acidic solutions, release drugs in a timely manner, are synthetically accessible, and have the ability to conjugate a variety of chemotherapeutics. In addition, researchers have also found that DDSs with a higher drug loading are more effective. This is one area where acid-sensitive linkers have been lacking. While drug loading has improved in the past decade, it is still a major challenge to covalently conjugate many drugs to a DDS. There has been more interest in increasing the payload of DDSs by improving carriers. Some efforts use dendrimers to increase the drug loading of DDSs.^{44, 85} Another method employed to increase drug loading is conjugation of drugs to polymer building blocks via hydrazone linkers which self-assemble into micelles.

A new strategy for increasing the payload of drugs is encapsulation-based while still incorporating acid-sensitive linkers. To improve drug loading, many pH-sensitive linkers are being developed for use with polymers and in micelles with drug encapsulation.^{69, 86} Examples of this strategy were highlighted in section 1.3, but, in addition to those, acid-sensitive gates and acid-sensitive caps⁸⁷ have been developed to encapsulate drugs using the chemistry developed from acid-sensitive linkers.

While acid-sensitive linkers are traditionally used to conjugate drugs to carriers, a combination of acid-labile linkers with encapsulation may be the key to increasing drug loading. The extensive research on acid-sensitive linkers and their properties has laid the foundation for these acid-sensitive linkers to be translated into acid-sensitive components in polymers and materials. Continued research on improving acid-sensitive linkers and development of new moieties will continue to lay the foundation for further research in DDSs.

The Yang Lab has developed a novel acid-sensitive linker for use in DDSs. We believe this linker may be superior to other linkers because the rates of hydrolysis can be tuned by various mechanisms, it can be used to conjugate amine and alcohol containing drugs, and it is synthetically accessible from fairly inexpensive starting materials. The remainder of this thesis will focus on describing the development and characterization of the *N*-ethoxybenzylimidazoles platform for use as linkers in cancer drug delivery.

Chapter 2

The development of *N*-ethoxybenzylimidazoles (NEBIs) as an acid-sensitive hydrolyzable group

2.1 Introduction

The *N*-ethoxybenzylimidazole (NEBI) family of compounds was first explored by Dr. Seong Deok Kong, a former graduate student in the Yang Lab. Inspired by methylene ether imidazole protecting groups, which were shown to be hydrolytically unstable in aqueous acidic conditions and at elevated temperatures (Figure 2.1A),⁸⁸ ⁸⁹ Dr. Kong investigated protected imidazoles for acid triggered hydrolysis for potential use in drug delivery systems (DDSs). Since protonated imidazoles are known to have pKa's in the range of 1.5-7.75,⁹⁰ it was hypothesized that *N*-linked imidazoles in the protonated state would be useful for hydrolysis in mild

acid (e.g., pH 5.5), but would be more stable in solutions of normal, physiological pH (pH 7.4, Figure 2.1B). This chapter describes the initial development and evaluation of *N*-linked imidazoles as linkers for DDSs.

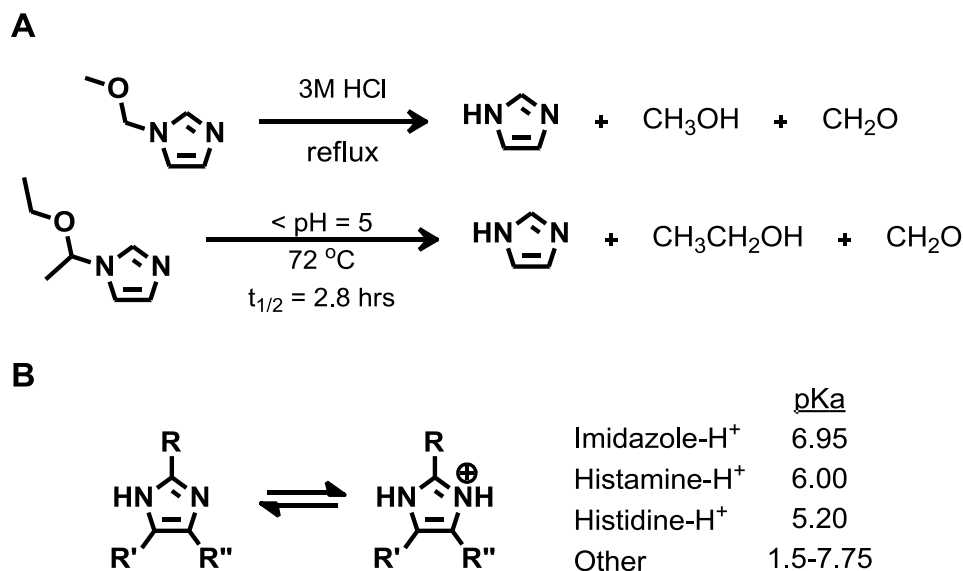


Figure 2.1 A) Acidic hydrolysis of protected imidazoles. B) The pKa of known protonated-imidazoles.

The cleavage of ethoxyethyl groups on imidazoles had been proposed to involve the protonation of the imidazole nitrogen (N3 in Figure 2.2) followed by breaking of the C6-N1 bond as the rate-determining step (RDS, Figure 2.2).⁸⁸ To determine if *N*-linked imidazoles could undergo acid catalyzed hydrolysis at physiological temperatures, substitution of the ethyl group (i.e., bearing the C6 carbon in Figure 2.2) with benzyl groups were explored for lowering the temperature required for this hydrolysis reaction and facilitate the cleavage of the C6-N1 bond under physiological conditions.

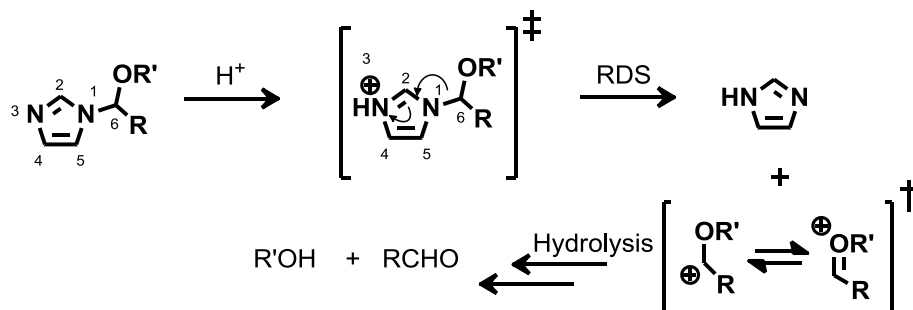


Figure 2.2 The proposed deprotection mechanism of *N*-linked imidazoles.

Substitution of R with substituted benzene group led to rates of hydrolysis at physiological temperatures that were potentially applicable for drug delivery. This class of compounds, *N*-ethoxybenzylimidazoles (**2.1**), was nicknamed “NEBI” for short (Figure 2.3). The NEBI group hydrolyzed to give benzaldehyde, imidazole and ethanol. The observed half-life of hydrolysis of the parent NEBI at 37 °C was 1.7 h and 25 h at pH 5.5 and pH 7.4, respectively (Figure 2.3).

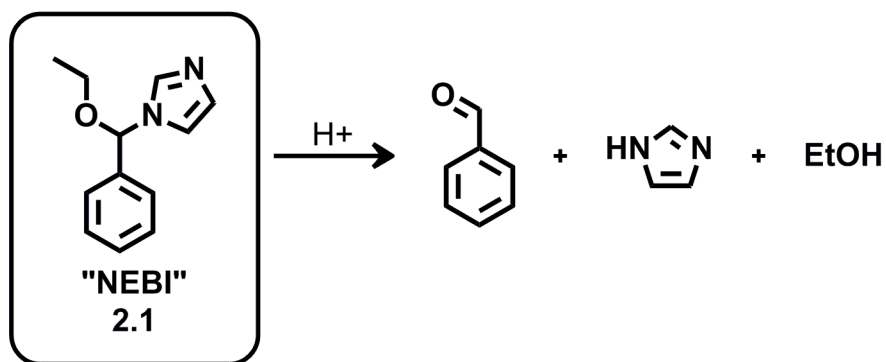


Figure 2.3 Hydrolysis of the NEBI gives benzaldehyde, imidazole and EtOH.

2.2 Kinetic analysis of the NEBI

Kinetic analysis indicated that the hydrolysis of **2.1** is first-order dependent on the concentration of **2.1** and zero-order dependent on the concentration of buffering agent (Figure 2.4).⁹¹ This was expected from the proposed mechanism shown in Figure 2.2, where the benzyl group (R = phenyl) appears to stabilize the transition state of the rate-determining step better than the previously reported ethyl group (R = methyl),⁸⁸ thus facilitating the hydrolysis of **2.1** at physiological temperatures.

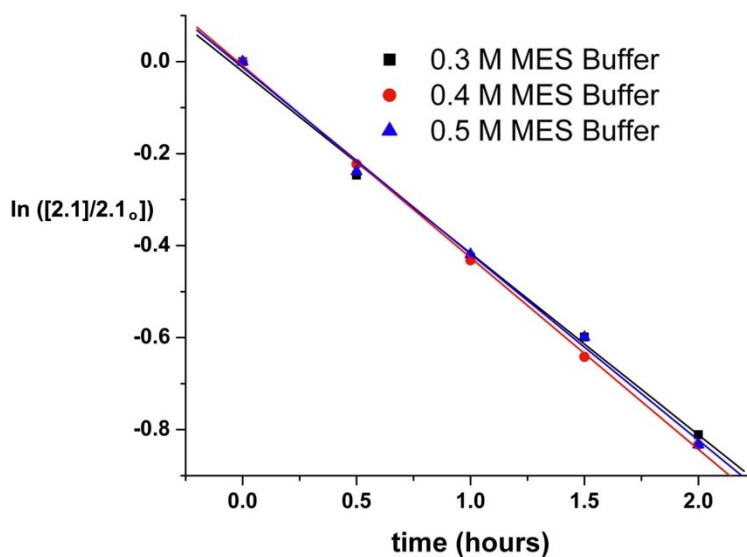


Figure 2.4 The dependence of the concentration of 2-[N-morpholino]ethanesulfonic acid (MES) buffer on the rates of hydrolysis of N-ethoxybenzylimidazole **2.1**.

2.3 Electronic effects on NEBI hydrolysis

To investigate whether electronic effects might influence the rate of hydrolysis of NEBIs, electron donating groups (EDG) and electron withdrawing groups (EWG) were incorporated at the ortho or para positions of the phenyl ring.

Compounds **2.1-2.8** were synthesized by refluxing commercially available benzaldehydes with triethyl orthoformate, ethanol and catalytic amounts of concentrated HCl. The resulting acetals were refluxed with imidazoles and TsOH for 3 days (Figure 2.5). The rates of hydrolysis were compared for **2.1-2.8**. Incorporation of an electron donating methoxy group at the ortho position in **2.6**, for instance, resulted in a half-life of 0.6 h for the hydrolysis of **2.6** at 37 °C in 0.5 M MES buffered D₂O (pD = 5.5); a slower rate was observed for hydrolysis for **2.6** ($t_{1/2}$ = 5 h) at 37 °C in 0.5 M N-[2-hydroxyethyl]piperazine-N'-[2-ethanesulfonic acid] (HEPES) buffered D₂O (pD = 7.4) compared to the rates of hydrolysis at pD = 5.5 (Figure 2.6). Incorporation of electron withdrawing substituents at the ortho or para positions of the phenyl ring of **2.1**, on the other hand, resulted in lower rates of hydrolysis in acidic and neutral solutions. Incorporation of a relatively weak electron withdrawing bromo substituent at the ortho position in **2.5**, for example, resulted in a significant decrease in the rate of cleavage of the NEBI moiety, with measured half-lives of 280 and 2300 h for the hydrolysis of **2.5** at 37 °C in buffered D₂O at pD = 5.5 and pD = 7.4, respectively. Furthermore, incorporation of strong electron withdrawing nitro substituents at the ortho or para position of the phenyl ring resulted in remarkably slow rates of hydrolysis of the NEBI moiety at 37 °C, with measured half-lives of 6900 h for both **2.3** and **2.8** in buffered D₂O at pD = 5.5 and no hydrolysis detected after >8 weeks at pD = 7.4.

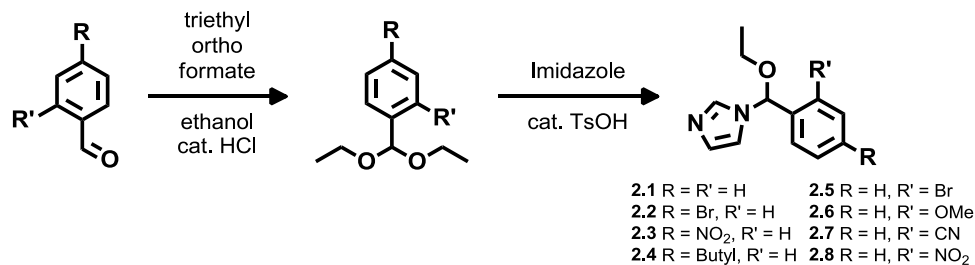


Figure 2.5 General procedure for the synthesis of *N*-ethoxybenzylimidazoles (NEBIs) 2.1-2.8 from the corresponding benzaldehydes.

	R	R'	pH=5.5 ^a		pH=7.4 ^b	
			<i>t</i> _{1/2} [h]	<i>k</i> [h ⁻¹]	<i>t</i> _{1/2} [h]	<i>k</i> [h ⁻¹]
2.1	H	H	1.7	0.41	25	0.028
2.2	Br	H	16.2	0.04	270	0.003
2.3	NO ₂	H	6900	<0.001	N/A ^c	-
2.4	Bu	H	1.0	0.69	8.8	0.079
2.5	H	Br	280	0.003	2310	< 0.001
2.6	H	OMe	0.6	1.13	5.1	0.136
2.7	H	CN	3500	<0.001	N/A ^c	-
2.8	H	NO ₂	6900	<0.001	N/A ^c	-

Figure 2.6 Half-lives (*t*_{1/2}) and rate constants (*k*) for the hydrolysis of NEBIs in D₂O at pD = 5.5 and pD = 7.4. ^a0.5M MES buffer solution ^b0.5M HEPES buffer ^cNo hydrolysis detected after > 8 weeks.

To further probe the mechanism of cleavage of NEBIs in acidic solutions, the linear free energy relationship for the hydrolysis of **2.1-2.4** in D₂O at pD = 5.5 was plotted (Figure 2.7). The calculated *p*-value of -4.2 for the hydrolysis of the NEBIs was consistent with an increase in positive charge (e.g., on the benzylic carbon of

2.1-2.8) in the rate-determining step of the reaction. This observed linear Hammett correlation, combined with the finding that the rate of hydrolysis of **2.1** is independent of the concentration of buffering agent, supports a specific acid-catalyzed mechanism⁹² for the hydrolysis of **2.1-2.8** as shown in Figure 2.2.

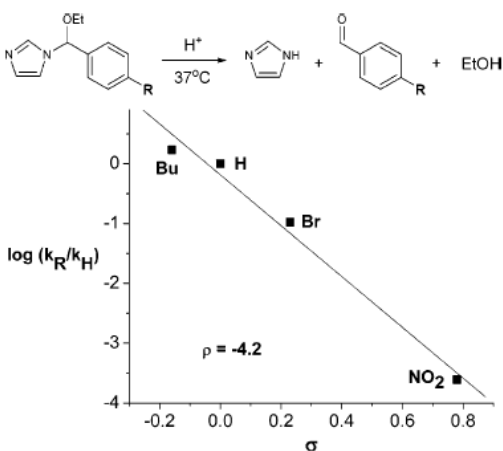


Figure 2.7 Linear Hammett correlation for the hydrolysis of 2.1-2.4 in 0.5 M MES buffered D₂O (pD = 5.5) at 37 °C, where R = n-butyl (Bu), H, Br, and NO₂.

I, together with Rina Fong, also investigated the electronic effects of an EDG and EWG on the 2 position of the imidazole on the NEBI. We found that an EDG methyl group (**2.9**) decreased the rates of hydrolysis and shifted the pH-range of hydrolysis towards a high pH when compared to **2.1**. An EWG morpholine amide (**2.10**) increased the rate of hydrolysis over a range of pH's and shifted the pH range of hydrolysis to a lower pH when compared to **2.1** (Figure 2.8, unpublished results). This demonstrated that the pKa of the imidazole could change the rate of hydrolysis and the pH range of hydrolysis. The inflection points were measured to be 4.68, 5.28 and 7.29 for **2.10**, **2.1** and **2.10**, respectively. The addition of substituents on the imidazole group would allow us to dial into a specific pH range for acid-catalyzed hydrolysis. Due to electronic effects from the phenyl ring, the inflection point is not a

directly match that of the pKa of the imidazole ion, but the trend shows that lower the pKa of the imidazole ion, the lower the active pH range for hydrolysis. This feature of the NEBI makes it versatile as a linker for DDSs, and may offer advantages over other acid-sensitive linkers under current development.

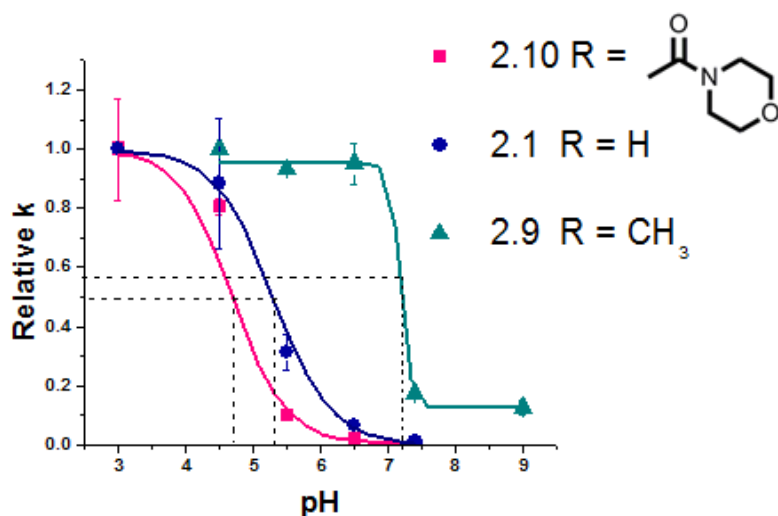


Figure 2.8 A comparison of hydrolysis rates of 2.1, 2.9 and 2.10.

2.4 NEBI stability studies

An important feature of acid-sensitive linkers is their stability in physiological conditions. To determine if components found in physiological conditions influenced the rate of NEBI hydrolysis, NEBI groups were assessed for their hydrolytic stability in the presence of common metal Lewis acids found in the body or in buffered solutions containing 10% fetal bovine serum (FBS) at pH 7.4. These hydrolysis studies revealed that the metal Lewis acids (at concentrations corresponding to their reported total concentration in blood or FBS) did not significantly affect the rate of hydrolysis of NEBI groups compared to hydrolysis in buffer alone (Figure 2.9⁹³).

These results collectively demonstrate that pH-sensitive NEBI groups are relatively stable to biological fluids such as blood.

Additive	Total concentration in blood (mM)	k (h^{-1})	k_{rel}
None	N/A	0.0211	1
Zn(II)	0.107	0.0241	1.14
Cu(II)	0.016	0.0249	1.18
Mg(II)	1.56	0.0222	1.05
Fe(III) ^a	8.00	0.0228	1.08
Ca(II)	1.51	0.0238	1.13
Na(I)	85.6	0.0222	1.13
K(I)	41.5	0.0221	1.05
10% Serum	N/A	0.0221	1.05

Figure 2.9 Hydrolysis of NEBI groups in buffered solutions containing biologically-relevant Lewis Acids or FBS. ^a $[\text{FeCl}_3]$ used in these experiments was 0.01 mM due to solubility limitations of FeCl_3 in buffer.

2.5 Temperature dependence of NEBI hydrolysis

A characteristic of the NEBI that would improve its versatility, and utility as a linker in a DDSs is temperature sensitivity. The dual ability to be acid-sensitive and temperature-sensitive would improve the tunability of a NEBI group. In order to explore the temperature dependence on hydrolysis of NEBI groups, I measured the rate of hydrolysis of **2.1** at 27.0 °C, 32.0 °C, 37.0 °C, 41.0 °C, 45.0 °C. The hydrolysis of **2.1** was monitored by UV absorption using a Molecular Devices SpectraMax 190 microplate reader at 235 nm. As expected, I found that the rate of hydrolysis was temperature dependent (Figure 2.10A). Plotting the $\ln k$ of hydrolysis against the inverse of the temperature (Figure 2.10B) provided the ΔH^\ddagger and ΔS^\ddagger of the reaction. Since $\ln k = (\Delta H^\ddagger/R)1/T + \Delta S^\ddagger/R$, I was able to determine

ΔH^\ddagger of hydrolysis of the NEBI to be 62.1 kJ/mol (14.8 kcal/mol). An estimate of ΔS^\ddagger was determined from the y-intercept to be 127.1 J/mol•K (30.4 cal/mol•K). A large positive entropy value was expected, as the NEBI hydrolyzes from one compound to three. Although we were initially interested in the acid-sensitivity of the NEBI groups, this information can be used to develop an acid-sensitive and temperature-sensitive linker, which can be used jointly for targeted controlled release of drugs.

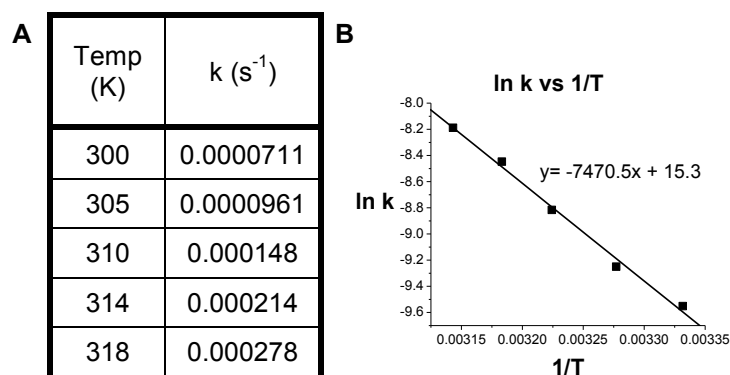


Figure 2.10 A) The rate of hydrolysis for 2.1 at pH 5.5 and varying temperatures. B) The Eyring Plot used to relate temperature and rate. The slope from this graph allowed for calculation of ΔH^\ddagger , while the y-intercept may be used to calculate ΔS^\ddagger .

2.6 Conclusions

Inspired by imidazole protecting groups, the Yang lab developed a novel acid-sensitive functional group that had exhibited increased rates of hydrolysis in mildly acidic environments, but were more stable at physiological pH and temperature. Experimental evidence supports a specific acid catalyzed mechanism for hydrolysis of the NEBI, with first order kinetic dependence on the concentration of NEBI. The rates of hydrolysis of the NEBI can be tuned by EDG and EWG on the phenyl ring. Substitution on the imidazole ring can be used to tune the pH range of

hydrolysis and also speed up the rate of hydrolysis. In addition to flexibility of tuning the rates of hydrolysis, temperature studies show that the NEBI also has the potential to be a temperature sensitive moiety. These properties will be advantageous when the NEBI is applied towards DDSs since studies have shown that the effectiveness of DDS depends on the rate of release of drugs from the drug carrier.⁴³

Notes about the chapter:

A large portion of this chapter is taken from a published reference.⁹² Reproduced with permission from S. D. Kong, A. Luong, G. Manorek, S. B. Howell and J. Yang, *Bioconjugate Chemistry*, 2007, **18**, 293-296. Copyright 2011 American Chemical Society. <http://pubs.acs.org/doi/abs/10.1021/bc060224s>

The NEBI stability studies was taken from a published manuscript, pH-Sensitive, *N*-ethoxybenzylimidazole (NEBI) bifunctional crosslinkers enable triggered release of therapeutics from drug delivery carriers, that appears in *Organic and Biomolecular Chemistry* 2010. Alice Luong, Tawny Issarapanichkit, Seong Deok Kong, Rina Fong and Jerry Yang, Royal Publishing Society, 2010. The dissertation author was the primary investigator and author of this paper. The figures from this publication are reproduced by permission of The Royal Society of Chemistry. <http://pubs.rsc.org/en/Content/ArticleLanding/2010/OB/c0ob00228c>

I would like to thank Prof. Yang for directing this research. Dr. Seong Deok Kong deserves credit for performing initial synthesis and studies on the NEBI compounds **2.1-2.8**. I would like to thank Rina Fong for tirelessly measuring the rates of hydrolysis of compounds in the presence of metal Lewis acids and FBS.

Tawny Issarapanichkit was very helpful in making starting materials. I would also like to thank Lynn Tross for the synthesis of compound **2.10**.

2.7 Experimentals

All reagents were purchased from Sigma-Aldrich, Inc., TCI, or Alfa Aesar and used without further purification. NMR spectra were recorded on a Varian 400 (FT, 400 MHz, ^1H ; 100 MHz, ^{13}C) spectrometer. HR-MS (high-resolution mass spectra) were obtained in the Department of Chemistry & Biochemistry, University of California, San Diego. Kinetic analysis by reverse-phase high performance liquid chromatography (RP-HPLC) was performed with a Agilent 1100 Series HPLC using an analytical reverse-phase column (SPHERI-5 Phenyl 5 micron, 250 x 4.6 mm).

General Procedure for the synthesis of *N*-ethoxybenzylimidazoles (2.1-2.8)

A solution of benzaldehyde (6.82 mmol), triethyl orthoformate (3.3 g, 22.5 mmol), and conc. HCl (10 μL , 90 μmol) was refluxed in 3.7 mL of ethanol for 24 hrs. Diethyl ether was added and the organic layer was extracted with 2 M NaOH. The organic layer was dried over anhydrous Na_2SO_4 . After removal of diethyl ether under reduced pressure, the crude mixture was distilled under vacuum (55-65 $^\circ\text{C}$ / 0.5 mmHg) to give pure benzaldehyde diethylacetal (82-91 % yield). All acetals were characterized by ^1H -NMR and used without further purification.

A mixture of imidazole (1.0 g, 14.7 mmol), benzaldehyde diethylacetal (58.8 mmol), and TsOH (84 mg, 0.441 mmol) was heated neat at 110 $^\circ\text{C}$ for 1-3 days, accompanied by concurrent distillation of ethanol. After cooling, sodium carbonate (0.47 g, 4.41 mmol) was added and the crude mixture was distilled under vacuum

(150-170 °C/ 0.5 mmHg) to give *N*-ethoxybenzylimidazole derivatives (**2.1-2.8**) (15-75 % yield).

Characterization of **2.1**: ^1H NMR (CDCl_3 , 400 MHz) δ 1.258 (t, 3 H), 3.539 (m, 2 H), 6.178 (s, 1 H), 6.955 (s, 1 H), 7.078 (s, 1 H), 7.290-7.327 (m, 5 H), 7.673 (s, 1 H); ^{13}C NMR (CDCl_3 , 100 MHz) δ 14.839, 64.469, 86.854, 116.970, 125.654, 128.357, 128.766, 129.647, 136.249, 137.616; HR-MS (m/z) calcd for $\text{C}_{12}\text{H}_{14}\text{N}_2\text{O}$ (M^+), 202.1101; found, 202.1102.

Characterization of **2.2**: ^1H NMR (CDCl_3 , 400 MHz) δ 1.254 (t, 3 H), 3.523 (m, 2 H), 6.136 (s, 1 H), 6.920 (s, 1 H), 7.091 (s, 1 H), 7.177 (d, 2 H), 7.474 (d, 2 H), 7.673 (s, 1 H); ^{13}C NMR (CDCl_3 , 100 MHz) δ 14.954, 64.686, 86.308, 116.948, 123.043, 127.563, 130.088, 131.631, 136.398, 136.885; HR-MS (m/z) calcd for $\text{C}_{12}\text{H}_{13}\text{BrN}_2\text{O}$ (M^+), 280.0206; found, 280.0207.

Characterization of **2.3**: ^1H NMR (CDCl_3 , 400 MHz) δ 1.297 (t, 3 H), 3.573 (m, 2 H), 6.268 (s, 1 H), 6.927 (s, 1 H), 7.132 (s, 1 H), 7.506 (d, 2 H), 7.724 (s, 1 H), 8.217 (d, 2 H); ^{13}C NMR (CDCl_3 , 100 MHz) δ 14.979, 65.019, 85.813, 116.881, 123.804, 127.031, 130.682, 136.535, 144.476, 148.155; HR-MS (m/z) calcd for $\text{C}_{12}\text{H}_{13}\text{N}_3\text{O}_3$ (M^+), 247.0951; found, 247.0954.

Characterization of **2.4**: ^1H NMR (CDCl_3 , 400 MHz) δ 0.902 (t, 3 H), 1.260 (t, 3 H), 1.322 (m, 2 H), 1.562 (m, 2 H), 2.588 (t, 2 H), 3.547 (m, 2 H), 6.162 (s, 1 H), 6.974 (s, 1 H), 7.085 (s, 1 H), 7.157 (d, 2 H), 7.211 (d, 2 H), 7.677 (s, 1 H); ^{13}C NMR (CDCl_3 , 100 MHz) δ 13.998, 14.882, 22.346, 33.539, 35.324, 64.428, 86.955, 116.981, 125.596, 128.392, 129.707, 135.003, 136.274, 143.633; HR-MS (m/z) calcd for $\text{C}_{16}\text{H}_{22}\text{N}_2\text{O}$ (M^+), 258.1727; found, 258.1728.

Characterization of **2.5**: ^1H NMR (CDCl_3 , 400 MHz) δ 1.258 (t, 3 H), 3.583 (m, 2 H), 6.417 (s, 1 H), 6.959 (s, 1 H), 7.049 (s, 1 H), 7.218 (t, 1 H), 7.370 (t, 1 H), 7.536 (d, 1 H), 7.645 (d, 1 H), 7.701 (s, 1 H); ^{13}C NMR (CDCl_3 , 100 MHz) δ 14.874, 64.754, 85.960, 116.979, 122.396, 127.356, 127.605, 129.400, 130.410, 132.916, 136.490, 136.632; HR-MS (m/z) calcd for $\text{C}_{12}\text{H}_{13}\text{BrN}_2\text{O}$ (M^+), 280.0206; found, 280.0203.

Characterization of **2.6**: ^1H NMR (CDCl_3 , 400 MHz) δ 1.253 (t, 3 H), 3.549 (m, 2 H), 3.747 (s, 1 H), 6.472 (s, 1 H), 6.841 (d, 1 H), 6.966-7.340 (m, 4 H), 7.638-7.667 (m, 2 H); ^{13}C NMR (CDCl_3 , 100 MHz) δ 15.257, 55.762, 64.738, 82.219, 110.872, 117.093, 120.806, 126.206, 126.532, 129.261, 130.293, 136.770, 156.288; HR-MS (m/z) calcd for $\text{C}_{13}\text{H}_{16}\text{N}_2\text{O}_2$ (M^+), 232.1206; found, 232.1209.

Characterization of **2.7**: ^1H NMR (CDCl_3 , 400 MHz) δ 1.300 (t, 3 H), 3.664 (m, 2 H), 6.491 (s, 1 H), 7.059 (s, 1 H), 7.127 (s, 1 H), 7.450-7.546 (m, 2 H), 7.615-7.706 (m, 2 H), 7.763 (s, 1H); ^{13}C NMR (CDCl_3 , 100 MHz) δ 14.926, 65.643, 85.159, 111.088, 116.643, 117.062, 126.209, 129.568, 130.139, 133.254, 136.386, 141.222; ^{13}C NMR (Acetone- d_6 , 100 MHz) δ 14.495, 65.035, 84.882, 111.161, 116.563, 117.125, 126.592, 129.744, 129.846, 133.435, 133.606, 137.071, 141.789; HR-MS (m/z) calcd for $\text{C}_{13}\text{H}_{13}\text{N}_3\text{O}$ (M^+), 227.1053; found, 227.1055.

Characterization of **2.8**: ^1H NMR (CDCl_3 , 400 MHz) δ 1.213 (t, 3 H), 3.583 (m, 2 H), 6.907 (s, 1 H), 7.030 (s, 1 H), 7.134 (s, 1 H), 7.289 (d, 1 H), 7.517-7.627 (m, 2 H), 7.725 (s, 1 H), 7.933 (d, 1H); ^{13}C NMR (CDCl_3 , 100 MHz) δ 14.683, 65.873, 83.735, 117.508, 125.062, 127.500, 130.140, 130.241, 132.873, 133.443, 136.940, 148.102; HR-MS (m/z) calcd for $\text{C}_{12}\text{H}_{13}\text{N}_3\text{O}_3$ (M^+), 247.0951; found, 247.0950.

General procedure for hydrolysis of 2.1 at varying concentrations of buffer (Figure 2.4)

Solutions of **2.1** (50 mM) in buffered D₂O solutions containing 20% *d*₆-DMSO (v/v) were incubated in a 37 °C constant temperature bath. NaCl was added to solutions containing less than 0.5 M MES buffer to maintain a constant ionic strength for all measurements. Rates of hydrolyses were obtained by ¹H-NMR (400 MHz) measurements. The relative ¹H NMR integrations of the benzylic proton and the aldehyde proton of the benzaldehyde product resulting from hydrolysis were compared over the time in order to estimate the rate of hydrolysis for the *N*-ethoxybenzylimidazoles.

General procedure for hydrolysis of *N*-ethoxybenzylimidazole derivatives (2.1-2.8)

Compounds **2.1-2.8** (0.05 mmol) were placed in 0.5 mL of 0.5 M MES buffer (pH= 5.5) or 0.5 M HEPES buffer (pH= 7.4) containing 20-40% DMSO-*d*₆ (v/v) and incubated at 37 °C in a constant temperature bath. The rates of hydrolysis were obtained by ¹H-NMR measurements. The relative ¹H NMR integrations of the benzylic protons of **2.1-2.8** and the aldehyde proton of the benzaldehyde product resulting from hydrolysis were compared over the time in order to estimate the rate of hydrolysis for the compounds **2.1-2.8**.

Synthesis of *N*-ethoxybenzyl-2-methylimidazole (2.9)

A mixture of 2-methylimidazole (1.21 g, 14.7 mmol), benzaldehyde diethylacetal (10.6g, 58.8 mmol), and TsOH (84 mg, 0.441 mmol) was heated neat

at 110 °C for 3 days, accompanied by concurrent distillation of ethanol. After cooling to room temperature, sodium carbonate (0.47 g, 4.41 mmol) was added and the crude mixture was distilled under vacuum (150-170 °C/ 0.5 mmHg) to give *N*-ethoxybenzyl-2-methylimidazole (30-80 % yield). ¹H NMR (CDCl₃, 400 MHz) δ 1.285 (t, 3 H), 2.365 (s, 3H), 3.558 (m, 2 H), 6.198 (s, 1 H), 6.899 (s, 1 H), 6.939 (s, 1 H), 7.239-7.337 (m, 5 H); ¹³C NMR (CDCl₃, 100 MHz) δ 13.750, 14.763, 64.437, 86.039, 117.658, 125.859, 127.431, 128.558, 128.787, 138.005, 144.716; HR-MS (*m/z*) calcd for C₁₃H₁₆N₂O (M⁺), 216.1263; found, 216.1261.

Synthesis of *N*-ethoxybenzyl-2-(carboxypiperidinyl)imidazole (2.10)

Ethyl imidazole-2-carboxylate (500 mg, 3.57 mmol) and 15 mL of piperidine were heated to 65 °C for overnight. The piperidine was removed under reduced pressure and 520 mg of 1H-piperidinylimidazole-2-carboxamide was collected. No further purification was carried out and the proton NMR indicated pure 1H-piperidinylimidazole-2-carboxamide was synthesized. White solid (81% yield). ¹H-NMR (400 MHz, CDCl₃) δ 7.12 (s, 2H), 4.52 (d, 2 H), 3.72 (t, 2 H), 1.69 (s, 6 H). ¹³C-NMR(400 MHz CDCl₃) δ 158.4, 141.7, 129.4, 118.6, 47.9, 44.4, 26.9, 26.1, 24.8. HR-MS (*m/z*) calcd for C₉H₁₃N₃O (M⁺), 179.1053; found, 179.1055

Diethyl acetal benzaldehyde (900 mg, 4.94 mmol), thionyl chloride (0.2 mL 2.76 mmol) and acetyl chloride (1.0 ml 14 mmol) was refluxed for one hour under inert conditions. The excess thionyl chloride, acetic acid was removed to obtain yellow oil. The crude product was characterized by ¹H (CDCl₃) NMR to identify the formation of chloro-ethoxymethyl benzene from the benzylic proton shift of δ = 6.58

(60% yield). The crude material was immediately taken onto the next step without further purification.

Under nitrogen atmosphere, sodium hydride (90 mg 3.8 mmol) and 1H-piperidinylimidazole-2-carboxamide (500 mg 2.8 mmol) was stirred for one hour in 10 mL dry THF at room temperature. The crude mixture of chloro-ethoxymethyl benzene was added dropwise. The reaction was allowed to stir at room temperature for three h. After quenching with saturated NaHCO₃, extraction with ethyl acetate, the combined organic layer was washed with water, brine and dried over Na₂SO₄. The crude material was purified by flash chromatography (Acetone-DCM, 1:9 w/ 1% Et₃N). ¹H-NMR (400 MHz, CDCl₃) δ 7.31 – 7.39 (m, 5H), 7.06 (s, 1H), 7.05 (s, 1H), 6.99 (s, 1H), 3.57 – 3.85 (m, 6H), 1.66 (s, 6H), 1.25 – 1.28 (t, 3H). ¹³C-NMR(400 CDCl₃) δ 160.0, 140.9, 138.9, 128.9, 128.7, 128.6, 128.2, 126.2, 118.9, 86.1, 64.9, 48.7, 43.7, 26.9, 25.9, 24.8, 15.2. HR-MS (*m/z*) calcd for C₁₈H₂₃N₃O₂ (M⁺), 313.1785; found, 313.1779.

General procedure for measurement of the rate of hydrolysis of *N*-ethoxybenzylimidazole derivatives (2.1, 2.9, 2.10) as a function of pH.

The rate of hydrolysis was measured for NEBI derivatives (**2.1**, **2.9**, **2.10**) at pH 3.0, 4.5, 5.5, 6.5, 7.4, 8.5, and 9.0. These experiments were carried out in 0.01 M buffers made with citric acid, acetate, MES, N,N-Bis(2-hydroxyethyl)-2-aminoethanesulfonic Acid (BES), HEPES, N-tris[hydroxymethyl]methyl-3-aminopropanesulfonic acid (TAPS), and N-[2-hydroxyethyl]piperazine-N'-[3-propanesulfonic acid] (EPPS), respectively. Compounds (**2.1**, **2.9**, **2.10**) were dissolved in acetonitrile (ACN) into 1 mM or 2 mM concentrations. A solution of **2.1**,

2.9 and **2.10** (20 μ L) was combined with 180 μ L of buffer in a 96 well plate. The plate was incubated at 37 $^{\circ}$ C and the absorbance of the compounds was monitored with a Molecular Devices SpectraMAX 190 plate reader at various time intervals at 235 nm.

Measurement of the rate of hydrolysis of N-ethoxybenzylimidazole 2.1 in the presence of Metal Lewis Acids or Serum.

Solutions of **2.1** (0.5 mM) were incubated in 0.1 M HEPES (pH 7.4) buffer and incubated at 37 $^{\circ}$ C. The hydrolysis of **2.1** in the presence of various metal Lewis acids was monitored by observing the formation of benzaldehyde product by UV absorbance at 235 nm. Solutions of metal ions were made from the following salts: $\text{Zn}(\text{NO}_3)_2$, $\text{Cu}(\text{NO}_3)_2$, MgCl_2 , FeCl_3 , CaCl_2 , NaCl , and KCl . For measurement of the hydrolysis of **2.1** in the presence of FBS, FBS was dialyzed against the solution of 0.5 mM **2.1** (in 0.1 M PBS buffer, pH 7.4) during the course of the hydrolysis experiment. The dialysis chamber was removed only during measurement of the formation of benzaldehyde product by UV spectroscopy; the dialysis chamber was necessary for these studies since the UV absorption of serum proteins in FBS interfered with the analysis of the hydrolysis of **2.1**.

Measuring the rate of hydrolysis of 2.1 at varying temperatures

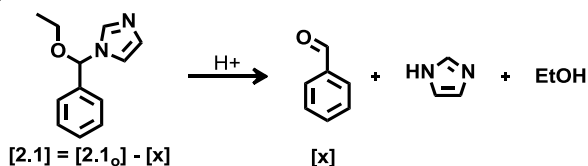
A solution of **2.1** (2 mM) was made in acetonitrile (ACN). The solution of **2.1** (20 μ L) was combined with 180 μ L of 10 mM MES buffer at pH 5.5 with 10% ACN. The UV absorption at 235 nm was monitored using a Molecular Devices SpectraMAX 190 microplate reader. The buffer was incubated at the correct temperature before mixing with the **2.1** solution. Readings were taken immediately

after mixing at 27.0 °C, 32.0 °C, 37.0 °C, 41.0 °C, 45.0 °C, and then again once every 10 - 60 seconds. The increase in absorption was monitored over time.

Calculations:

The rate of hydrolysis of the NEBI was calculated using Beer's Law.

Hydrolysis of **2.1**.



The extinction coefficient of **2.1** and benzaldehyde were determined by measuring the absorbance of 200 μL of varying concentrations of **2.1** and benzaldehyde. The absorbance was plotted against the concentration, and the slope from the trend line was used as the extinction coefficient. The extinction coefficient for **2.1** and benzaldehyde were determined to be 182 mM^{-1} and 3564 mM^{-1} respectively.

In order to calculate the rate of hydrolysis, we needed to plot $\ln([A]/[A_0])$ vs. t , where the rate is the slope of the graph. The absorbance measured by the plate reader is the sum of the absorbance of **2.1** and benzaldehyde. It can be expressed in the following equation:

$$\text{Absorbance} = 182\text{mM}^{-1}([\mathbf{2.1}]_0 - x) + 3564\text{mM}^{-1}x$$

The initial absorbance of **2.1** can be used to calculate $[\mathbf{2.1}]_0$ from the extinction coefficient of **2.1**, 182 mM^{-1} . From this information, and the equation above, you can calculate x , which corresponds to the concentration of

benzaldehyde. The formation of benzaldehyde = the hydrolysis of 2.1, and can be expressed in the following equation:

$$[2.1_0] - [x] = [2.1]$$

Knowing the value of x , and $[2.1_0]$, I calculated $[2.1]$. With all of these values, we were able to plot $\ln([2.1]/[2.1_0]) = -kt$ to determine the rate of hydrolysis.

Chapter 3

Hydrolysis and Cytotoxicity Studies of a doxorubicin-linked NEBI

3.1 Introduction

Chapter 2 described the stability and hydrolytic properties of the NEBI groups in acidic and neutral aqueous solutions. This chapter describes the development and synthesis of doxorubicin conjugated to the NEBI platform through an amide bond. We investigated this doxorubicin-NEBI conjugate for its hydrolytic properties and its cytotoxic effect on human ovarian carcinoma 2008 cells.

We chose doxorubicin (Figure 3.1) to be our model drug in these experiments because it is a well known chemotherapeutic that is often the model drug in the development of DDSs. Doxorubicin's anti-cancer mechanism of action is thought to include the intercalation of doxorubicin into DNA, and inhibition of

DNA and RNA synthesis.⁹⁴ While doxorubicin has been effective in treating patients, it has many side effects due to the non-specific cytotoxicity towards healthy and unhealthy cells. Side effects associated with doxorubicin include alopecia, cardiomyopathy, nausea, and vomiting. The principal clinical limitation of doxorubicin is the risk of cardiotoxicity, which ranges from a delayed and insidious cardiomyopathy to irreversible heart failure.⁹⁵ DDSs for doxorubicin have been explored by several groups through encapsulation or covalent conjugation onto carriers.^{69, 81, 96-98} The targeted delivery of doxorubicin to cancerous cells through DDSs may greatly reduce the side effects currently associated with doxorubicin.

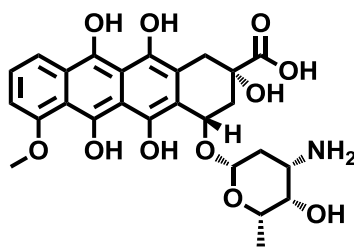


Figure 3.1 Doxorubicin

3.2 Conjugation of doxorubicin to the NEBI platform

To conjugate doxorubicin to a NEBI, a carboxylic acid functional group was incorporated to the parent NEBI (**2.1**) on the para position of the phenyl ring (Figure 3.2). Formation of the NEBI functional group did not occur in the presence of a carboxylic acid, so 4-carboxybenzaldehyde was protected as an ethyl ester (**3.1**). Although we previously published this synthesis using thionyl chloride and ethanol as reagents in the first step,⁹² I subsequently found that the ester formation via ethyl iodide and potassium carbonate improved yields and simplified purification. An ethyl ester was

used as a protecting group for the carboxylate to avoid mixtures of esters resulting from the synthesis of ethyl acetal. We also later found that using TsOH instead of concentrated HCl provided better yields in step b (Figure 3.2).

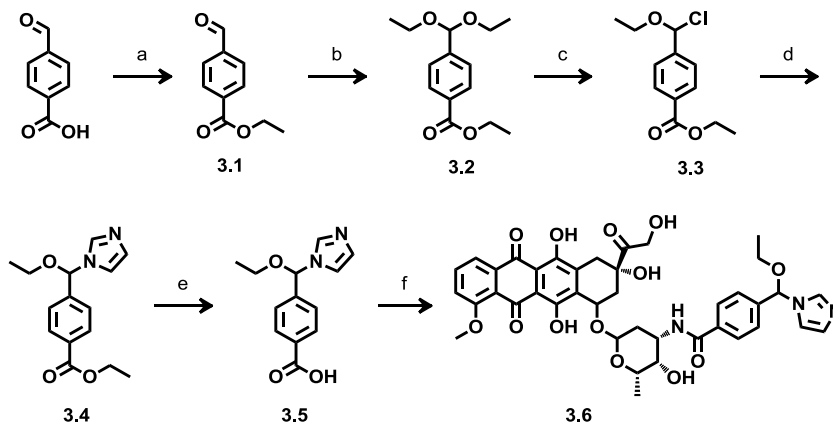


Figure 3.2 Synthetic scheme for *para*-*N*-ethoxybenzylimidazole-doxorubicin conjugate **3.6**. Reagents: a) SOCl_2 , ethanol; b) triethyl orthoformate, HCl, ethanol, 78% yield for two steps; c) SOCl_2 , acetyl chloride, neat; d) NaH, imidazole, THF, 33% yield for two steps; e) NaOH, THF/ H_2O , 90% yield; f) doxorubicin, EDC, THF, 54% yield.

The synthesis of compound **3.3** required freshly distilled acetyl chloride refluxed with compound **3.2** and thionyl chloride for one hour. We later found that 1.2 equivalents of thionyl chloride alone, refluxed with compound **3.2** for one hour also results in compound **3.3** with similar yields and without the need to freshly distill acetyl chloride. The thionyl chloride and acetyl chloride were removed under reduced pressure. Compound **3.3** was added in a dropwise manner to a solution of imidazole and sodium hydride in THF to give an ester protected NEBI (**3.4**). Although compound **3.4** was originally purified with silica chromatography using a mixture of DCM and MeOH as eluent, we found a mixture of EtOAc and hexanes with 2% triethylamine (TEA) gave higher purity compounds. The TEA is essential for purification to prevent hydrolysis of the NEBI on the silica column.

Hydrolysis of compound **3.4** was achieved with lithium hydroxide in THF and water to give compound **3.5**. An amide bond was formed by coupling doxorubicin to **3.5** using EDC, and DMAP to give *para-N*-ethoxybenzylimidazole-doxorubicin (**3.6**).

3.3 Hydrolysis of a doxorubicin-linked NEBI

Hydrolysis studies were performed on compound **3.6** to determine if the NEBI group retained its expected hydrolytic properties in mildly acidic environments. Compound **3.6** was dissolved in DMSO and buffer, incubated at 37 °C, and monitored at pH 5.5 (18.6 mM MES buffer) and 7.4 (18.6 mM HEPES buffer) via HPLC. We found that compound **3.6** hydrolyzed to give *N*-(4-formylbenzoyl)doxorubicin (**3.7**, Figure 3.3A). Compounds **3.6** and **3.7** were monitored by the absorption of the doxorubicin moiety at 470 nm using an Agilent 1100 series HPLC machine. We found the half-life of hydrolysis at 37 °C to be 55 h at pH 5.5 and 1150 h at pH 7.4 (Figure 3.3B). Confirmation of the hydrolysis product **3.7** was made through LC-MS and also matched by comparing the retention time of compound **3.7** on the column compared to known **3.7** that was synthesized. We found that hydrolysis of compound **3.6** followed first order kinetics and was pH dependent as found with other NEBI groups.⁹² The observed rate of hydrolysis of compound **3.6** at pH 5.5 was consistent with the expected value for a NEBI group containing an amide functionality attached to the *para* position of the phenyl ring as predicted from the linear free energy relationship shown in Chapter 2 (Figure 2.6, R = CONHR₂).

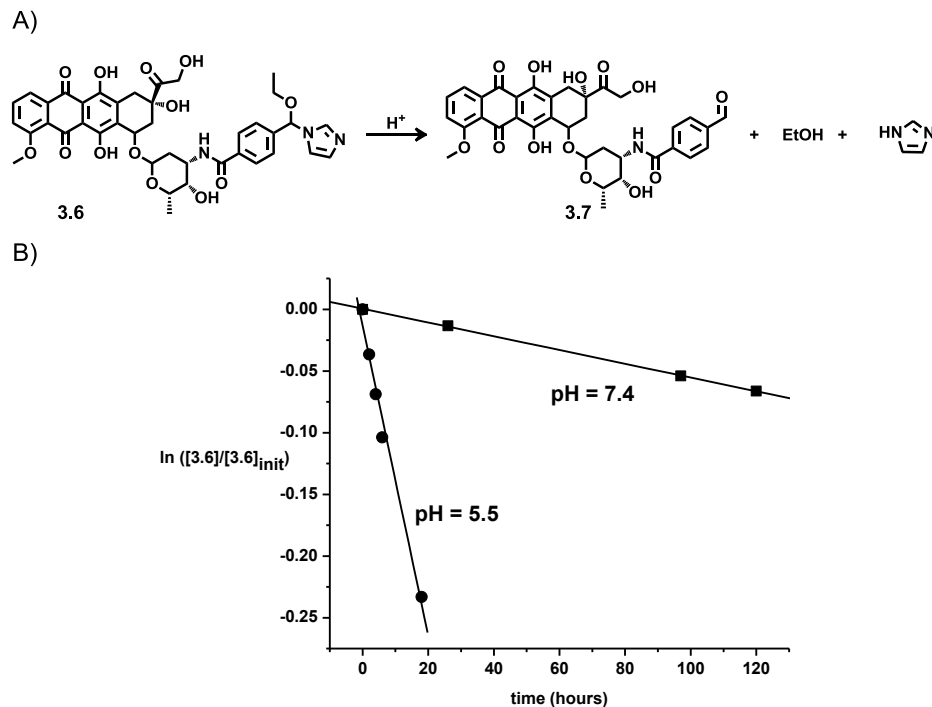


Figure 3.3 A) The schematic for hydrolysis of 3.6. B) Hydrolysis of 3.6 at 37 °C at pH 5.5 and pH 7.4, monitored at 470 nm using HPLC methods.

3.4 Cytotoxicity studies of 3.6 and 3.7

N-(4-formylbenzoyl)doxorubicin (**3.7**) was synthesized through coupling of doxorubicin to 4-carboxybenzaldehyde with EDC and DMAP. Gerald Manorek (Howell group, UCSD, School of Medicine) previously tested the cytotoxicity of compound **3.7** and **3.6** on human ovarian carcinoma 2008 cells. Compound **3.7** was found to have an IC_{50} of 12 μ M in a colony formation assay, while **3.6** was found to an IC_{50} about 2 times higher than **3.7**.⁹² I also independently tested the cytotoxicity of compound **3.6** on 2008 cells, but used an SulforhodamineB (SRB) cytotoxicity assay instead.⁹⁹ The SRB cytotoxicity assay was used because it is a faster method to measure cell viability compared to the colony formation assay. The

SRB cytotoxicity assay revealed that compound **3.7** had an IC_{50} of 5.8 μM (Figure 3.4).¹⁰⁰ This result was within the same order of magnitude of cytotoxicity found in the colony formation assay.

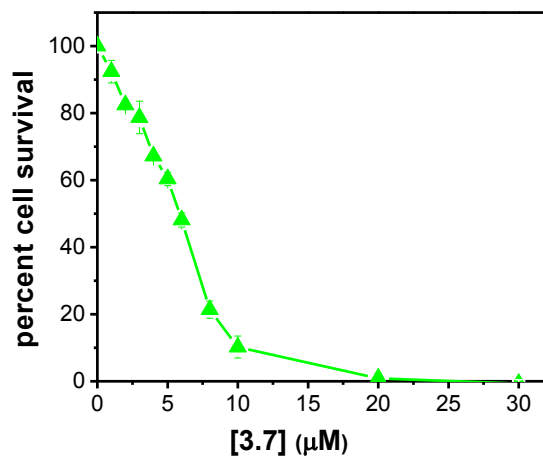


Figure 3.4 Cytotoxicity of **3.7** tested on 2008 human ovarian carcinoma cells using the SRB Assay.

3.5 Conclusions

In this chapter, I synthesized a NEBI coupled to doxorubicin (**3.6**) via an amide bond that exhibited accelerated rates of hydrolysis in acidic solution compared to at neutral pH. Hydrolysis of compound **3.6** under acidic conditions gave compound **3.7** at pH 5.5 and 7.4, which showed potentially useful cytotoxic activity against human ovarian carcinoma 2008 cells. Previous studies have shown that drugs conjugated to delivery vessels via acid-sensitive linkers with hydrolytic properties similar to those of **3.6** can exhibit useful antitumor activity *in vivo*.^{69, 70, 73, 81} These drugs conjugated to delivery vessels using acid-sensitive linkers also showed

reduced toxicity to normal, healthy tissues compared to administration of equivalent concentrations of free drug. This study demonstrated proof-of-concept that the NEBI functional groups can be used to release active drugs after hydrolysis from carriers in mildly acidic environments.

Notes about the chapter:

A portion of this chapter is taken from a published reference.⁹² Reproduced with permission from S. D. Kong, A. Luong, G. Manorek, S. B. Howell and J. Yang, *Bioconjugate Chemistry*, 2007, **18**, 293-296. Copyright 2011 American Chemical Society. <http://pubs.acs.org/doi/abs/10.1021/bc060224s>

I would like to thank Dr. Seong Deok Kong for performing the hydrolysis studies shown in Figure 3.1. I would like to thank Gerald Manorek for his contribution with the colony formation assay. Many thanks to Linnie Tross who helped optimize the synthesis of NEBI compounds and increased the yields. Finally, I would also like to thank Prof. Jerry Yang for directing the research and preparing the manuscript.

3.6 Experimentals

All reagents were purchased from Sigma-Aldrich, Inc., TCI, or Alfa Aesar and used without further purification. NMR spectra were recorded on a Varian 400 (FT, 400 MHz, ¹H; 100 MHz, ¹³C) spectrometer. HR-MS (high-resolution mass spectra) were obtained in the Department of Chemistry & Biochemistry, University of California, San Diego. Kinetic analysis by reverse-phase high performance liquid

chromatography (RP-HPLC) was performed with an Agilent 1100 Series HPLC using an analytical reverse-phase column (SPHERI-5 Phenyl 5 micron, 250 x 4.6 mm).

Synthesis of *N*-ethoxybenzylimidazole-doxorubicin conjugate (**3.6**)

We synthesized compound **3.6** using a synthetic route outlined in Figure 3.2. 4-carboxylbenzaldehyde (13.5 mmols) and thionyl chloride (27 mmols) was refluxed in 50 mL anhydrous dichloromethane (DCM) and 20 mL distilled ethanol for 12 h. An additional 3 mL of thionyl chloride (41 mmols) was added and the solution was allowed to reflux for another 24 h. The solution was cooled and the solvents were removed under reduced pressure. The product mixture was dissolved in DCM and washed with 10% NaCO₃. The organic layer was dried over anhydrous Na₂SO₄. Crude NMR indicated a mixture of **3.1** and ethyl 4-formylbenzoate and was taken on without further purification.

The crude mixture of **3.1** was combined with triethyl orthoformate (44.5 mmol) and conc. HCl (19.5 μ L, 178 μ mol) in 2.6 mL of absolute ethanol and allowed to reflux for 24 h. After removal of ethanol and excess orthoformic acid under reduced pressure, the crude mixture was taken up in diethyl ether and the solution was washed with saturated NaCO₃. The organic layer was dried over anhydrous Na₂SO₄, and the diethyl ether was removed under reduced pressure. Compound **3.2** was distilled from the crude mixture under vacuum (141 °C, 0.7 Torr) to give pure compound (78 % isolated yield from 4-carboxybenzaldehyde). Characterization of **3.2**: ¹H NMR (CDCl₃, 400 MHz) δ 1.170 (t, 6H), 1.318 (t, 3H), 3.481 (m, 4 H), 4.295 (q, 2H), 5.476 (s, 1H), 7.478 (d, 2H), 7.969 (d, 2H) ¹³C NMR

(CDCl₃, 100 MHz) 14.465, 15.316, 61.157, 100.956, 126.834, 129.587, 130.526, 144.045, 166.411 ESI-MS: 224.96 (M⁺ -ethyl), 206.99 (M⁺ - ethoxy).

The synthesis of **3.4** was performed in using a modified procedure as previously reported.¹⁰¹ A solution of **3.2** (1.13 mmol), freshly distilled acetyl chloride (1.8 mmol) and thionyl chloride (0.227 mmol) was refluxed for one hour under N₂. The excess thionyl chloride and acetic acid were removed under reduced pressure and the crude mixture was characterized by ¹H NMR. ¹H-NMR (in CDCl₃) indicated a new peak at 6.203 ppm, presumably corresponding to the benzylic H in **3.3**. The crude yield of **3.3** by ¹H-NMR was ~54%, with the remainder of the material identified as starting material **3.2** (~8%) as well as a large amount (~38%) of **3.1**. The crude material was immediately taken on to the next step without further purification. **Note:** I observed hydrolysis of **3.3** (presumably from moisture in the air) over the course of several h when left open to air. Compound **3.3** should, therefore, be prepared fresh and used immediately. Hydrolysis could have also been from water in the CDCl₃ in later studies, yields of **3.3** improved when I ensured the CDCl₃ was dry through addition of sieves to the bottle.

In a dry flask, NaH (0.612 mmol) and imidazole (0.612 mmol) was allowed to stir for one hour in 0.5 mL of anhydrous THF. A solution of a crude mixture of **3.3** (0.612 mmols) was added to the imidazole solution. The solution was stirred for 12 h at 23 °C. After removal of the solvent under reduced pressure, **3.4** was isolated by silica chromatography using as eluent a 95:5 mixture of DCM:MeOH. The isolated yield of **3.4** was 33%. Characterization of **3.4**: ¹H NMR (CD₃OD, 400 MHz) δ 1.270 (t, 3H), 1.368(t, 3H), 3.526 (m, 1H), 3.674 (m, 1H), 4.358 (q, 2H), 6.527 (s, 1H), 7.089 (d, 2H), 7.509 (d, 2H), 7.946 (s, 1H), 8.034 (d, 2H). ¹³C NMR (MeOH,

100 MHz) δ 15.621, 15.158, 62.349, 65.760, 87.583, 118.570, 127.252, 129.949, 130.777, 132.216, 138.103, 144.535, 167.464 ESI-MS: 274.54 (M+H⁺)

A solution of the **3.4** (0.151 mmol) and LiOH (0.151 mmol) in 0.8 mL of a 5:3 THF:water solution was allowed to stir for 12 h at 23 °C. The THF and water were removed under reduced pressure and the crude solid was washed with chloroform. ¹H-NMR of the crude in CD₃OD indicated only the desired carboxylate was present (presumably as the lithium salt). The yield was estimated as 90% by weight.

The crude mixture from ester hydrolysis of **3.5** (.134mmol) was dissolved in 1.5 mL DMF. Doxorubicin (16.7 μ mol) and 1-(3-dimethylaminopropyl)-3-ethylcarbodiimide hydrochloride (EDC, 66.8 mmol) were added to the DMF solution and stirred for 12 h at 23 °C. Product **3.6** was isolated by silica chromatography using as eluent a 92:8 mixture of DCM:MeOH. The isolated yield of **3.6** was 54%. Characterization of **3.6**: ¹H NMR (CD₃OD, 400 MHz) δ 1.242 (t, 3H), 1.283 (m, 6H), 1.833 (d, 1H), 2.136 (m, 2H), 2.356 (d, 1H), 2.915 (d,1H), 3.017 (d, 1H), 3.491 (m, 1H), 3.635 (m, 1H), 3.741 (s, 1H), 3.955 (s, 3H), 4.326 (t, 2H), 4.753 (d, 2 H), 5.069 (s, 1H), 5.435 (s, 1H), 5.492 (s, 1H), 6.471 (s, 1H), 6.990(s, 1H), 7.081 (s, 1H), 7.433 (m, 3 H), 7.740 (t, 1H), 7.809 (d, 3H), 7.885 (s, 1H). HR-MS (*m/z*) calcd for C₄₀H₄₂O₁₃N₃ (M+H⁺) 772.2712; found, 772.2721.

Synthesis of *N*-(4-formylbenzoyl)doxorubicin (**3.7**)

Doxorubicin (6.9 μ mol) was stirred in 660 μ L of acetonitrile and 340 μ L of water. 4-carboxybenzaldehyde (13.8 μ mol), and EDC (17.6 μ mol) were added to the solution and the solution was stirred for 18 h at 23 °C. Product **3.7** was isolated by silica chromatography using as eluent a 90:10 mixture of DCM:MeOH. The isolated yield of **3.7** was 51%. Characterization of **3.7**: ¹H NMR (CDCl₃, 300 MHz) 1.341 (s,

3H) 1.873 (d, 1H), 2.004(m, 2H), 2.172 (d, 1H), 2.227 (d,1H), 2.353 (d, 1H), 3.103 (d, 1H), 3.301 (d, 1H), 3.760 (s, 1H), 4.266 (m, 1H), 4.788 (s, 3H), 5.337 (d, 1H), 5.556 (d, 1H), 6.519 (d, 1H), 7.416 (d, 1H), 7.800 (t, 1H), 7.919 (m, 5H), 8.051 (d, 1H), 10.064 (s, 1H). ESI-MS: 698.01 (M+Na⁺)

Hydrolysis of *para-N*-ethoxybenzylimidazole conjugated to doxorubicin (3.6)

The *para-N*-ethoxybenzylimidazole conjugated with doxorubicin (**3.6**) (0.37 μ mol) was dissolved in 0.5 mL of 18.6 mM MES buffer (pH=5.5) or 18.6 mM HEPES buffer (pH=7.4) containing 30% DMSO (v/v) and incubated at 37 °C in a constant temperature bath. The hydrolysis of **3.6** at pH=5.5 and pH=7.4 was monitored by RP-HPLC by injection of small aliquots (20 μ L) of the solutions at regular time intervals and analyzing the chromatograms at λ = 470 nm. The products were eluted with an isocratic solvent mixture of 70% MeOH and 30% H₂O with a flow rate of 1 mL/min. The retention time of **3.6** and **3.7** were 8.11 minutes and 6.25 minutes, respectively. We determined the rates of hydrolysis of the NEBI moiety in **3.7** by comparison of the relative integrated HPLC peak areas of **3.6** and **3.7** at 470 nm at each time point.

Cytotoxicity Assays:

Colony formation assay of 3.6 and 3.7 on human ovarian carcinoma 2008 cells

Human ovarian carcinoma 2008 cells were plated in 6-well plates at a density of 200 cells in 3 mL of media (RPMI-1640 + 10% Fetal Bovine Serum) per well and incubated overnight to allow the cells to adhere to the bottom of the wells. After overnight incubation the media was removed from each well and fresh growth media containing different concentrations of **3.6** and **3.7** was added to the wells. The cells were incubated for 1 hour in the presence of **3.6** and **3.7**. Following the

removal of the solutions containing **3.6** and **3.7**, the cells were incubated with fresh media for 10 days to allow surviving cells to form colonies. After removal of media, the plates were washed with 2 mL of room temperature PBS buffer (pH 7.4, 0.138 M NaCl, 0.003 mM KCl, 14.2 mM potassium phosphate), and then fixed and stained for 15 minutes with 1 mL of 0.1% crystal violet solution that contains 10% methanol. Clusters containing >50 cells were scored as colonies using an AlphaInotech Imager. We performed this colony formation assay in triplicate on 3 independent occasions.

SRB Cytotoxicity studies of (3.7) on human ovarian carcinoma 2008 cells

Human ovarian carcinoma 2008 cells were plated into each well of a 96 well plate (3000 cells/well) using RPMI-1640 media with 10% FBS. The cells were incubated for 24 h at 37°C with 5% CO₂. After the incubation period, cells were dosed with various concentrations of *N*-(4-formylbenzoyl)doxorubicin (**3.7**). The cells were allowed to incubate with the molecules for 72 h. After incubation, cells were washed 3 times with 200 µL of PBS (Mediatech, 46-013CM) pH 7.4. Cells were then fixed with 200 µL of PBS and 50 µL of 50% trichloroacetic acid for one hour at 4 °C. After fixation, cells were washed 5 times with water and allowed to dry. A 0.4% sulforhodamine B (SRB, Sigma Aldrich, S1402) solution in 1% acetic acid was added to the cells and incubated for 15 minutes at room temperature. The cells were washed 3 times with 1% acetic acid and the 96 well plate was allowed to dry. Tris base solution (10 mM, 200 µL) was added to the wells for 15 minutes prior to measuring the absorbance at 515 nm.

IC₅₀ calculations are based on the concentration where cell survival is above 50% and the concentration when cell survival is just below 50%.

Equation: $IC_{50} = A + \frac{\log(0.5/A_1)}{\log(B_1/A_1)} * (B-A)$

A = concentration where cell survival is above 50%

A_1 = survival at concentration A

B = Concentration where cell survival is below 50%

B_1 = survival at concentration B.

Chapter 4

Development of a bifunctional NEBI crosslinker for use in a model drug delivery system

4.1 Introduction

In order to use the NEBI platform in a DDS, I developed a bifunctional NEBI crosslinker that would specifically conjugate a drug delivery carrier to a chemotherapeutic drug. I designed two bifunctional NEBI crosslinkers (**4.1** and **4.2**, Figure 4.1) on one side to carry a carboxylic acid functionality, and on the other side to carry an azide or alkyne functionality. The carboxylic acid functionality on the bifunctional crosslinker would allow conjugation of amine or alcohol-containing drugs through standard amidation or esterification conditions. The azide or alkyne functional group would allow for conjugation to alkyne or azide containing carriers respectively through “click” chemistry methods.

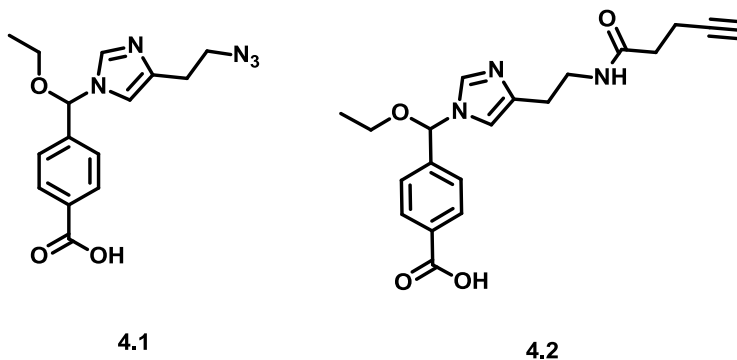


Figure 4.1 The structure of two bifunctional NEBI crosslinkers developed.

For this model DDS, we continued to use doxorubicin as our model drug and human serum albumin (HSA) as a model protein carrier. The amine functionality on doxorubicin allows for standard amidation to the bifunctional crosslinker. Also, work done in the previous chapter had already established the cytotoxicity and hydrolysis of a NEBI carrying doxorubicin. I choose HSA as a model drug delivery carrier since this protein is commercially available and is known to enter cancer cells through a endocytotic mechanism.¹⁰² HSA is also currently used as an FDA-approved drug carrier for paclitaxel for the treatment of breast cancer, and, therefore, is an excellent model for these studies.¹⁰³

We chose to use “click” chemistry in our design of a bifunctional NEBI crosslinker due to its many advantages. Azides and alkynes can be catalyzed by Cu^I for a Huisgen 1,3-dipolar cycloaddition very efficiently in aqueous conditions. These “click” reactions are bioorthogonal and not known to be naturally present in organisms. The reaction is also reported to be very high yielding reaction (up to 95% yield)¹⁰⁴ in mild aqueous conditions to cleanly give one product.^{79, 105} The NEBI platform and HSA was also readily functionalized with alkynes and azides.

In this chapter, I describe methods for the synthesis of bifunctional crosslinkers and methods used to create a model DDS. This model DDS was used to investigate whether a bifunctional NEBI crosslinker can have utility in a DDS. I investigated the effectiveness of the NEBI group in the DDS through cytotoxicity studies, and evaluated the cellular uptake and subcellular localization of the DDS using cell fluorescence studies.

4.2 Synthesis of bifunctional crosslinkers

Two bifunctional acid-sensitive NEBIs were created for conjugation of drugs to macromolecules. Figure 4.2 shows the synthesis of the bifunctional crosslinker *para-N*-ethoxybenzylimidazole-azide-carboxylic acid (**4.1**). Figure 4.3 shows the synthesis of the bifunctional crosslinker *para-N*-ethoxybenzylimidazole-alkyne-carboxylic acid (**4.2**). The synthesis of compounds **4.1** and **4.2** only differed in the imidazole compound that was used. While I was able to make two different bifunctional crosslinkers to show the versatility of the synthesis, I decided to conduct further tests on only **4.1** due to two main reasons. 1) The synthesis of **4.2** required compound **C** (Figure 4.3), which was not very soluble in THF or other dry reagents readily available. Dry DMSO was required to dissolve compound **C** during the synthesis of compound **4.2**. Using DMSO was problematic because it was difficult to remove after the reaction was completed, and DMSO had to be distilled for the reaction. 2) The yield for compound **4.2** was also slightly lower than that found for compound **4.1** due to other acidic protons found on compound **C** (alkyne proton and amide proton), which can also be deprotonated during the reaction with NaH. Alternatively, compound **A** was easily dissolved in tetrahydrofuran (THF) and could be used to synthesize the NEBI without any further complications.

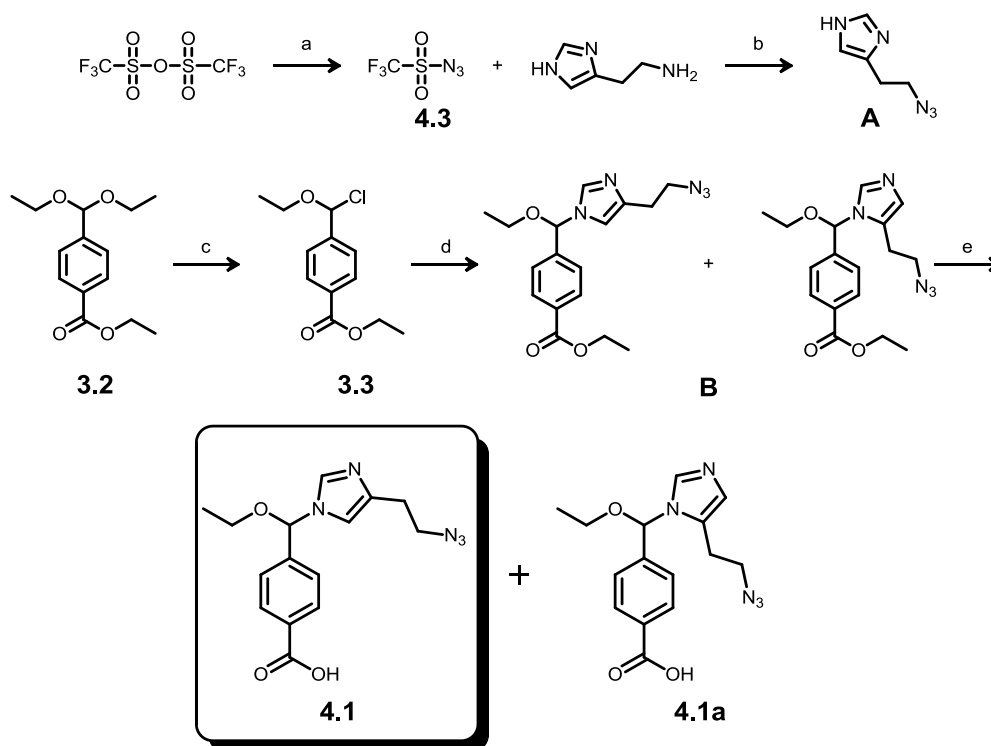


Figure 4.2 Synthetic scheme for bifunctional crosslinker para-N-ethoxybenzylimidazole-azide-carboxylic acid 4.1. Reagents: a) sodium azide, DCM and water; b) potassium carbonate, copper sulfate, in DCM, MeOH, and water 53 % yield for two steps; c) acetyl chloride, thionyl chloride; d) A, NaH, in THF, 28% yield over two steps; e) lithium hydroxide, water and THF.

Figures 4.1 and 4.2 show two final products **4.1**, **4.1a**, **4.2** and **4.2a** for each bifunctional crosslinker. While I synthesized two isomers, compounds **4.1** and **4.2** were the major products from the final step of the NEBI formation (Figures 4.2 and 4.3). Compounds **4.1a** and **4.2a** were minor products. I was able to separate and isolate the pure isomers by column chromatography, and characterized the isomers individually by NMR. In further studies, I used a mixture of compounds **4.1** and **4.1a**, because separation of these isomers, although possible, was difficult and impractical on the large scale. The isomers should have similar rates of hydrolysis, and would not interfere with the results of experiments when used as a mixture. By

NMR, the benzylic peaks of compounds **4.1** and **4.1a**, and **4.2** and **4.2a**, had different chemical shifts. The structure of pure **4.1** and **4.2** were determined by NOESY NMR, which showed a correlation between the benzylic proton and the proton on C-5 of the imidazole moiety. I did not observe this NOESY correlation in compounds **4.1a** and **4.2a**.

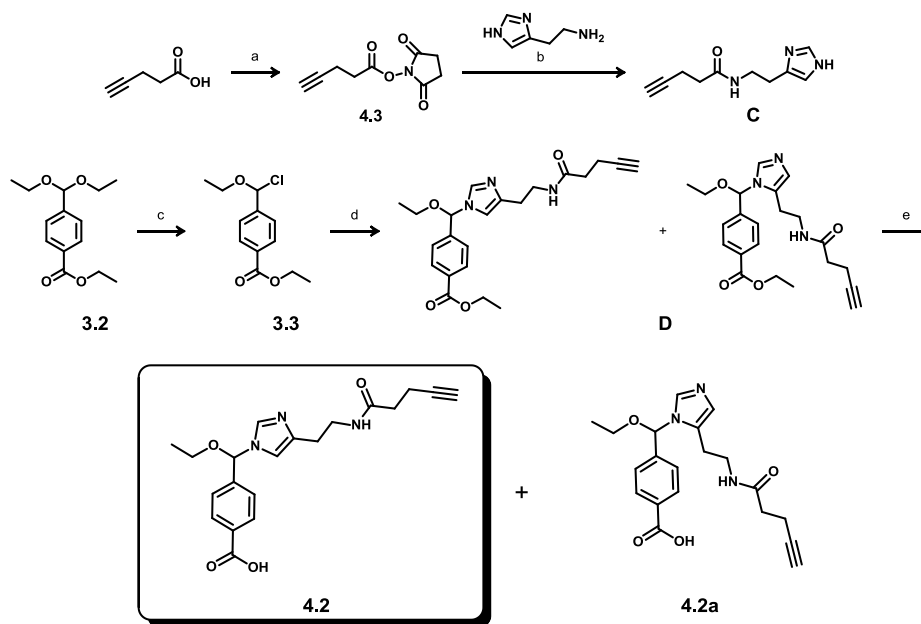


Figure 4.3 Synthetic scheme for bifunctional crosslinker *para*-*N*-ethoxybenzylimidazole-alkyne-carboxylic acid **4.2**. Reagents: a) NHS, EDC, DCM; b) 0.1 M HEPES buffer 53 % yield; c) acetyl chloride, thionyl chloride; d) B, NaH, in THF, 21% yield over two steps; e) lithium hydroxide, water and THF.

4.3 Conjugation of doxorubicin to HSA

In order to conjugate **4.1** to HSA, some of the lysine residues on HSA were functionalized with alkynes. We incorporated alkyne functionalities on the lysines of HSA by reacting compound **4.3** with HSA in 0.1 M HEPES buffer (pH 8.3) to afford HSA-alkyne **4.6** (Figure 4.4). Compound **4.3** was added dropwise during the course of the reaction. The pH was monitored, and maintained at pH 8.3 by addition of

0.01 M NaOH solution as needed. Compound **4.6** represents a mixture of isomers, since there are multiple lysine residues present in HSA. Figure 4.4 outlines the procedure used to conjugate doxorubicin to HSA via compound **4.1**.

After coupling doxorubicin to the carboxyl functionality of compound **4.1** using standard amide coupling conditions, we reacted this NEBI-doxorubicin conjugate with **4.6** under copper-mediated “click” conditions to afford HSA-NEBI-doxorubicin conjugate (**4.7**).¹⁰⁶

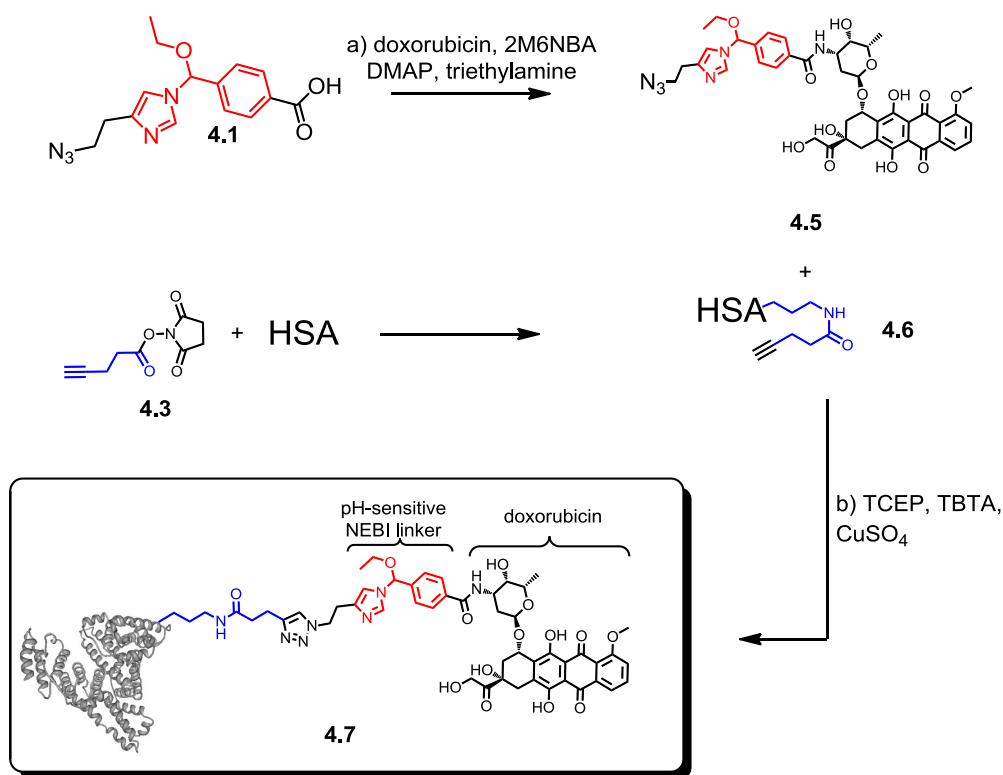


Figure 4.4 Conjugation of doxorubicin to HSA via a NEBI linker using click chemistry. TCEP = tris(2-carboxyethyl)phosphine, TBTA = tris(benzyltriazolylmethyl)amine

In order to provide a comparison for the utility of the bifunctional NEBI crosslinker, (**4.1**) for drug delivery applications, we also synthesized a doxorubicin containing an azide (**4.8**, Figure 4.5A) and conjugated it to **4.6** to generate a stable

HSA-doxorubicin conjugate (**4.9**). Click chemistry conditions were once again employed to construct this stable HSA-doxorubicin conjugate (Figure 4.5B). Comparison of the cytotoxicity between **4.7** and **4.9** would allow us to determine the utility of the acid-sensitive NEBI linker.

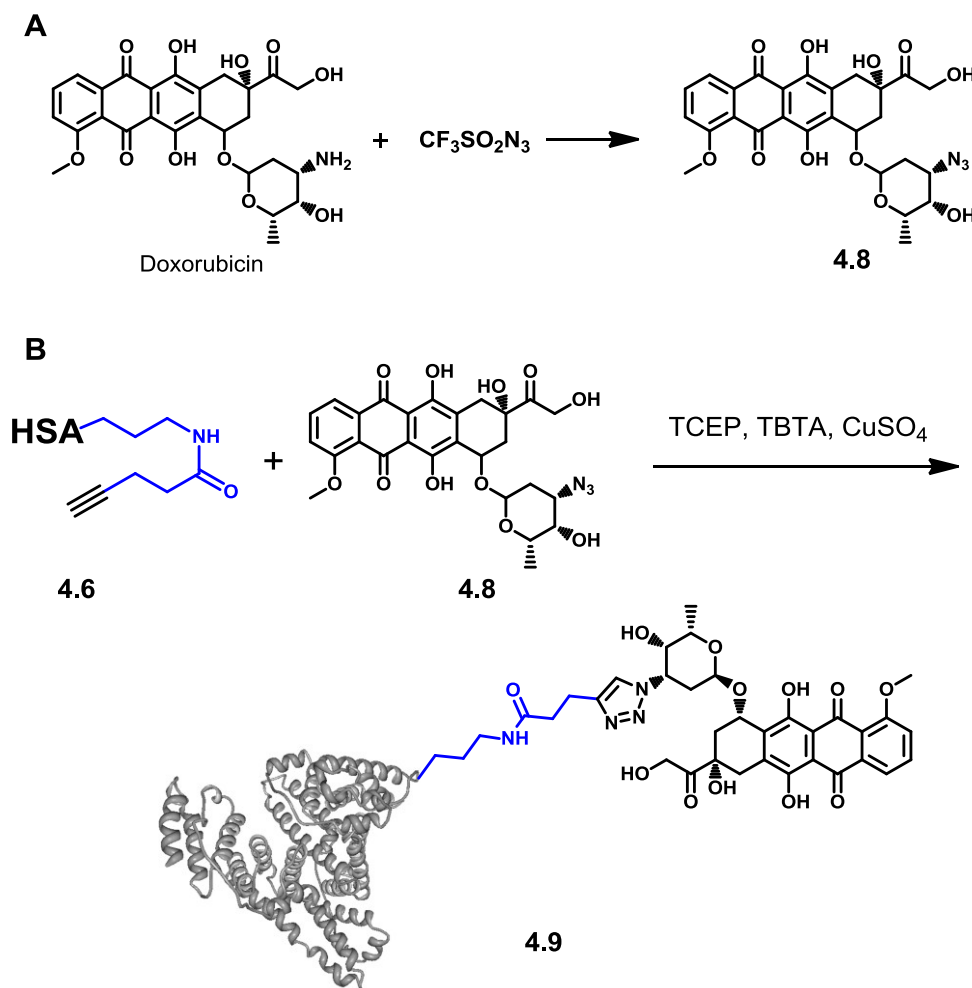


Figure 4.5 A) Synthetic scheme for azido-doxorubicin **4.8**. Reagents: potassium carbonate, copper sulfate, in DCM, MeOH. B) Synthetic scheme for **4.9**

4.4 Characterization of doxorubicin conjugates **4.7** and **4.9**

The Bradford assay¹⁰⁷ was used to determine the concentration of HSA in each sample. The extinction coefficient (ϵ) of doxorubicin in PBS pH 7.4 at $\lambda = 480$ nm was measured (3.37 mM^{-1}), and the Beer-Lambert Law¹⁰⁷ was used to determine the concentration of doxorubicin in the sample. This analysis afforded an estimate of ~ 1 doxorubicin molecule per HSA molecule in compound **4.7**. Similarly, this procedure afforded an estimate of ~ 1 doxorubicin molecule per HSA molecule in compound **4.9**.

Compounds **4.7** and **4.9** were also characterized by 4-20% SDS PAGE gel (Figure 4.2). The gel was analyzed for fluorescence using a Typhoon imager (Ex: 488nm, Em/bp: 580/30nm), followed by staining with Coomassie blue. Figure 4.6 shows an image of the SDS-PAGE gel by fluorescence analysis and by Coomassie blue staining for HSA, **4.7**, **4.9** and for crude samples from control reactions.

Lanes 5 and 6 in Figure 4.6 contained a mixture of compound **4.8** or **4.5** (respectively) with **4.6** that were reacted in the same manner as for the synthesis of **4.7** and **4.9**, but without the addition of the copper catalyst. The absence of fluorescence on the HSA resulting from these control reactions strongly supports that doxorubicin is covalently conjugated to HSA in **4.7** and **4.9**, presumably through the designed “click” reactions. Importantly, these control reactions demonstrate that the conditions used to synthesize and to purify **4.7** and **4.9** do not result in non-specific association of doxorubicin derivatives with HSA.

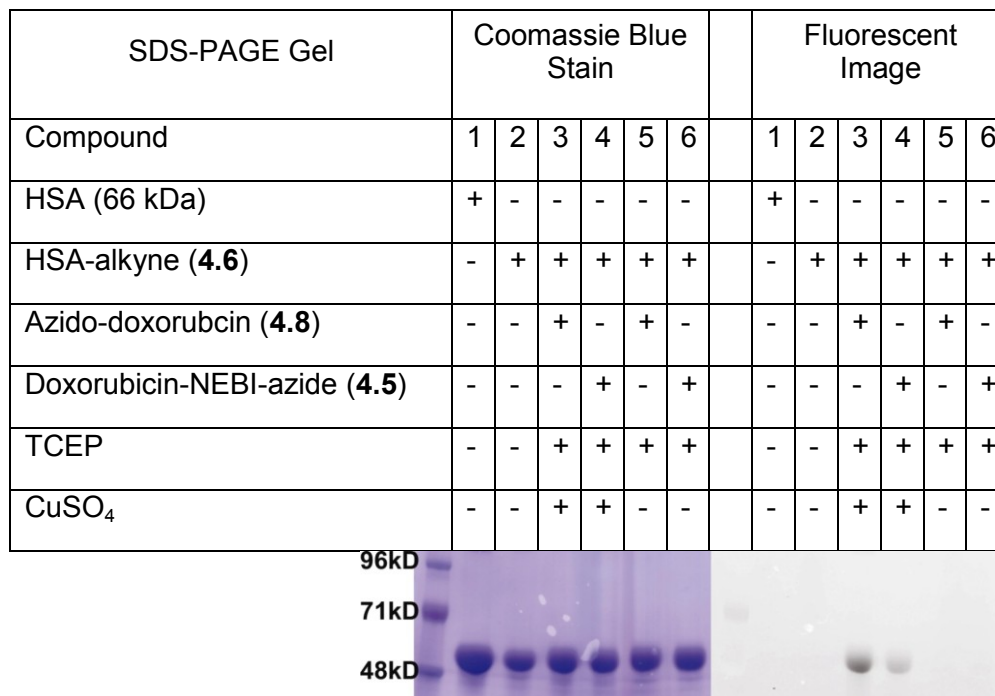


Figure 4.6. SDS-PAGE gel characterization of compounds 4.6, 4.7, 4.9. 4.6 is in lane 2. 4.5 is in lane 4. 4.9 is in lane 5. The gel was analyzed by Coomassie Blue staining (left) and fluorescence imaging (right). The legend indicates the components used to generate the protein species in each lane of the gel.

4.5 Colocalization studies of 4.7 in cells

To determine whether the conjugate **4.7** could internalize and localize within acidic compartments of cells, we examined the uptake and subcellular localization of **4.7** in human ovarian carcinoma 2008 cells. Figure 4.7 illustrates that incubation of cells with **4.7** (red) for 24 h resulted in significant cellular uptake. Subsequent treatment of these cells with LysoTracker Blue revealed the location of the lysosomes (blue regions in Figure 4.7C). Figure 4.7D shows that a significant fraction of **4.7** co-localized (green) with LysoTracker Blue in these cells, suggesting that **4.7** indeed localized primarily within the lysosomes of

these cells. This result is in agreement with previous reports for the uptake and subcellular localization of HSA in the lysosomes of cells.¹⁰² The Pearson coefficient for colocalization of LysoTracker Blue and **4.7** was calculated to be 0.71. Since these imaging studies confirm that conjugate **4.7** internalizes and localizes in acidic compartments of cancer cells, and since NEBI groups exhibit accelerated hydrolysis in mild acidic solutions,⁹² we hypothesized that incubation of these cells with **4.7** will result in intracellular release of doxorubicin analog **3.7**, resulting in reduced viability of the cells.

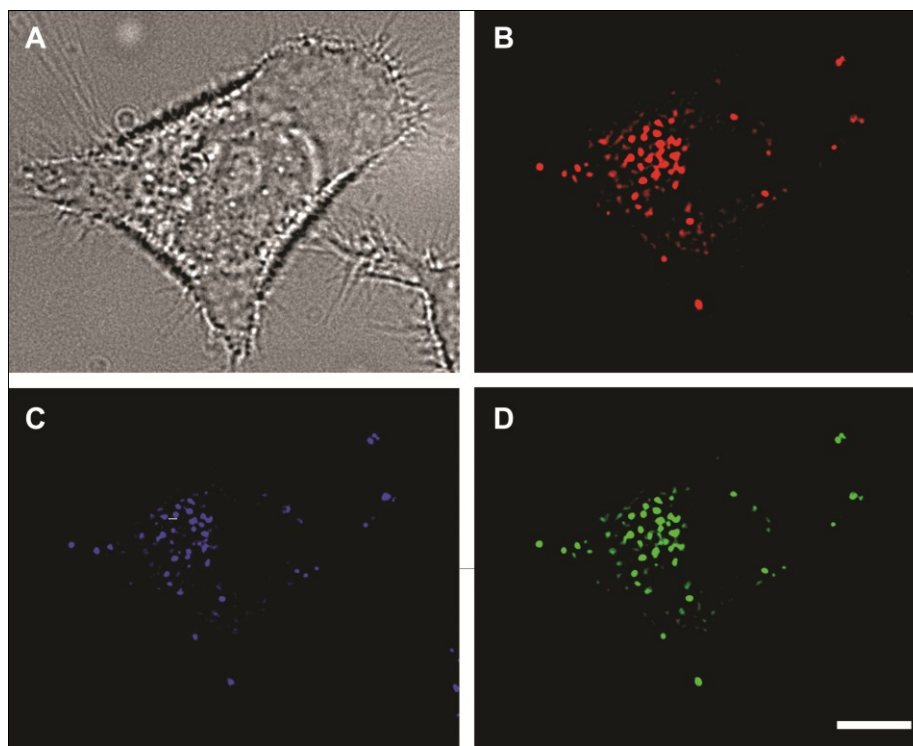


Figure 4.7 Fluorescence imaging studies for the internalization and localization of 4.7 in human ovarian carcinoma 2008 cells. A) Differential interference contrast image of a human ovarian carcinoma 2008 cell. B) Fluorescence micrograph from a z-slice through the cell showing the location of 4.7 (red) inside the cell. The subcellular distribution of 4.7 was determined by monitoring the intrinsic fluorescence of doxorubicin C) Fluorescence micrograph from the same z-slice through the cells as shown in (B), except showing only the location of the lysosomes, which were stained with Lyotracker blue. D) A merged fluorescence micrograph of (B) and (C) indicating areas of co-localization of 4.7 and the Lyotracker Blue. Scale bar = 5 μm .

4.6 Cytotoxicity studies of 4.7

In order to assess whether **4.7** indeed exhibits cytotoxic activity to cancer cells, we determined the viability of human ovarian carcinoma 2008 cells that were exposed to **4.7**. Indeed exposure of cells to increasing concentrations of **4.7** resulted in reduced cell viability with an IC_{50} of 1.6 μM (Figure 4.8). Figure 4.8A shows that conjugate **4.7** was ~ 4 times more cytotoxic than **3.7** alone (i.e., the

doxorubicin analog expected to accumulate in cells after hydrolysis of the NEBI group, $IC_{50} = 5.8 \mu\text{M}$, see Chapter 3). The HSA-NEBI-doxorubicin conjugate **4.7** was also 10 times more potent than HSA-doxorubicin conjugate **4.9** ($IC_{50} = 16 \mu\text{M}$), which lacked an acid-sensitive linker. We hypothesize that the observed weak toxicity of **4.9** arises from the natural degradation of HSA in the lysosomes, which results in the release of a small amount of some active derivatives of doxorubicin in the cell over the course of the 3 day incubation. These results from cytotoxicity experiments demonstrated that a drug conjugate comprising acid-sensitive NEBI linkers was more potent compared to a conjugate that did not comprise an acid-labile group (**4.9**) or compared to free **3.7** alone.

As expected, control experiments revealed that native HSA and HSA-alkyne (**4.6**, Figure 4.8B), were not toxic to cells within the same protein concentration range (Figure 4.8B). Cytotoxicity studies of 4-carboxybenzaldehyde (Figure 4.8C), showed no cytotoxicity up to $50 \mu\text{M}$, which is also beyond the range used for the cytotoxicity studies of **4.7** and **3.7**

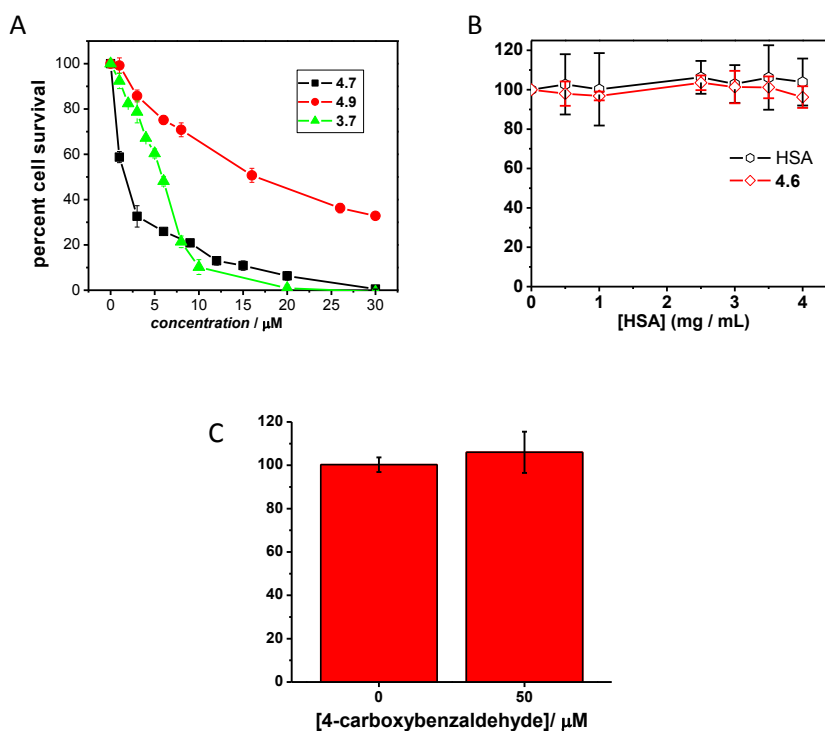


Figure 4.8 A) Cytotoxicity study of 4.7, 4.9 and 3.7, showed that conjugate 4.7 was the most cytotoxic of all the doxorubicin containing compounds. B) Control studies showed that HSA and HSA-alkyne (4.6) did not contribute towards the cytotoxicity found in compounds 4.7 and 4.9 in A. C) Comparison of the viability of human ovarian carcinoma 2008 cells with or without exposure to a 50 μM concentration of 4-carboxybenzaldehyde.

4.7 Cellular uptake studies of 4.7 vs 3.7

We hypothesized that the observed improved toxicity of **4.7** compared to free **3.7** was due to the capability of **4.7** to exhibit improved uptake of doxorubicin in the cells through an HSA-mediated, pinocytotic process.¹⁰⁸ To support this hypothesis, we incubated the human ovarian carcinoma 2008 cells with conjugate **4.7** (or doxorubicin analog **3.7** (with an equal concentration of total doxorubicin in both experiments). After 3 h, the cells were washed to remove excess extracellular molecule **4.7** or **3.7** and the cells were examined for the uptake of doxorubicin by

deconvolution microscopy (Figures 4.9A and 4.9B). This analysis revealed that cells incubated with conjugate **4.7** had an average of ~ 5.5 times the amount of doxorubicin within the cells compared to cells incubated with molecule **3.7** (Figure 4.9C). This increased uptake of doxorubicin conjugated with HSA via the NEBI linker correlated well with the observed increased toxicity of conjugate **4.7** compared to doxorubicin analog **3.7** (Figure 4.8A).

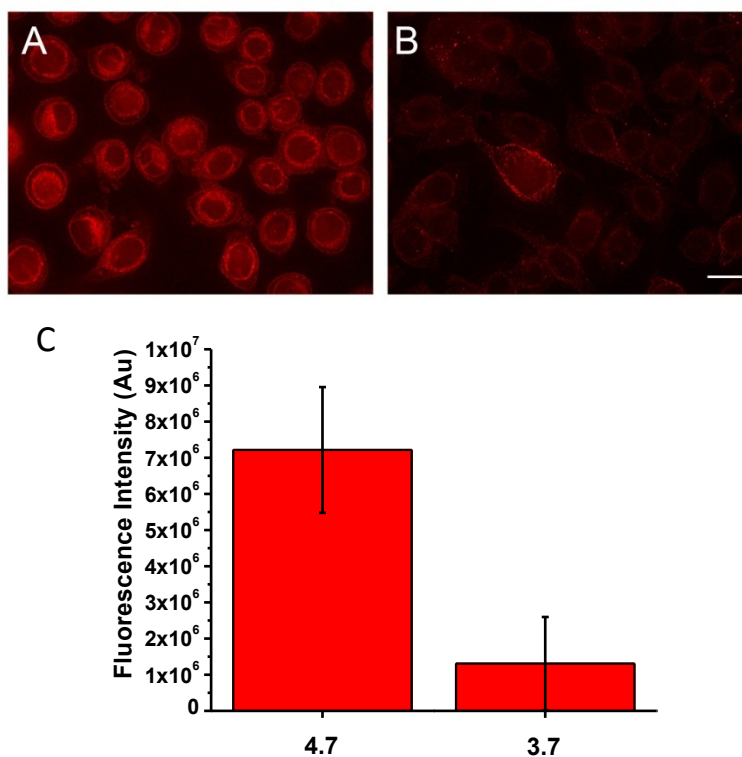


Figure 4.9 Analysis of the uptake of 4.7 and 3.7 by human ovarian carcinoma 2008 cells. A) and B) are micrographs of representative z-slices through cells that were incubated with molecule 4.7 (A) or molecule 3.7 (B) for 3 h. Here, the intrinsic fluorescence of doxorubicin is shown in red. Scale bar = 15 μm . C) The bar graph indicates that there is approximately 5.5 times the amount of doxorubicin in the cells incubated with molecule 4.7 compared to cells incubated with molecule 3.7. Average total fluorescence per cell was determined from analysis of 10 cells in each sample image. Analysis of the data in (C) revealed a p -value of 3.2×10^{-9} .

4.8 Metabolism of 4.7

Additionally, to gain some insight for the origin of the observed toxicity from conjugate **4.7**, we incubated the human ovarian carcinoma 2008 cells with **4.7** for 72 h. The cell lysate was then analyzed by LC-MS. This analysis revealed a complex mixture of doxorubicin-derived species, with at least three known metabolites^{109, 110} of doxorubicin identified by LC-MS (Figure 4.10). These combined results support that conjugation of doxorubicin to an HSA carrier via the acid-sensitive NEBI crosslinker can result in improved uptake and toxicity compared to un-conjugated molecule, with cytotoxic activity originating from the release of active derivatives of doxorubicin in the cells.

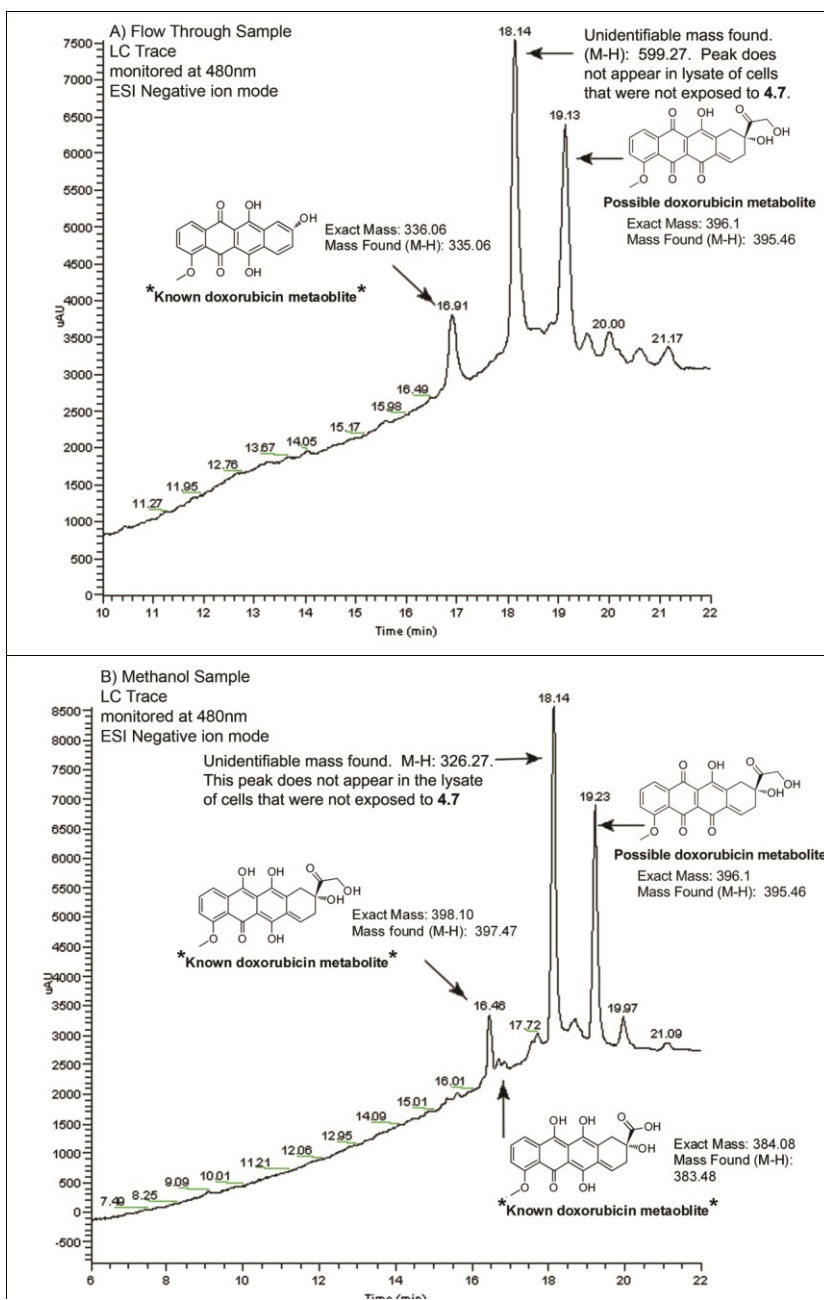


Figure 4.10 LC-MS analysis of the lysate of human ovarian carcinoma 2008 cells treated with 4.7. A) The LC trace of the flow through sample. B) The LC trace of the MeOH sample. The samples were monitored at 480 nm (the absorbance of doxorubicin) to highlight possible doxorubicin metabolites. ESI-Negative ion mode was used to determine the mass of the peaks observed at 480 nm.^{109, 110}

4.9 Conclusions

This work demonstrates that a new acid-sensitive, bifunctional NEBI crosslinker (**4.1**) can be employed for facile conjugation of macromolecules with small molecules. Here, I present one application for such an acid-sensitive crosslinker by demonstrating its use for conjugating an anticancer agent (**3.7**) to a protein-based drug carrier (here, HSA) as a proof-of-concept. The resulting DDS (**4.7**) exhibited improved cellular uptake and cytotoxic activity in cancer cells compared to free molecule **3.7** alone. Conjugate **4.7** also exhibited 10-fold improved cytotoxic activity compared to a conjugate that did not comprise an acid-labile group (**4.9**), supporting that the cleavable, acid-sensitive NEBI group can have a strong influence on the potency of therapeutics conjugated to HSA. Although several factors may contribute to the observed cytotoxic activity of **4.7** in human ovarian carcinoma 2008 cells (Figure 4.8A), the results presented here strongly support that the activity of **4.7** is likely due to the accelerated hydrolysis of the NEBI crosslinker upon uptake and intracellular localization of **4.7** in the acidic lysosomes of cancer cells.

Bifunctional crosslinkers based on NEBI groups such as **4.1** possess several attractive features as a tool for generating acid-responsive materials. For instance, they afford facile methods to attach a broad range of amine- and alcohol-containing molecules to macromolecules through standard amide or ester bond-forming reactions.¹¹¹⁻¹¹⁶ Additionally, the ability to incorporate functional groups on NEBI crosslinkers with orthogonal reactivity to amide or ester bond-forming reactions (e.g., alkyne or azide functional groups for “click” reactions) facilitates conjugation of small molecules to a range of natural and synthetic macromolecules. These

bifunctional NEBI crosslinkers are attractive since they are synthetically accessible from readily available and cheap starting materials. These advantageous features make it possible, for instance, to rapidly synthesize a range of DDSs carrying a variety of therapeutic agents that can be released from drug delivery carriers at controlled rates within acidic compartments of targeted cells.

Notes about the chapter:

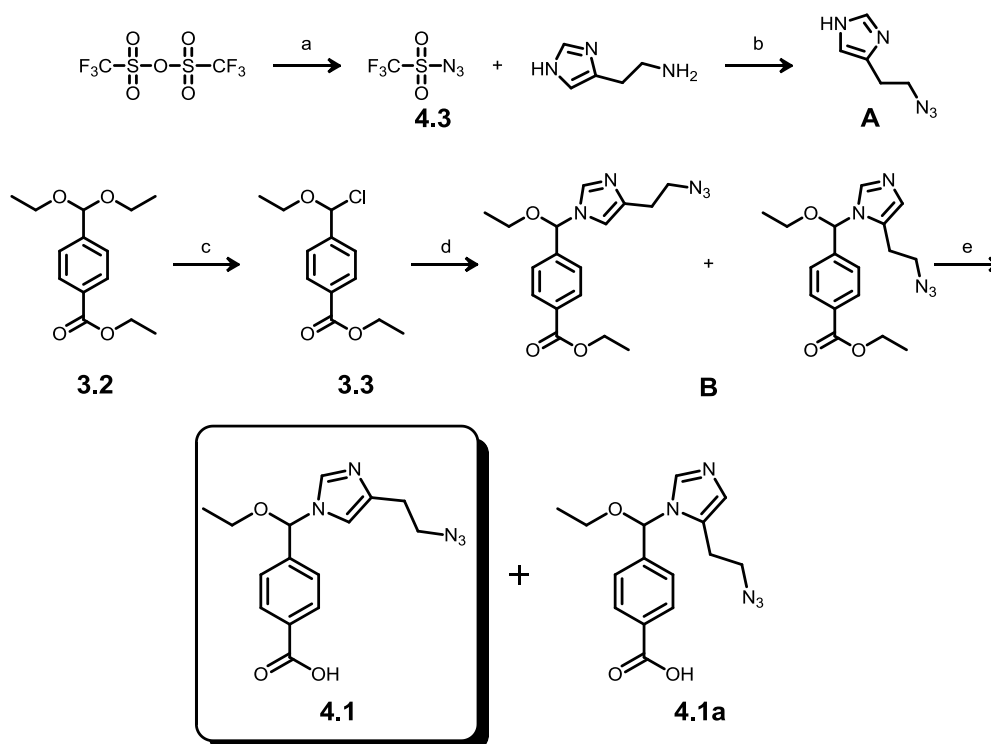
A large portion of this chapter was taken from a published reference,¹⁰⁰ pH-Sensitive, *N*-ethoxybenzylimidazole (NEBI) bifunctional crosslinkers enable triggered release of therapeutics from drug delivery carriers, that appears in *Organic and Biomolecular Chemistry* 2010. Alice Luong, Tawny Issarapanichkit, Seong Deok Kong, Rina Fong and Jerry Yang, Royal Publishing Society, 2010. The dissertation author was the primary investigator and author of this paper. The figures from this publication are reproduced by permission of The Royal Society of Chemistry. <http://pubs.rsc.org/en/Content/ArticleLanding/2010/OB/c0ob00228c>

I would like to thank my intern, Tawny Issarapanickit, for her many hours of work towards synthesis of starting materials. Kersi Pestonjamas from the UCSD Microscopy Facility was instrumental in training me to use the fluorescent microscopes and in obtaining fluorescent images. I would also like to acknowledge Dr. Yongxuan Su at the UCSD Department of Chemistry and Biochemistry Small Molecular Mass Spectrometry facility for his help with identifying doxorubicin metabolites through LC-MS. I would also like to thank Prof. Jerry Yang for directing the research and his patience with me while preparing this manuscript.

4.10 Experimentals

All reagents were purchased from Sigma-Aldrich, Inc., TCI, or Alfa Aesar and used without further purification. Doxorubicin (aka Adriamycin) was from Bedford Laboratories. NMR spectra were recorded on a Varian 400 (FT, 400 MHz, ^1H ; 100 MHz, ^{13}C) and Joel ECA-500 (FT, 500MHz ^1H) spectrometer. HR-MS (high-resolution mass spectra) were obtained in the Department of Chemistry & Biochemistry, University of California, San Diego using a ThermoFinnigan MAT900XL-MS. ESI-MS (electrospray ionization mass spectra) were obtained using ThermoFinnigan LCQDECA-MS. Kinetic analysis by reverse-phase high performance liquid chromatography (RP-HPLC) was performed with an Agilent 1100 Series HPLC using an analytical reverse-phase column (SPHERI-5 Phenyl 5 micron, 250 x 4.6 mm). Purification of HSA conjugates were performed with an Atka Purifier 10 using a HiLoad 16/60 superdex 200 prep grade column.

Synthesis of 4.1



Synthesis of triflyl azide (4.3)

Triflyl azide was prepared following the procedure reported by Pelletier and coworkers.¹¹⁷ A solution of sodium azide (7.12 g, 110 mmol) was dissolved in distilled H₂O (18 mL) with dichloromethane (DCM, 30 mL) and cooled in an ice bath. Triflyl anhydride (3.7 mL, 20.6 mmol) was added slowly over 20 minutes with vigorous stirring continued for an additional two hours. The mixture was placed in a separatory funnel and the organic phase removed. The aqueous portion was extracted with DCM (2 × 30 mL). The organic fractions containing the triflyl azide (4.3), were pooled and washed once with saturated sodium carbonate and used without further purification.

Synthesis of A

Histamine•2HCl (2.0 g, 11.2 mmol), potassium carbonate (2.31 g, 16.7 mmol), and CuSO₄•pentahydrate (28 mg, 111 μmol) were dissolved in distilled H₂O (15 mL, pH adjusted to 8.3) and MeOH (30 mL). The **4.3** in DCM (90 mL) was added and the mixture was stirred at ambient temperature overnight. The mixture was washed 3 times with EtOAc. The organic layers were pooled and dried over sodium sulfate, and solvent was removed under reduced pressure. Compound **A** was isolated by silica chromatography using as eluent a 96:4:2 mixture of DCM:MeOH:TEA. The isolated yield of compound **A** was 94%. Characterization of **A**: ¹H NMR (CDCl₃, 400 MHz) δ 2.904 (t, 2H), 3.587 (t, 2H), 6.899 (s, 1H), 7.630 (s, 1H) ESI-MS (*m/z*, M+H⁺): 137.99

Synthesis of **B**

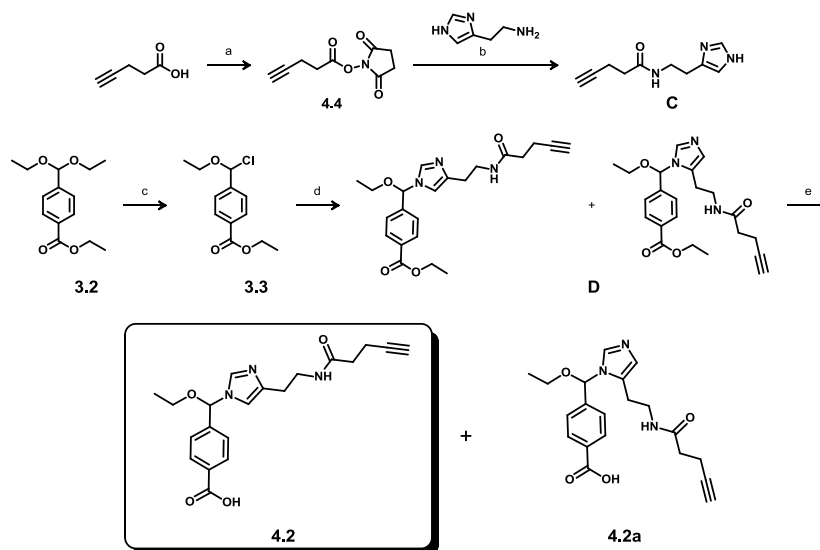
The synthesis of **3.2** was described in previous work by Kong et al. and Chapter 3.⁹² Compound **3.2** (555 mg, 2.2 mmol), freshly distilled acetyl chloride (250 μL, 3.52 mmol) and thionyl chloride (52 μL, 440 μmol) were combined without additional solvent and refluxed for 1 hour at 65 °C under N₂. The excess thionyl chloride and acetyl chloride were removed under reduced pressure and the crude mixture was characterized by ¹H NMR. ¹H-NMR (in CDCl₃) indicated a new peak at 6.203 ppm, presumably corresponding to the benzylic H in **3.3**. The crude yield of **3.3** by ¹H-NMR was ~54%, with the remainder of the material identified as starting material **3.2** (~8%) as well as a large amount (~38%) of ethyl 4-formylbenzoate. The crude material was immediately taken on to the next step without further purification.

In a separate dry flask, NaH (2.86 mmol) was added to a solution of **A** (300 mg, 2.2 mmol) dissolved in dry THF. The solution was allowed to stir for 1 hour at 23 °C, and then the crude mixture of **3.3** was added dropwise to the **A**/NaH. The combined solution was stirred for 12 h at 23 °C. Saturated sodium carbonate was added to the solution and washed 3 times with DCM. The organic layers were pooled and dried over sodium sulfate. The solvent was removed under reduced pressure. The product was isolated by silica chromatography using as eluent a 97:2:1 mixture of DCM:MeOH:TEA. This procedure produced a ~ 1:1 mixture of isomers (with respect to the nitrogens on the imidazole moiety) in 36% isolated yield over two steps. Although the desired isomers could be resolved and purified by chromatography for characterization by ¹H NMR, ¹³C NMR and HR-MS, we used this mixture of isomers for the synthesis of **B** since using this mixture significantly simplified the synthesis and purification of the conjugates and since separating these isomers was not expected to affect the results of the described fluorescence imaging and cytotoxicity studies. Characterization of **B**: ¹H NMR (CDCl₃, 400 MHz) δ 1.296 (t, 3H), 1.390 (t, 3H), 2.849 (t, 2H), 3.570 (m, 4H), 4.388 (q, 2H), 6.198 (s, 1H), 6.773 (s, 1H), 7.426 (d, 2H), 7.758 (s, 1H), 8.056 (d, 2H). ¹³C NMR (CDCl₃, 100 MHz) δ 14.268, 14.708, 28.415, 50.647, 61.146, 64.635, 86.383, 114.358, 125.942, 129.824, 131.118, 136.295, 139.944, 142.295, 165.977. HR-ESI-FT-MS calcd (*m/z*): 344.1717; found: 344.1721. Inspection by NOESY indicated a correlated peak between the benzylic hydrogen and the hydrogen on C-5 of the imidazole moiety, confirming the probable identity of isomer **B** with respect to the two nitrogens on the imidazole group.

Synthesis of **4.1**

Compound **B** (6.6 mg, 9.7 μmol) was dissolved in 200 μL of THF and 100 μL of distilled H_2O . A solution of LiOH (10.0 μL of a 1M solution). The solvent was removed under reduced pressure. The crude was taken up in 10% MeOH and DCM, and filtered. The solvent was then removed under reduced pressure to give **4.1** in 81% isolated yield. Characterization of **4.1**: ^1H NMR (CD_3OD , 400 MHz) δ 1.230 (t, 3H), 2.762 (t, 2H), 3.271 (t, 2H), 3.447 (t, 2H), 6.374 (s, 1H), 6.937 (s, 1H), 7.331 (d, 2H), 7.825 (s, 1H), 7.893 (d, 2H) ^{13}C NMR (CD_3OD , 100 MHz) δ 15.400, 29.242, 52.066, 65.785, 88.265, 116.293, 126.698, 130.701, 138.113, 140.033, 140.452, 141.687, 174.975. HR-ESI-FT-MS (m/z) calcd: 316.1404; found: 316.1410.

Synthesis of 4.2



Synthesis of 4.4

A solution of pent-4-ynoic acid (10.1 mmol, 1 g), 1-Ethyl-3-(3-dimethylaminopropyl) carbodiimide (EDC, 12.2 mmol, 2.34 g), *N*-hydroxysuccinimide (12.2 mmol, 1.41 g) was stirred at room temperature in 100 mL of dry DCM for 24 h. Saturated Sodium carbonate was added to the solution, and washed 3 times with DCM. The organic layers were pooled, dried over sodium sulfate and solvent removed under reduced pressure to give a 76% crude yield of compound 4.4. The crude sample was used in subsequent reaction with HSA without further purification. Characterization of 4.4: ^1H NMR (CDCl_3 , 400 MHz) δ 2.049 (t, 1H), 2.621 (m, 2H), 2.848-2.903 (m, 6H).

Synthesis of C

A solution of 4.4 (20 mmol in dioxane) was added dropwise to a solution of Histamine \cdot 2HCl (3 g, 0.1M HEPES buffer, pH 8.3). The reaction was monitored by

a pH meter, and kept at pH 8.3 by addition of 0.01M NaOH. The solution was stirred for another hour after all of **4.4** was added. Compound **C** was purified using a mixture of 1:8:91 ammonium hydroxide:MeOH:DCM. Yield: 70%. Characterization of **C**: ^1H NMR (CD_3OD , 400 MHz) δ 2.37 (m, 2H), 2.44 (m, 2H), 2.77 (m, 2H), 3.42 (m, 3H), 6.85 (s, 1H), 7.89 (s, 1H) ESI-MS (m/z , $\text{M}+\text{H}^+$): 192.10

Synthesis of **3.3**

The synthesis of **3.2** was described in previous work by Kong et al. and Chapter 3¹¹⁸ Compound **3.2** (171 mg, .68 mmol), freshly distilled acetyl chloride (77 μL) and thionyl chloride (10 μL) were combined without additional solvent and refluxed for 1 hour at 65°C under N_2 .

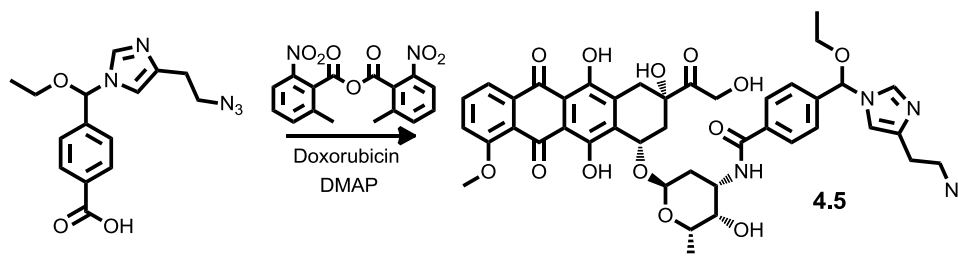
Synthesis of **D**

In a separate dry flask, NaH (2.86 mmol) was added to a solution of **C** (300 mg, 2.2 mmol) dissolved in dry DMSO. The solution was allowed to stir for 1 hour at 23 °C, and then the crude mixture of **3.3** was added dropwise to the **C**/NaH. The combined solution was stirred for 12 h at 23 °C. Saturated sodium carbonate was added to the solution and washed 3 times with DCM. The organic layers were pooled and dried over sodium sulfate. The solvent was removed under reduced pressure. The product was isolated by silica chromatography using as eluent a 97:2:1 mixture of DCM:MeOH:TEA. Yield: 21% Characterization of **D**: ^1H NMR (CDCl_3 , 400 MHz) δ 1.29 (t, 2H), 1.38 (t, 3H), 2.36 (d, 2H), 2.39 (m, 2H), 2.61 (t, 2H), 3.52 (m, 5H), 4.36 (m, 2H), 6.15 (s, 1H), 6.71 (s, 1H), 7.39 (d, 2H), 7.60 (s, 1H), 8.05 (d, 2H) ESI-MS (m/z , $\text{M}+\text{H}^+$) = 397.47

Synthesis of 4.2

Compound **D** (11.8 mg) was dissolved in a solution of THF/H₂O. A solution of LiOH (32.7 μ L of a 1M solution) was added and allowed to stir for 12 h. The solvent was removed under reduced pressure, and the crude product was dissolved in 10% MeOH and DCM. The solvent was then removed under reduced pressure. Yield: 92%. Characterization of **4.2**: ¹H NMR (CD₃OD, 400 MHz) δ 1.26 (t, 3H), 2.31 (m, 2H), 2.40 (m, 2H), 2.71 (t, 2H), 3.35 (s, 1H), 3.40 (t, 2H), 3.48-3.69 (m, 2H), 6.39 (s, 1H), 6.91 (s, 1H), 7.36 (d, 2H), 7.82 (s, 1H), 7.93 (d, 2H) ESI-MS (*m/z*, M+H⁺) = 371.02

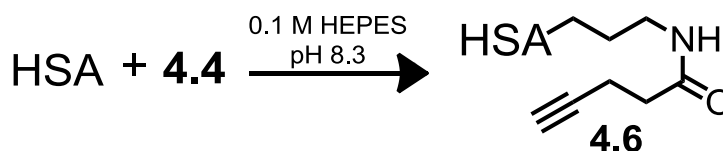
Synthesis of 4.5



A solution of **4.1** (3.0 mg, 9.5 μ mol), 2-Methyl-6-nitrobenzoic anhydride (2.9 mg, 8.6 μ mol), Dimethylaminopyridine (DMAP, 1 crystal) in DMF was stirred for 2 h at 23 °C. Doxorubicin•HCl (5 mg, 8.6 μ mol) dissolved in 1 mL DMF was added to the solution and allowed to stir for an additional 12 h. The DMF was removed under reduced pressure. The product was isolated by silica column chromatography using as eluent 96:3:1 mixture of DCM:MeOH:TEA. The isolated yield of **E** was 44%. Characterization of **4.5**: ¹H NMR (CDCl₃, 500 MHz) δ 1.270 (t, 3H), 1.305/1.318 (d, 3H), 1.968 (s, 1H), 2.014 (s, 1H), 2.171 (d, 1H), 2.179 (d, 1H), 2.814 (t, 2H), 3.309

(m, 2H), 3.526 (t, 2H), 3.566 (m, 2H), 3.746 (s, 1H), 4.078 (s, 3H), 4.221 (m, 1H), 4.369 (t, 1H), 4.781 (s, 2 H), 5.321 (s, 1H), 5.549 (s, 1H), 6.131 (s, 1H), 6.730 (s, 1H), 7.359 (m, 3H), 7.622 (s, 1H), 7.726 (d, 2H), 7.794 (t, 1H), 8.042 (d, 1H). HR-MS (m/z) calcd: 841.3039; found: 841.3054.

Synthesis of HSA-alkyne 4.6



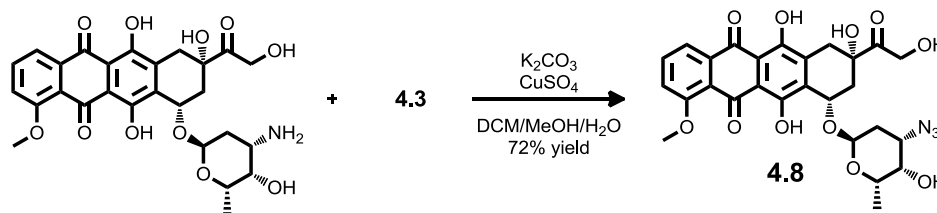
Human serum albumin (HSA, 200 mg, 3 μ mol) was dissolved in 12 mL of 0.1 M HEPES buffer, pH 8.3. Compound 4.4 (300 μ mol) was dissolved in 1 mL of DMSO and added to the HSA solution dropwise at 23 $^{\circ}$ C. The reaction was monitored on a pH meter. Aliquots of 0.1M NaOH were used to maintain a pH of 8.3 over the course of the reaction of HSA with 4.4. After complete addition of 4.4, the reaction was allowed to stir for an additional 1 hour at 23 $^{\circ}$ C. Compound 4.6 was exchanged into phosphate buffered saline (PBS, pH 8.0) using Amicon ultra centrifugal filter devices (30kD MW cut off, catalog number: UFC903024).

Synthesis of HSA-NEBI-doxorubicin (4.7)

The click reaction was performed following the general procedure previously reported by Speers, et. al.¹⁰⁶ A solution containing 43 mL of a 1.5 mg/mL solution of 4.6 in PBS (pH 8.0) was combined with 1 mL of a 2.5 mM solution of 4.5 in DMSO at 23 $^{\circ}$ C. The solution was vortexed for 5 seconds. A solution of freshly made tris(2-carboxyethyl)phosphine (TCEP, 1 mL, 50 mM) and tris-

(benzyltriazolylmethyl)amine (TBTA) in 1:4 DMSO:t-BuOH (3.0 mL, 1.7 mM) were added to the solution containing **4.5** and **4.6**, and vortexed for 5 seconds. A solution of CuSO_4 in water (1 mL, 50 mM) was added and the solution was vortex again for 5 seconds. The reaction was stirred for 1 hour at ambient temperature. The solution was exchanged into PBS pH 7.4 using Amicon Ultra Centrifugal Filter devices (30kD MW cut off). Compound **4.7** was purified by FPLC using a superdex 200 prep grade column with PBS at pH 7.4 with a flow rate of 1 mL min^{-1} . The retention time was 40-50 minutes.

Synthesis of Azido-doxorubicin (**4.8**)



Triflyl azide was prepared following the procedure reported by Pelletier and coworkers.¹¹⁷ A solution of sodium azide (1.78 g, 27.5 mmol) was dissolved in distilled H_2O (4.5 mL) with DCM (7.5 mL) and cooled in an ice bath. Triflyl anhydride **4.3** (0.9 mL, 5.55 mmol) was added slowly over 5 minutes with stirring continued for an additional 2 h at 23 °C. The mixture was placed in a separatory funnel and the organic phase removed. The aqueous portion was extracted with DCM ($2 \times 3.75 \text{ mL}$). The organic fractions containing the triflyl azide, were pooled and washed once with saturated sodium carbonate and used without further purification. The total volume of triflyl azide in DCM was $\sim 15 \text{ mL}$. Triflyl azide (150 μL in DCM solution) was added to a solution containing doxorubicin•HCl (8.62 μmol), CuSO_4 (86 nmol), and potassium carbonate (12.9 μmol) in a 1:1:1 mixture of

DCM:H₂O:MeOH. The solution was stirred for 12 h at ambient temperature. The solvent was removed under reduced pressure and **4.8** was purified over silica using as eluent 97:3 DCM:MeOH. The yield of **4.8** was 20%. Characterization of **4.8**: ¹H NMR (CDCl₃, 500 MHz) δ 1.343 (d, 3H), 1.928 (m, 1H), 2.109 (m, 1H), 2.202 (m, 1H), 2.331 (d, 1H), 3.078 (d, 1H), 3.286 (d,d 1H), 3.591 (m, 1H), 3.735 (s, 1H), 4.035 (d, 1H), 4.098 (s, 3H), 4.753 (s, 2H), 5.330 (m, 1H), 5.593 (d, 1H), 7.419 (d, 1H), 7.802 (t, 1H), 8.042 (d, 1H). HR-ESI-FT-MS: calcd (*m/z*, M+Na⁺): 592.1547; found = 592.1538.

Compound **4.8** was also evaluated for cytotoxic activity against human ovarian carcinoma 2008 cells using a standard SRB assay as described in the main text. These studies revealed that compound **4.8** reduced the viability of the cells with an IC₅₀ of 80 nM.

Synthesis of HSA-doxorubicin conjugate (4.9)

The click reaction was performed following the general procedure previously reported by Speers, et. al.¹⁰⁶ A solution containing 43 mL of a 1.5 mg/mL solution of HSA-alkyne (**4.6**) in PBS (pH 8.0) was combined with 1 mL of a 2.5 mM solution of doxorubicin-azide **4.8** in DMSO. The solution was vortexed for 5 seconds. A solution of freshly made TCEP (1 mL, 50 mM) and TBTA in 1:4 DMSO:t-BuOH (3.0 mL, 1.7 mM) were added to the solution containing **4.6** and **4.8** and vortexed for 5 seconds. A solution of CuSO₄ in water (1 mL, 50 mM) was added and the solution was vortex again for 5 seconds. The reaction was stirred for 1 hour at ambient temperature. The solution was exchanged into PBS pH 7.4 using Amicon Ultra Centrifugal Filter devices (30kD MW cutoff). Compound **4.9** was purified by FPLC

using a superdex 200 prep grade column with PBS at pH 7.4 with a flow rate of 1 mL min⁻¹; the retention time was 40-50 minutes.

Fluorescence Cellular Imaging Studies

Human ovarian carcinoma 2008 cells were plated with RPMI-1640, (Invitrogen 11835-030) phenol red free media supplemented with 10% FBS (Omega Scientific, FB-01) on 35 mm glass bottom dishes (MatTek Co., Ashland, MA) and incubated overnight. HSA-NEBI-doxorubicin (**4.7**) was added to the cells to give a final concentration of 10 μ M of **4.7** and allowed to incubate for 24 h. LysoTracker Blue (Invitrogen, L7525) was added to the cells and incubated for 30 minutes. The remaining living cells were washed three times with phenol red free RPMI-1640 media without FBS and then immediately imaged with a Delta Vision Deconvolution Microscope System (Applied Precision, Issaquah, WA) equipped with a Nikon TE-200 inverted light microscope with infinity corrected lenses and with a mercury arc lamp as the illumination source. The co-localization was determined using softWoRx image analysis software (Applied Precision, Issaquah, WA).

The intrinsic fluorescence of doxorubicin (Abs/Em: 480/550, 585 nm) was used to visualize the location of **4.7** and was observed by excitation with bandpass (bp) filtered light (Ex/bp: 490/20nm) and the emission monitored at Em/bp: 617/53 nm. The fluorescence of the LysoTracker Blue (Abs/Em: 373/422 nm) was detected using an Ex/bp: 360/40 nm excitation filter and an Em/bp: 457/50 nm emission filter.

In order to provide a quantifiable value for the co-localization of LysoTracker Blue and **4.7**, we determined the extent of overlap of the fluorescence of

Lysotracker Blue and **4.7**. This imaging analysis afforded a Pearson's correlation coefficient¹¹⁹ of 0.71.

Cytotoxicity Studies

Human ovarian carcinoma 2008 cells were plated into each well of a 96 well plate (3000 cells/well) using RPMI-1640 media with 10% FBS. The cells were incubated for 24 h at 37°C with 5% CO₂. After the incubation period, cells were dosed with various concentrations of HSA, **3.7**, **4.6**, **4.7**, **4.9**, or 4-carboxybenzaldehyde. The cells were allowed to incubate for 72 h. After incubation, cells were washed 3 times with 200 µL of PBS (Mediatech, 46-013CM) pH 7.4. Cells were then fixed with 200 µL of PBS and 50 µL of 50% trichloroacetic acid for one hour at 4°C. After fixation, cells were washed 5 times with 200 µL of water and allowed to dry. A 0.4% sulforhodamine B (SRB, Sigma Aldrich, S1402) solution in 1% acetic acid was added to the cells and incubated for 15 minutes at room temperature. The cells were washed 3 times with 200 µL 1% acetic acid and the 96 well plate was allowed to dry. Tris base solution (10 mM, 200 µL) was added to the wells for 15 minutes prior to measuring the absorbance at 515 nm.

HSA-NEBI-doxorubicin (4.7) Cell Uptake Studies

Human ovarian carcinoma 2008 cells were plated with RPMI-1640, phenol red free media supplemented with 10% FBS on 35 mm glass bottom dishes and incubated overnight. HSA-NEBI-doxorubicin (**4.7**) and doxorubicin analog (**3.7**) were incubated with cells for 3 h. The final concentration of doxorubicin in the samples was 20 µM. The cells were washed three times with media to remove excess molecules and then immediately imaged with a Delta Vision Deconvolution

Microscope System (Applied Precision, Issaquah, WA) equipped with a Nikon TE-200 inverted light microscope with infinity corrected lenses and with a mercury arc lamp as the illumination source. Doxorubicin was observed by excitation with bandpass (bp) filtered light (Ex/bp: 490/20nm) and the emission monitored at Em/bp: 617/53 nm. The average fluorescence intensity per cell was determined using softWoRx image analysis software (Applied Precision, Issaquah, WA).

LC-MS analysis of the breakdown of HSA-NEBI-doxorubicin (4.7) in cells

Human ovarian carcinoma 2008 cells were plated into 60 mm x 15 mm tissue culture treated dishes with RPMI-1640 phenol red free media with 10% FBS. The cells were incubated at 37 °C with 5% CO₂ until ~ 80% confluent. HSA-NEBI-doxorubicin (**4.7**) was added to the cells and allowed to incubate for 3 days. After 3 days, the cells were lysed with 0.1% triton X in PBS solution. The media and PBS was combined and run through a Supelclean™ Hisep™ SPE Tube. The flow through was collected. Additionally, we subsequently eluted the Hisep SPE Tube with MeOH. LC-MS was used to analyze both the flow through and MeOH samples. The LC was monitored at 480nm, the absorbance of doxorubicin, to highlight the chromatographic peaks that possibly contained doxorubicin-derived species^{110, 120}. The method used for elution was a gradient from 30% MeOH and 70% water to 70% MeOH and 30% water over 20 minutes with a flow rate of 1 ml min⁻¹ on a reverse phase column (Phenomenex Synergi Polar-RP LC column 4 micron, 150mm x 4.6mm). Negative ion mode The mass spectrometry data was obtained using ThermoFinnigan LCQDECA-MS in ESI-Negative ion mode.

Chapter 5

***Ortho-N*-ethoxybenzylimidazoles (o-NEBI): a two step hydrolysis for release of alcohol containing drugs**

5.1 Introduction

In Chapter 4, I described the development of an acid-sensitive bifunctional NEBI crosslinker (**4.1**) for use in a model DDS (**4.7**).¹⁰⁰ While characterization of conjugate **4.7** showed that the NEBI was useful in a model DDSs (**4.7**), the conjugate had an IC_{50} of 1.6 μ M, which was less potent than native doxorubicin (IC_{50} = 1.6 nM). This decrease in potency in conjugate **4.7** may be contributed to the release of doxorubicin analog **3.7** (IC_{50} = 5.8 μ M), rather than native doxorubicin from conjugate **4.7**. The goal of the research described in this chapter is to improve the NEBI linker by investigating methods to release native, unmodified chemotherapeutics from a DDS comprised of a NEBI linker. A NEBI linker that

could release free drug would be more preferred for two reasons: 1) a DDS releasing the free drug would be more potent, and 2) release of the free drug, which is already FDA approved, would not require extensive testing for FDA approval.

The design of this work was inspired by work previously performed by Bender *et. al.*¹²¹ which showed the accelerated hydrolysis of *ortho*-formylbenzoyl esters (Figure 5.1A). The rates of ester hydrolysis were dependent on the pH, with slowest rates at approximately pH 3-4. The rates of hydrolysis increased as the pH decreased from ~3 and increased from ~4.¹²² With this precedence, we hypothesized that a methyl ester in the *ortho* position to the NEBI (**5.1**) would undergo hydrolysis of the NEBI, followed by an assisted hydrolysis of *ortho*-formylbenzoyl ester (Figure 5.1B). The goal of this chapter is to develop a NEBI platform that can be used in a future DDS for the delivery of native unmodified chemotherapeutics (Figure 5.1C).

This chapter describes the synthesis and characterization of an *o*-NEBI that was designed to undergo two separate steps of hydrolysis. An *o*-NEBI conjugate with an alcohol containing chemotherapeutic, 5-fluoro-2'-deoxyuridine (5-FU), was constructed and characterized by hydrolysis and cytotoxicity studies.

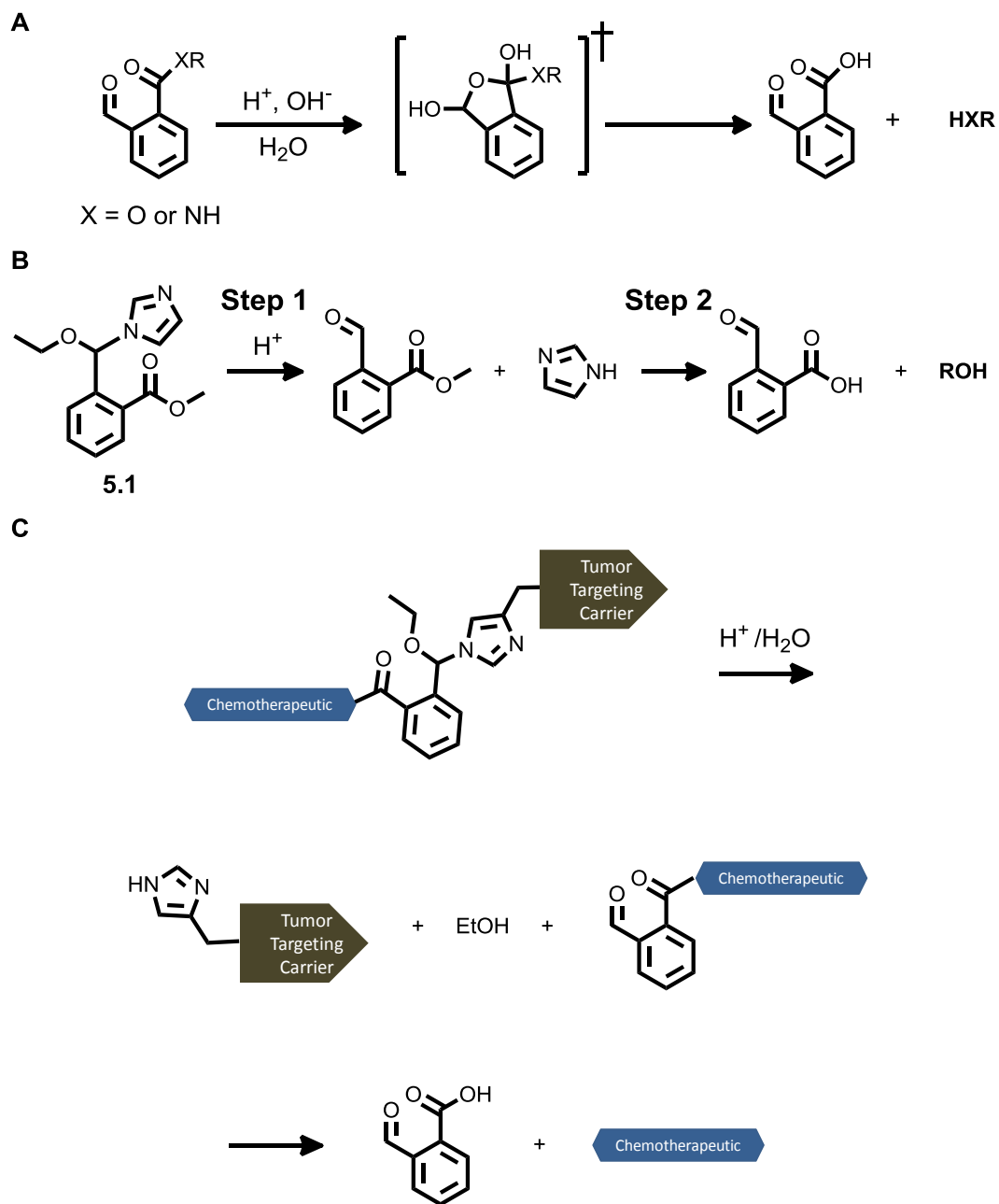


Figure 5.1 A) Assisted hydrolysis of *o*-formylbenzoates. B) The hypothesized hydrolysis of an *o*-NEBI methyl ester. C) Schematic of the goal for the new *o*-NEBI platform.

5.2 o-NEBI-methyl ester: proof-of-concept

To determine if an alcohol containing drug could be released in free form from an o-NEBI platform, I synthesized **5.1** according to Figure 5.2 as a proof-of-concept. The synthesis of the o-NEBI, **5.1**, started with 2-carboxybenzaldehyde and followed a synthesis scheme very similar to that of the original NEBI functional group in Chapter 3 and 4.

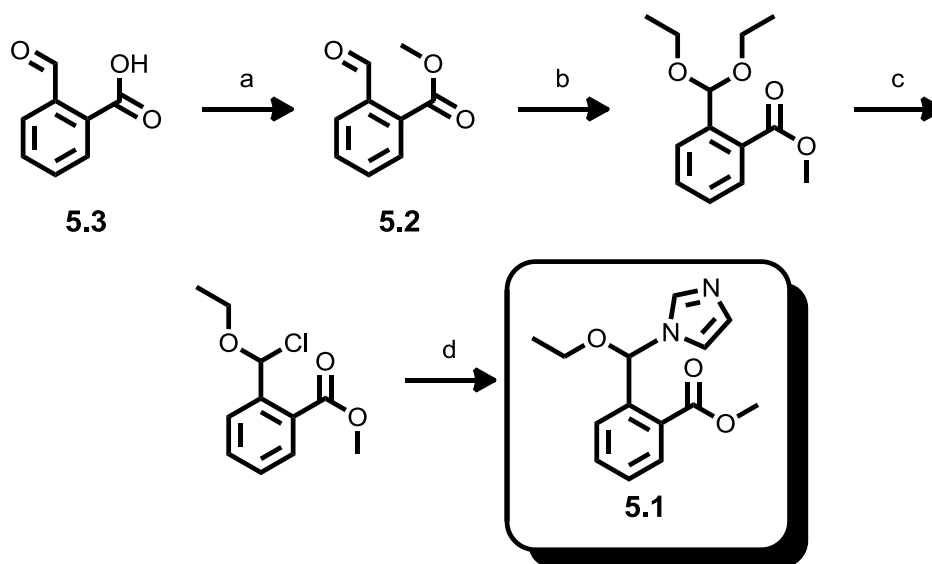


Figure 5.2 The synthetic scheme for o-NEBI carrying a methyl ester **5.1**. Reagents: a) MeI and potassium carbonate in DMF, 88% yield b) ethylorthoformate, EtOH, and TsOH, 76% yield c) acetyl chloride, thionyl chloride d) imidazole, NaH, in THF, 28% yield over two steps

Compound **5.1** was incubated at 37 °C and monitored by HPLC at pH 5.5 and 7.4. Compound **5.1** underwent a two-step hydrolysis as hypothesized (Figure 5.3). At pH 5.5, compound **5.1** hydrolyzed into the o-formylbenzoyl methyl ester (**5.2**), which accumulated but continued to hydrolyze into 2-carboxybenzaldehyde (**5.3**) in a second step. At pH 7.4, I found that **5.1** converted cleanly to **5.3**, without accumulation of **5.2**. The hydrolysis of the **5.1**, continued to follow first order

kinetics (as described in Chapter 2) while incubated at 37 °C, with a half-lives of 78 h and 3600 h at pH 5.5 and 7.4 respectively for step one (Figure 5.3B). An individual study of the second step of hydrolysis, **5.2** to **5.3**, showed the half-life at pH 5.5 to be 130 h, but only 5.1 h at pH 7.4 while incubated at 37 °C (Figure 5.3C). This data showed that at pH 5.5, the hydrolysis of **5.2** to **5.3** was the rate-determining step for the formation of **5.3**, which is why **5.2** accumulated at pH 5.5. However, at pH 7.4, the hydrolysis of the NEBI functional group in step 1 was much slower ($t_{1/2} = 3600$ h) and therefore the rate-determining step for the formation of **5.3**, so we did not see the accumulation of **5.2** by HPLC. The increased rates of hydrolysis for the second step of hydrolysis at pH 7.4 were expected, as it was described previously by Bender *et. al.* Since step one was acid catalyzed, there was no concern that the hydrolysis of step two was faster at pH 7.4. This increased rate of hydrolysis of step two at pH 7.4 might actually be beneficial to the NEBI system in the context of drug delivery, if the aldehyde intermediate eventually escapes the endosomes and lysosomes into the cytosol, which has a pH of 7.2-7.4.

The hydrolysis of **5.1** to **5.2** and **5.3** proceeded cleanly without the buildup of any other intermediates as determined by HPLC. No other peaks formed during this hydrolysis on the HPLC trace. The concentrations were calculated by using Beer's Law and the absorption of the compounds on the HPLC trace (Figure 5.3D). The ester hydrolysis always followed the hydrolysis of the NEBI. These peaks were verified by LC-MS by Dr. Su at the mass spectrometry facility, and the retention times were also matched to the retention times of pure **5.2** (synthesized) and **5.3** (commercially available).

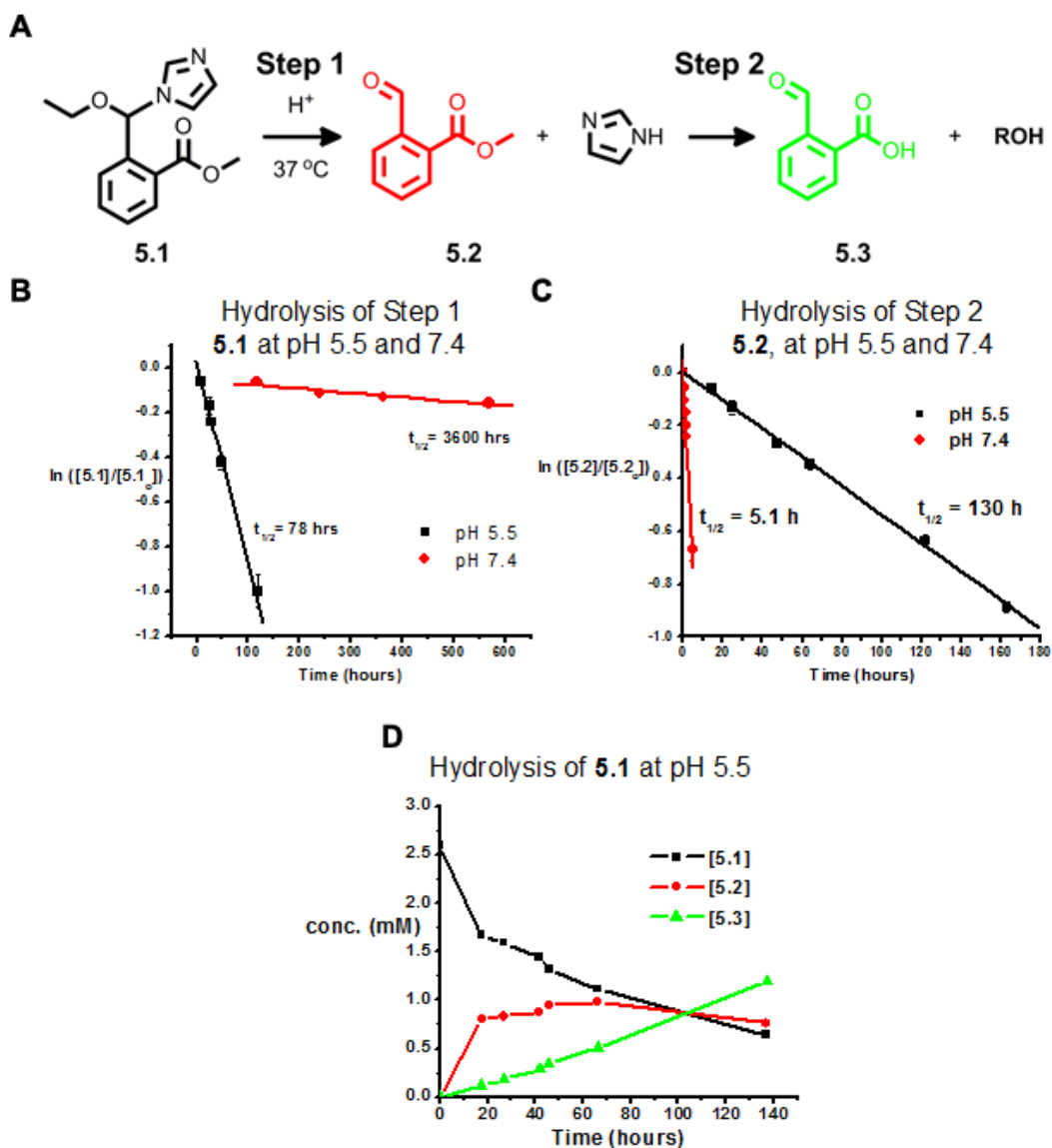
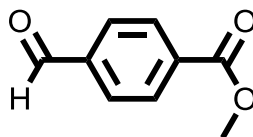


Figure 5.3 A) A schematic of the hydrolysis of **5.1** into **5.2** in step one, followed by the hydrolysis of **5.2** in step two to give **5.3**. B) Hydrolysis of **5.1** at pH 5.5 and 7.4 while incubated at 37 °C. C) Hydrolysis of **5.2**, step two, measured independently at pH 5.5 and 7.4 while incubated at 37 °C. D) The concentrations of **5.1**, **5.2** and **5.3** at pH 5.5 monitored over time by HPLC.

To verify that the hydrolysis of **5.2** was assisted by the aldehyde in the ortho position to the ester, I also synthesized **5.4** (Figure 5.4), which had the aldehyde in the para position to the ester. I found that there was no hydrolysis at pH 5.5 and 7.4

by HPLC monitoring after 6 days while incubated at 37 °C, and concluded that the hydrolysis of the ester on **5.2** must be due to the assistance by the aldehyde functionality in the ortho position to the methyl ester.



5.4

Figure 5.4 Compound 5.4 showed no hydrolysis at pH 5.5 and 7.4 after 6 days while incubated at 37 °C.

5.3 Synthesis of an *o*-NEBI-alcohol containing drug conjugate

In order to determine if the *o*-NEBI platform would increase the cytotoxicity of a DDS comprised of a NEBI linker, I attempted to synthesize an *o*-NEBI containing an ester from a known alcohol containing chemotherapeutic. I first hydrolyzed the methyl ester of **5.1** to give **5.5** (Figure 5.5).

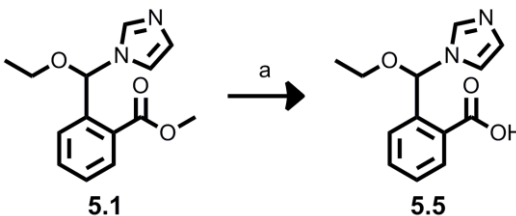


*Figure 5.5 Synthesis of an *o*-NEBI with a carboxylic acid, 5.5. Reagents: LiOH in THF/water.*

The synthesis of an *o*-NEBI containing an alcohol drug proved to be extremely challenging. I tried to couple paclitaxel, camptothecin, geldanamycin, and model fluorescent compounds such as dansyl alcohol to **5.5** with known coupling

agents. The NEBI, due to its acid and temperature sensitivity, is limited by the types of coupling agents that can be used for synthesis of esters. Although I was able to synthesize an *o*-NEBI with a NHS ester using EDC, I was unable to form any esters reacting this activated ester with alcohols and alkoxides under a variety of conditions. Coupling agents such as PyBOP, EDC, DCC, 2M6NBA with combinations of DMAP, DIPEA, and TEA all failed with camptothecin. I also tried couplings with ethylchloroformate with either DIPEA or TEA, which also failed. Coupling agents 1,1'-carbonyldiimidazole and 2-cyano-imidazole also failed to couple an alcohol containing drug to **5.5**. More exotic coupling methods such as vinyl acetate with Pd(OAc)₂ also failed.

As a last attempt, I decided to try using microwave assistance to push the reaction to ester formation. I knew that the NEBI could break down during the reaction due to the high temperature during the reaction. A reaction with paclitaxel, **5.5**, EDC and DMAP showed a new spot by thin layer chromatography. This spot was isolated by silica chromatography, but impure by NMR. Mass spectrometry indicated the presence of product, but the product was not fully characterized by NMR due to the presence of many impurities.

5.4 Synthesis and characterization of an *o*-NEBI conjugated to 5-fluoro-2'-deoxyuridine

With the newfound hope of making an ester on the *o*-NEBI platform using microwave assistance, I decided to try coupling 5-fluoro-2'-deoxyuridine (5-FU, **5.6**, Figure 5.6) to **5.5** as my model chemotherapeutic drug. 5-FU is a thymidylate synthase inhibitor, which leads to cell starvation of thymidine and eventually cell

death. It is an antimetabolite chemotherapeutic, which is broken down to 5-fluorouracil.¹²³ This drug is commercially available at a lower price than paclitaxel, and also has a lower molecular weight. This allowed me to perform my reactions at a larger scale.

My initial attempts in coupling **5.5** to **5.6** did not yield the *o*-NEBI-5-FU product (**5.7**). While I was able to verify the peaks associated with the NEBI from this synthesis by NMR methods, there were other peaks that I could not identify and the mass spectrometry data did not match. I finally realized that the product was an EDC adduct to the NEBI. So I decided to change coupling agents. When I used 2-methyl-6-nitro-benzoic anhydride (2M6NBA) as a coupling agent, I was able to isolate the desired **5.7** from the reaction mixture. Although I was able to synthesize **5.7**, the yield was very low (7%, Figure 5.6). This reaction provided enough product for preliminary studies. I contribute this low yield to the high microwave temperatures (100 °C) and 4 h reaction time that may have broken down **5.5** and product. This reaction has not yet been optimized. It is possible that a lower temperature and shorter reaction times may increase the product yield.

Examination of the hydrolysis of the NEBI group in **5.7** showed clean conversion to **5.6** (Figure 5.7) at both pH 5.5 and 7.4 when monitored by HPLC. In this case, there was no build up of an aldehyde intermediate at both pH 5.5 and 7.4 (Figure 5.7A). We hypothesized that the rate of the second step of hydrolysis was faster than the rate of the first step at both pH 5.5 and 7.4. We found that the hydrolysis of the NEBI continued to follow the expected first order kinetics, and had a half-life of 47 h and 2300 h at pH 5.5 and 7.4 respectively (Figure 5.7B). We monitored the decrease in concentration of **5.7** and the increase of **5.6** by HPLC.

These peaks were verified by LC-MS and also by matching retention time of commercially available **5.6** to the hydrolysis product by HPLC.

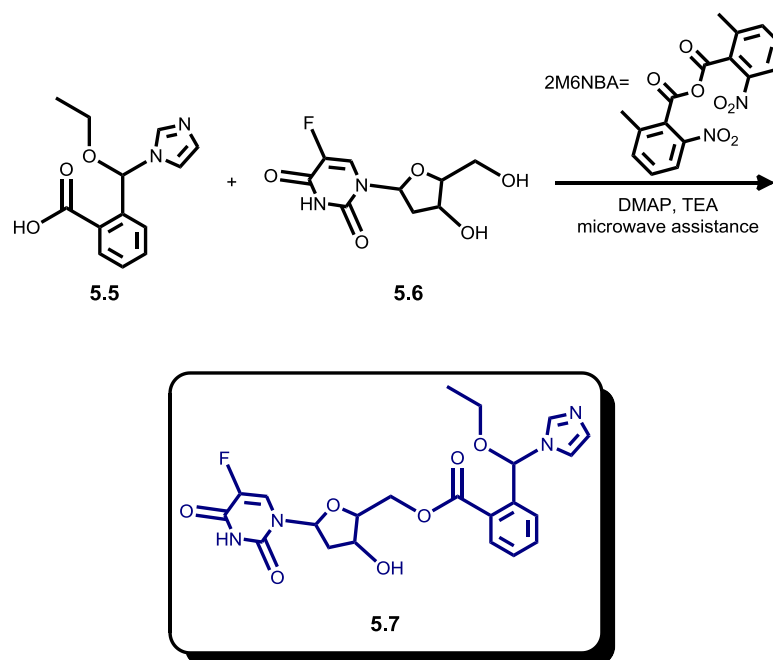


Figure 5.6 Schematic for the synthesis of **5.7**. Reagents: 2M6NBA, DMAP, TEA, Microwave, 100 °C. 7% yield.

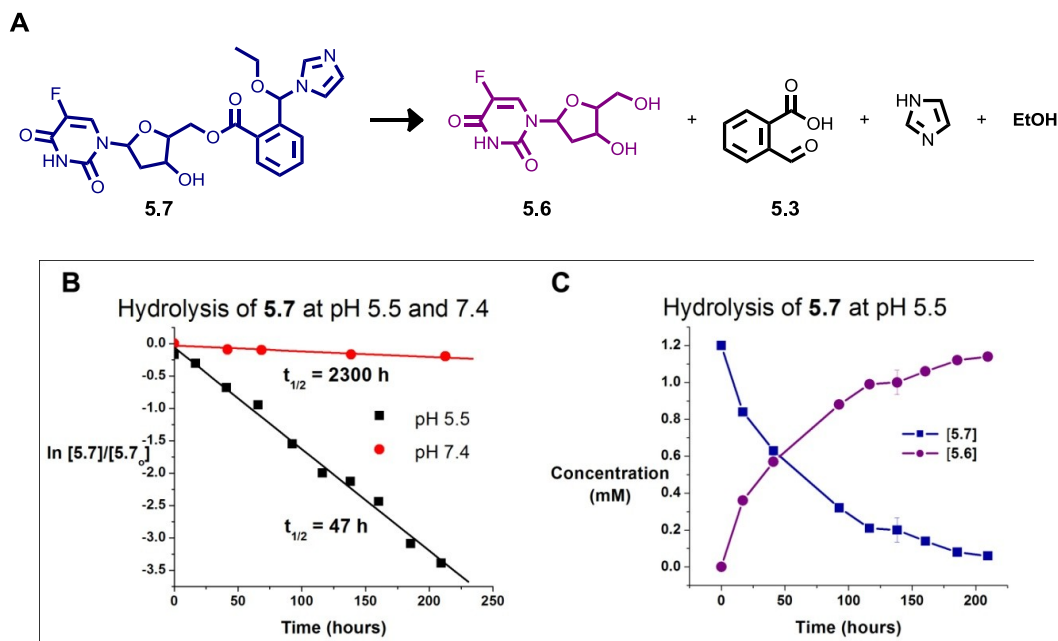


Figure 5.7 A) Schematic of **5.7** hydrolysis B) Hydrolysis of **5.7** and pH 5.5 and 7.4. C) Concentration of **5.7** and **5.6** over time as **5.7** hydrolyzes at pH 5.5.

To determine if compound **5.7** would be as potent as native 5-FU, cytotoxicity studies for compound **5.6** and **5.7** were performed on human ovarian carcinoma 2008 cells, and human mammary gland carcinoma MCF-7 cells. The IC_{50} for **5.6** was found to be 24 nM and 57 nM in 2008 and MCF-7 cells, respectively. Unfortunately, compound **5.7** was not as potent as **5.6**, and found to have an IC_{50} of 23.6 μ M and 2.37 μ M in 2008 and MCF-7 cells, respectively (Figure 5.8). I hypothesized that the loss of potency in **5.7** was due to the slow hydrolysis of the NEBI group under acidic conditions. Since the half-life for hydrolysis at pH 5.5 was 47 h, there were less than two half-lives that occurred during the 72 h incubation of **5.7** with the cells. Slow release of 5-FU may have hindered the potency of this *o*-NEBI-5-FU conjugate.

As expected, control experiments revealed that 2-carboxybenzaldehyde, the hydrolysis product, was not toxic to cells up to 200 μM , which is also beyond the range used for the cytotoxicity studies of **5.6** and **5.7** (data found in experimental section).

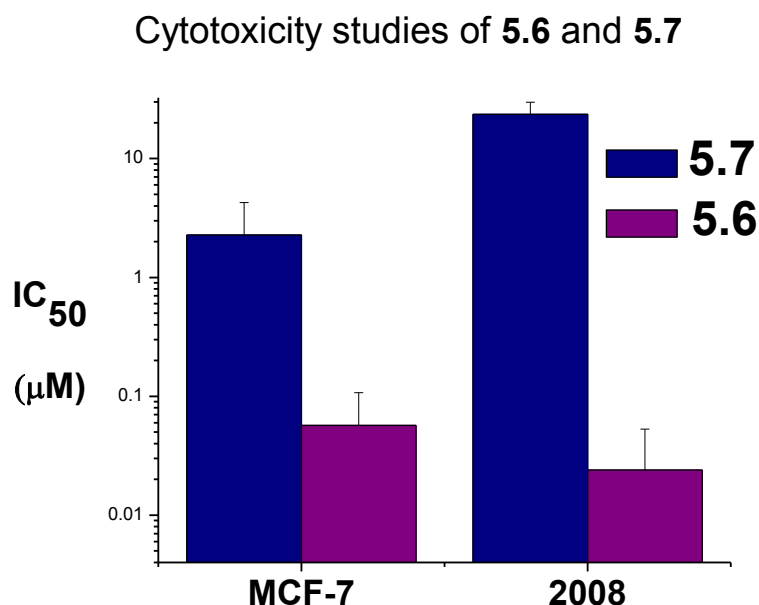


Figure 5.8 Cytotoxicity of 5.6 and 5.7 on 2008 and MCF-7 cells.

5.5 Increasing the rates of hydrolysis of *o*-NEBI

I hypothesized that increasing the rates of NEBI hydrolysis may improve the potency of *o*-NEBI-5-FU conjugate. We previously demonstrated that incorporating substituents to the phenyl ring of the NEBI group could significantly affect the hydrolysis rate in aqueous solution. To increase the rate of NEBI hydrolysis of the *o*-NEBI-5FU conjugate, an electron donating substituent was incorporated into compound **5.7** on the phenyl ring. When I incorporated a methoxy group on **5.1** to

give compound **5.8** (Figure 5.9), the rate of hydrolysis of the NEBI group in step one increased with a half-life of 0.47 h at pH 5.5 and 8.7 h at pH 7.4. The rate of the subsequent hydrolysis of the *ortho*-formylbezoyl ester, however, was significantly slowed ($t_{1/2} = 990$ h at pH 5.5). I found that increasing the hydrolysis of the first step through substitution with an EDG of the phenyl ring would decrease the rate of hydrolysis of the second step.

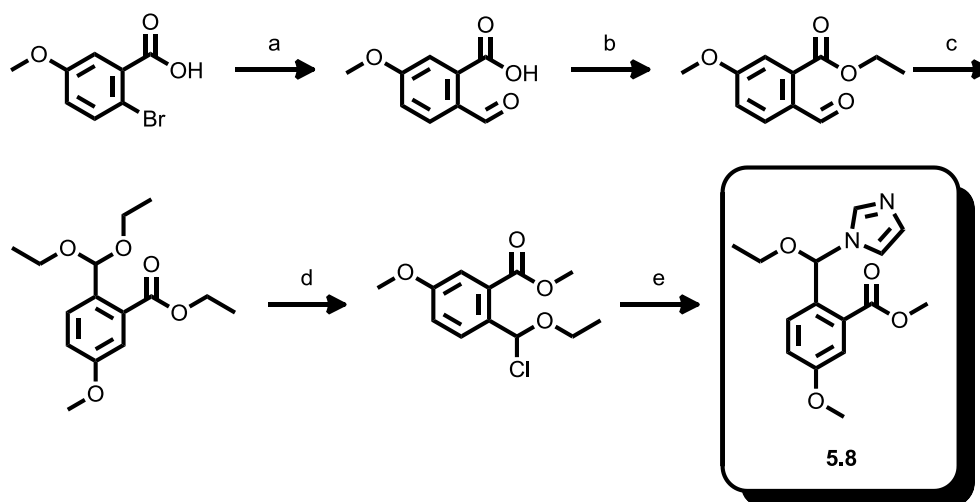


Figure 5.9 Schematic of the synthesis of **5.8**. Reagents: a) *n*-BuLi, DMF, -78 °C, 51% yield, b) EtI and sodium carbonate in DMF, 52% yield, c) ethyl orthoformate, EtOH, TsOH, 88% yield, d) thionyl chloride, reflux, neat e) imidazole, NaH in THF, 30% yield over two steps.

Since the hydrolysis of the second step was slowed considerably in **5.8**, I decided to take a different approach to increase NEBI hydrolysis. Fortunately, the NEBI system is very versatile and there is more than one way to adjust the rate of hydrolysis. Instead of substituting on the phenyl ring, I decided to explore the effect of adding a chloro substituent to the 2 position of the imidazole on **5.1** on the hydrolysis of the NEBI group in acidic solutions. I hypothesized that the lower pKa of the protonated form of 2-chloro-imidazole ($pK_a = 3.5^{124, 125}$) compared to

imidazole-H⁺ (pKa = 6.95) would increase the rate of NEBI hydrolysis (**5.9**, Figure 5.10) by stabilizing the protonated form of the imidazole. The lower pKa of the 2-chloro-imidazole-H⁺ ion suggests that the chloro substituent dominates over the π donating effects to stabilize the protonated form of the imidazole. Thus, in the context of a NEBI, the electron withdrawing characteristics of a chloro group on the 2 position of the imidazole will lead to weakening of the C6-N bond in the NEBI (Figure 2.2), and thus speed up the hydrolysis of the NEBI group.

The hydrolysis of **5.9** was measured by HPLC. The first step of hydrolysis was found to have a half-life of 5.9 h and 85 h at pH 5.5 and 7.4, respectively. The rate of the second step of hydrolysis (here, for **5.2**) was described previously (130 h at pH 5.5 and 5.1 h at pH 7.4). This hydrolysis data was promising because we were able to increase the first step of hydrolysis by incorporating a chloro substituent on the 2-position of the imidazole group in **5.8**. Since the second step of hydrolysis at pH 7.4 is fast, I hypothesized that the increase of the first step may be enough to increase the cytotoxicity of a NEBI drug conjugate.

Increasing the rate of hydrolysis via the chloro substituent on the imidazole moiety of the NEBI (**5.9**) was preferred over the addition of a methoxy substituent on the phenyl ring of the NEBI (**5.8**). While **5.8** increased the first step of NEBI hydrolysis, it slowed the rate of ester hydrolysis. I was concerned that the slowed second rate of hydrolysis would lower the potency of a NEBI drug conjugate, and, therefore, continued with **5.9**, since I was able to increase the rate of NEBI hydrolysis without slowing the rate of ester hydrolysis.

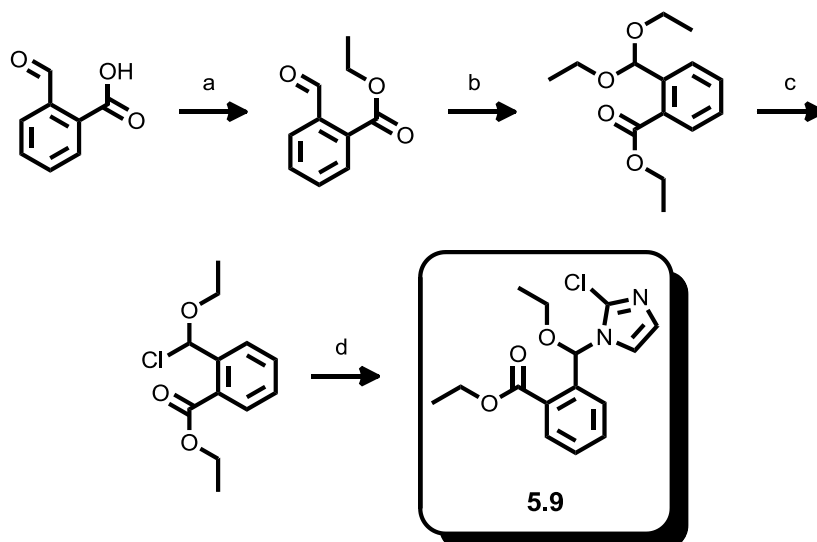


Figure 5.10 Schematic for the synthesis of 5.9. Reagents: a) EtI and potassium carbonate in DMF, 71% yield b) ethyl orthoformate, EtOH, TsOH, 67% yield, c) thionyl chloride, reflux neat d) 2-chloro-imidazole, NaH in THF, 60% yield over two steps.

5.6 Synthesis and characterization of chloro-*o*-NEBI-5-FU conjugate

To determine if increased rates of *o*-NEBI hydrolysis would improve the cytotoxicity of *o*-NEBI conjugates, I synthesized a chloro substituted NEBI coupled to **5.6** (**5.10**, Figure 5.11) using the same chemistry developed for the synthesis of compound **5.7**.

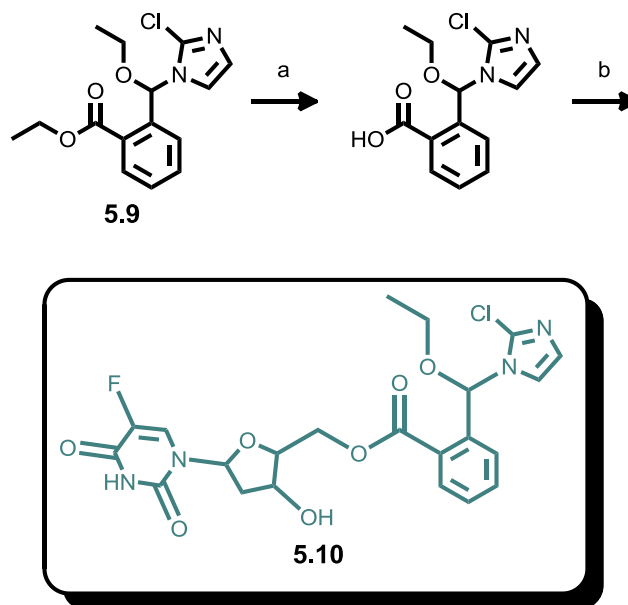
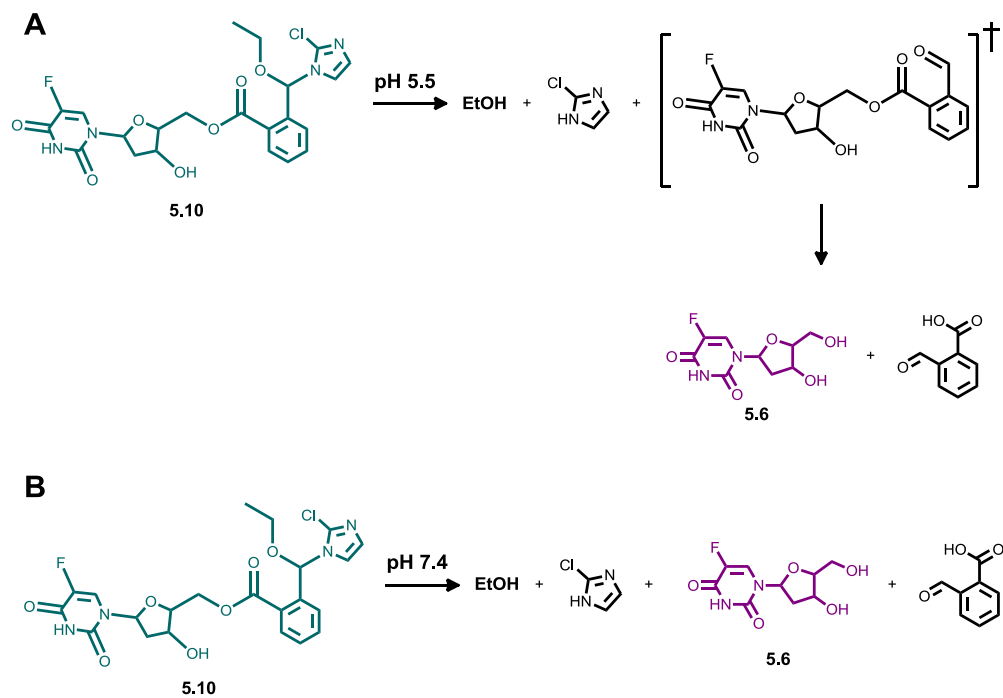


Figure 5.11 Schematic of the synthesis of 5.10. Reagents: a) LiOH in THF/water b) 5.6, 2M6NBA, DMAP, TEA, Microwave, 100 °C. 6% yield.

Hydrolysis studies of **5.10** showed a two-fold increase in the rate of NEBI hydrolysis compared to **5.7**. The half-life of hydrolysis was found to be 24 h and 276 h at pH 5.5 and 7.4, respectively, when incubated at 37 °C. Since we were able to increase the rate of hydrolysis at pH 5.5, we were able to detect the aldehyde intermediate in HPLC studies at pH 5.5 (Figure 5.12A). The second step of hydrolysis for the release of **5.6** was extrapolated to be approximately 30 h. We did not detect any of the aldehyde intermediate at pH 7.4 (Figure 5.12B), which is in-line with previous studies indicated that the rate of hydrolysis of this intermediate at pH 7.4 hydrolyzes at a rate that is faster than at pH 5.5 (Figure 5.3C).



C

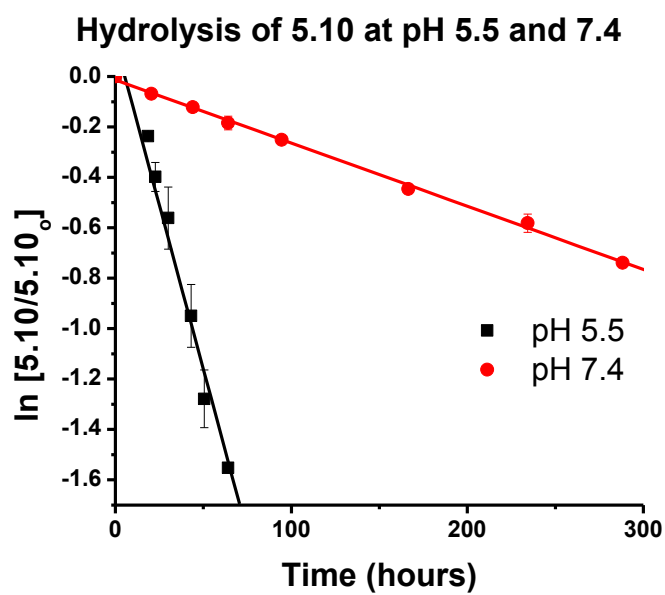


Figure 5.12 The hydrolysis of 5.10 at A) pH 5.5 and B) pH 7.4. C) Graph of 5.10 hydrolysis.

Cytotoxicity studies conducted on **5.10** showed a substantial improvement in the potency of the *o*-NEBI conjugate when compared to compound **5.7**. In addition, the IC₅₀ values measured for **5.10** was in the same order of magnitude as that found for native drug **5.6** (Figure 5.13). By increasing the rate of hydrolysis twofold, I was able to increase the potency >40 fold. This was very promising because not only was I able to release free unmodified 5-FU, I was also able achieve native 5-FU potency. These properties will be very useful in a future DDS with a NEBI platform.

As expected, control experiments revealed that 2-chloro-imidazole, a NEBI hydrolysis product, was not toxic to cells up to 200 μ M, which is also beyond the range used for the cytotoxicity studies of **5.10** (data found in experimental section).

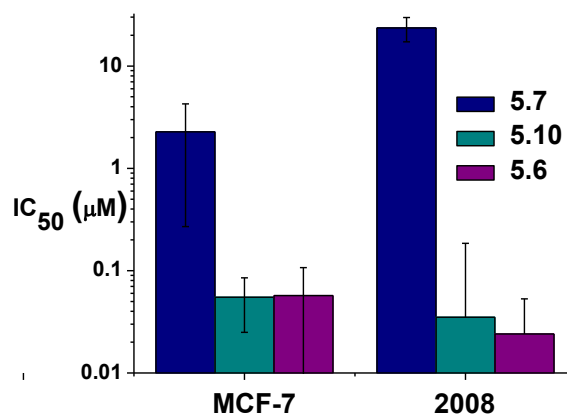
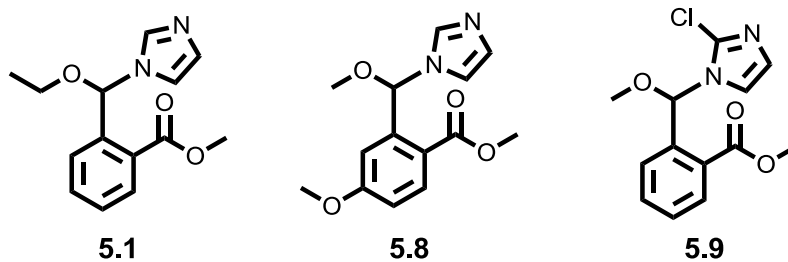


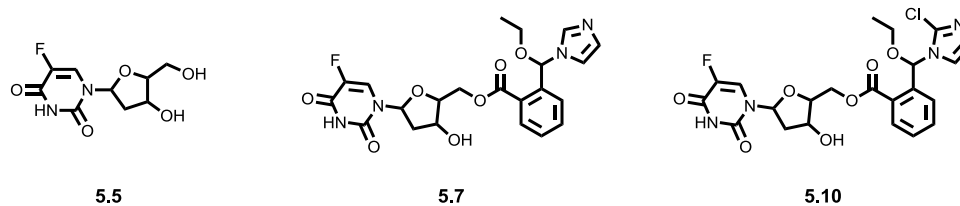
Figure 5.13 Cytotoxicity of studies 5.10 compared to 5.7 and 5.6 (native 5-FU).

5.7 Summary of data



Compound	Step 1 $t_{1/2}$ (hrs)		Step 2 $t_{1/2}$ (hrs)	
	pH 5.5	pH 7.4	pH 5.5	pH 7.4
5.1	78	3600	130	5.1
5.7	0.47	8.7	990	>8.7
5.9	5.9	85	N/A	N/A

Figure 5.14 The half-life of both steps of hydrolysis for *o*-NEBI derivatives 5.1, 5.8 and 5.9.



	Step 1 $t_{1/2}$ (hrs)		Step 2 $t_{1/2}$ (hrs)	IC_{50} (μ M)	
	pH 5.5	pH 7.4	pH 5.5	2008 Cells	MCF-7 Cells
5.7	47	2300	<47	23.6	2.37
5.10	24	276	30	0.035	0.055
5.5	N/A			0.024	0.057

Figure 5.15 A comparison of hydrolysis half-lives of 5.7 and 5.10, and cytotoxicity of 5.5, 5.7, and 5.10.

5.8 Conclusions

In this chapter, I demonstrated the release of an alcohol containing chemotherapeutic from an *o*-NEBI platform that maintained native drug potency. Compound **5.1** was synthesized and characterized as a proof-of-concept and found to undergo a two step hydrolysis mechanism to release an alcohol. This work was translated into constructing two *o*-NEBIs carrying an alcohol containing chemotherapeutic, 5-FU (**5.7** and **5.10**), via an ester bond.

The formation of the ester bond was a triumph in itself due to the many previous attempts that I have made towards ester formation on the NEBI platform. While the ester formation yields were low due to the high temperatures in the microwave reaction, we were still able to make enough of the 5-FU conjugates for characterization and evaluation. I believe that these yields can be optimized through tuning the temperature and time the reaction occurs at in the microwave.

I demonstrated that the potency of an *o*-NEBI conjugated to 5-FU was dependent on the rate of NEBI hydrolysis. Increased rates of NEBI hydrolysis led to the increase potency of the conjugate. While electronic effects on the phenyl ring influenced in both the first and second steps of hydrolysis, I was able to highlight the tunability of the NEBI by demonstrating that I could also tune the rate of hydrolysis by substitution of the 2 position on the imidazole ring. Substitution of the 2 position of the imidazole increased only the NEBI hydrolysis while leaving the ester hydrolysis rate unchanged, and was therefore favored over substitution of the phenyl ring with a methoxy group.

The results presented here strongly support the release of native **5.6** from the *o*-NEBI platform. Cytotoxicity activity of an *o*-NEBI drug conjugate was

comparable to native drug due to an increase rate of hydrolysis of the *o*-NEBI through the use of substituents placed on the imidazole group. The studies in this chapter are a proof-of-concept that the *o*-NEBI platform can be used towards improving the potency of a DDS comprised of a NEBI linker. Future studies for the *o*-NEBI platform include synthesis of a bifunctional crosslinker for conjugation of alcohol containing drugs to macromolecule targeting moieties.

Notes about this chapter:

The LC-MS studies in this chapter were conducted by Dr. Su at the Molecular Mass Spectrometry Facility. I would like to thank the Theodorakis Lab for allowing me to use their microwave for synthesis of 5-FU compounds. I would also like to thank Tawny Issarapanichkit for her help in synthesis and purification of starting materials. Finally, I would like to thank Prof. Jerry Yang for his support through all of the attempts made towards making an ester.

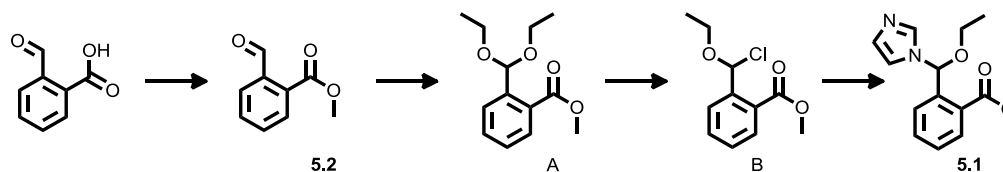
5.9 Experimentals

General Comments

All reagents were purchased from Sigma-Aldrich, Inc., TCI, or Alfa Aesar and used without further purification. NMR spectra were recorded on a Varian 400 (FT, 400 MHz, ¹H; 100 MHz, ¹³C) spectrometer. HR-MS (high-resolution mass spectra) were obtained in the Department of Chemistry & Biochemistry, University of California, San Diego. Kinetic analysis by reverse-phase high performance liquid chromatography (RP-HPLC) was performed with an Agilent 1100 Series HPLC

using an analytical reverse-phase column (SPHERI-5 Phenyl 5 micron, 250 x 4.6 mm).

Synthesis of 5.1 and 5.2:



Synthesis of *ortho*-formylbenzoyl ester **5.2**

A solution of 2-carboxybenzaldehyde (80 mmol), potassium carbonate (45 mmol) and methyl iodide (150 mmol) was stirred in DMF overnight. DCM and water was added to the solution. The organic layer was removed, and the aqueous layer washed two times with DCM. The organic layers were pooled, dried with sodium sulfate, and removed under reduced pressure to give **5.2**, 88% yield. Characterization of (**5.2**): $^1\text{H-NMR}$ (CDCl_3 , 400 MHz) δ 3.912 (s, 3H), 7.596 (d, 2H), 7.862 (dd, 1H), 10.547 (s, 1H) ESI-MS (m/z $\text{M}+\text{H}^+$ = 165.02)

Synthesis of **A**

A solution of **5.2** (71 mmol), triethyl orthoformate (213 mmol), and TsOH (0.7 mmol) was refluxed in 50 mL of EtOH for 24 hrs. After removal of EtOH under reduced pressured DCM was added and the organic layer was extracted with saturated sodium bicarbonate solution. The organic layer was dried over anhydrous sodium sulfate. After removal of diethyl ether under reduced pressure, the crude mixture was isolated by silica chromatography using as eluent of 80:20 hexanes:diethyl ether to give pure **A** (76 % yield). Characterization of (**A**): $^1\text{H-NMR}$ (CDCl_3 , 400 MHz) δ 1.226 (t,6H), 3.556 (m, 1H), 3.655 (m, 1H), 3.708 (s, 3H), 6.161 (s, 1H), 7.380 (t, 1H), 7.522 (t, 1H), 7.759 (d, 2H). ESI-MS (m/z $\text{M}+\text{H}^+$ = 261.0)

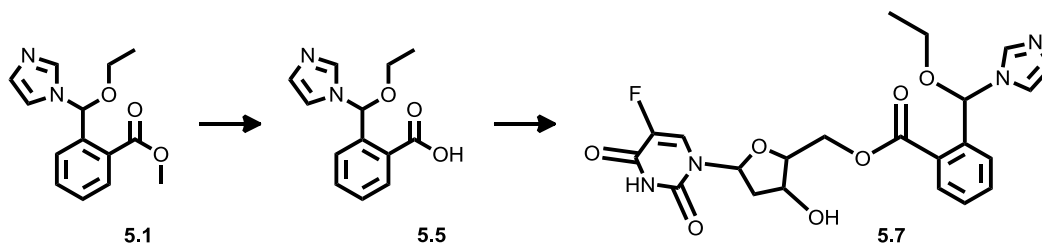
Synthesis of **B**

Compound **A** (1.2 mmol), freshly distilled acetyl chloride (1.2 mmol) and thionyl chloride (0.16 μ mol) were combined without additional solvent and refluxed for 1 hour at 65 °C under N₂. The excess thionyl chloride and acetyl chloride were removed under reduced pressure and the crude mixture was used without further purification

Synthesis of **5.1**

In a dry flask, NaH (1.6 mmol) was added to a solution of imidazole (1.2 mmol) dissolved in dry THF. The solution was allowed to stir for 1 hour at 23 °C, and then the crude mixture of **B** was added dropwise to the imidazole. The combined solution was stirred for 12 h at 23 °C. Saturated sodium carbonate was added to the solution and washed 3 times with DCM. The organic layers were pooled and dried over sodium sulfate. The solvent was removed under reduced pressure. **5.1** was isolated by silica chromatography using as eluent a 95:5 mixture of DCM:MeOH. The isolated yield over two steps was 22%. Characterization of (**5.1**): ¹H-NMR (CDCl₃, 400 MHz) δ 1.242 (t, 3H), 3.497-3.676 (m, 2H), 3.862 (s, 3H), 7.002 (s, 1H), 7.061 (s, 1H), 7.197 (d, 1H), 7.434 (t, 1H), 7.573 (t, 1H), 7.657 (d, 1H), 7.768 (s, 1H), 7.912 (d, 1H) ¹³C-NMR (CDCl₃, 100 MHz) 14.822, 52.327, 64.937, 83.823, 117.524, 126.358, 128.979, 130.628, 128.979, 130.628, 130.711, 132.378, 132.517, 136.963, 142.963, 142.455, 166.792 ESI-MS (m/z M+H⁺ = 260.86)

Synthesis of **5.7**



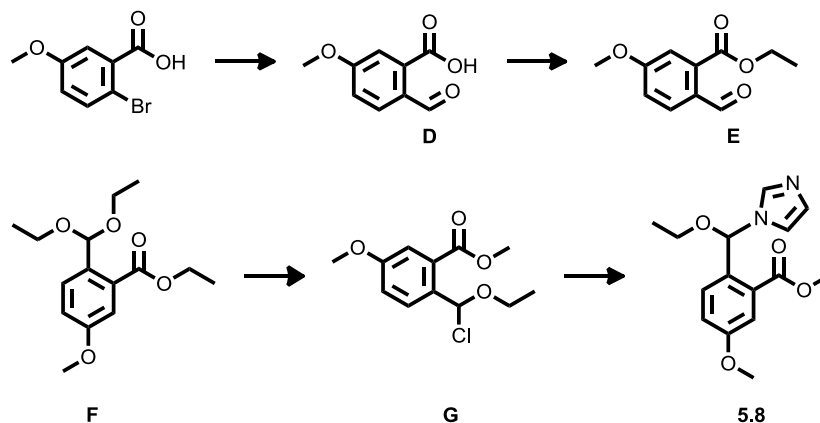
Synthesis of **5.5**

Compound **5.1** (148 μmol) and 1M LiOH (296 μL , 0.296 μmol) was stirred in a solution of THF/H₂O for 5 h. The solvent was removed under reduced pressure. The solid was washed with DCM 3 times and filtered. The filtrate was then washed 3 times with 2:8 MeOH:DCM and filtered. The solvents were removed under reduced pressure and **5.5** was used in the next step. Characterization of (**5.5**): ¹H-NMR (CD₃OD, 400 MHz) δ 1.25 (t, 3H), 3.4803.66 (m, 2H), 6.92 (s, 1H), 7.14 (s, 1H), 7.28 (s, 1H), 7.35 (m, 2H), 7.55 (d, 1H), 7.60 (d, 1H), 7.81 (s, 1H) ESI-MS (m/z M+H⁺ = 246.91)

Synthesis of **5.7**

Compound **5.5**, (0.1 mmol), 2M6NBA (0.06 mmol), triethylamine (17 μL), DMAP (0.03 mmol), and 5-fluoro-2'-deoxyuridine (0.06 mmol) were combined in a solution of THF and put into a microwave reactor for 4 h at 100 °C. The THF was removed under reduced pressure and the compound isolated by silica chromatography using as eluent a 5:93:2 mixture of MeOH:DCM:TEA. 7% yield. Characterization of **5.7** ¹H-NMR (CD₃OD, 400 MHz) δ 1.30 (t, 3H), 2.41-2.47 (m, 2H), 3.55-3.79 (m, 2h), 3.86 (d, 2H), 5.07 (s, 1H), 5.55 (d, 1H), 6.33 (m, 1H), 7.43 (s, 1H), 7.56 (s, 1H), 7.67 (m, 3H), 7.80 (t, 1H), 8.03 (m, 1H), 8.14 (d, 1H), 8.26 (m, 1H), 9.22 (s, 1H). ESI-MS (m/z M+H⁺ = 475.00)

Synthesis of 5.8



Synthesis of **D**

A solution of n-BuLi (1.6M in hexanes, 12.5 mL) was added dropwise to a solution of 2-bromo-5-methoxy benzoic acid (8.7 mmol) dissolved in 50 mL of dry THF in a -78 °C acetone and dry ice bath and allowed to stir for 15 minutes. Dry DMF (3 mLs) was then added to the solution. The solution was allowed to stir for another 15 minutes and then quenched with 2N sulfuric acid and extracted with EtOAc 3 times, and dried over sodium sulfate. The product was purified with column chromatography 30:68:2 EtOAc:hexanes:acetic acid. 51% yield
 Characterization of (**D**): ¹H-NMR (CD₃OD, 400 MHz) δ 3.91 (s, 3H), 7.30 (dd, 1H), 7.53 (d, 1H) 7.65 (dd 1H) ESI-MS (m/z M-H⁻ = 178.99)

Synthesis of **E**

Sodium carbonate (13 mmol) and ethyl iodide (5.2 mmol) was added to a solution of **D** in DMF and allowed to stir overnight. The product was extracted with DCM 3 times from saturated sodium bicarbonate. The product was used in the next step without further purification. 52% yield
 Characterization of (**E**): ¹H-NMR (CDCl₃, 400 MHz) δ 1.417 (t, 3H), 3.911 (s, 3H), 4.430 (q, 2H), 7.091-7.119 (d,d, 1H), 7.382

(d, 1H), 7.952 (d, 1H), 10.470 (s, 1H). ESI-MS (m/z $M+H^+$ = 208.94, $M+Na^+$ = 231.00)

Synthesis of **F**:

A solution of **E** (2.3 mmol), ethyl orthoformate (7.5 mmol) and EtOH (1.5 mL) and a crystal of TsOH was refluxed for 3 h. The crude was dried under reduced pressure and purified by column chromatography using as eluent 1:9 EtOAc: hexanes. 88 % yield. Characterization of (**F**): $^1\text{H-NMR}$ (CDCl_3 , 400 MHz) δ 1.213 (t, 3H), 1.389 (t, 3H), 3.538- 3.556 (m, 2H), 3.625, 3.642 (m, 2H), 3.828 (s, 3H), 4.350, 4.368 (m, 2H), 6.100 (s, 1H), 7.007, 7.029 (m, 1H), 7.280, 7.287 (d, 1H), 7.672, 7.694 (d, 1H). $^{13}\text{C-NMR}$ (CDCl_3 , 400 MHz) δ 14.471, 15.458, 55.690, 61.356, 62.548, 99.344, 115.124, 116.989, 128.543, 132.131, 159.300, 167.932. ESI-MS (m/z $M+Na^+$ = 305.09)

Synthesis of **G**:

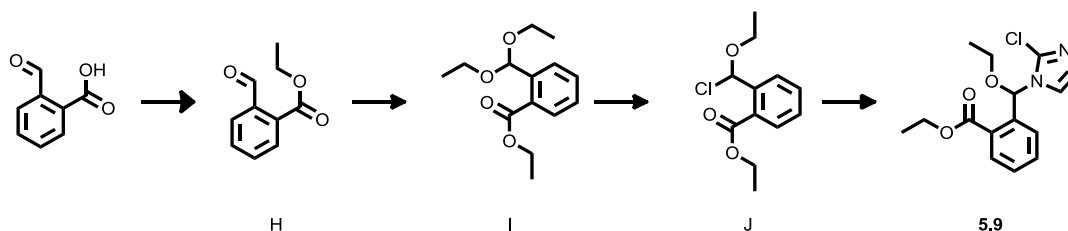
Compound **F** (1.2 mmol) and thionyl chloride (1.6 mmol) were combined without additional solvent and refluxed for one hour at 65 °C under N_2 . The excess thionyl chloride were removed under reduced pressure. The crude mixture was used directly in the next step.

Synthesis of **5.7**:

In a dry flask, NaH (3.6 mmol) was added to a solution of imidazole (1.8 mmol) dissolved in dry tetrahydrofuran (THF). The solution was allowed to stir for one hour at 23 °C, and then the crude mixture of **G** was added dropwise to the imidazole solution. The combined solution was stirred for 12 h at 23 °C. Saturated sodium carbonate was added to the solution and washed 3 times with DCM. The organic layers were pooled and dried over sodium sulfate. The solvent was

removed under reduced pressure. Compound **5.7** was isolated by silica chromatography using as eluent a 95:2:2 mixture of DCM:MeOH:TEA. 30% yield. Characterization of (**5.7**): $^1\text{H-NMR}$ (CDCl_3 , 400 MHz) δ 1.220 (t, 3H), 1.338 (t, 3H), 3.464- 3.624 (m, 2H), 3.834 (s, 3H), 4.310 (m, 2H), 6.966 (s, 1H), 7.032 (d, 1H), 7.061 (d, 1H), 7.101 (s, 1H), 7.411 (d, 1H), 7.549 (d, 1H), 7.691 (s, 1H). $^{13}\text{C-NMR}$ (CDCl_3 , 400 MHz) 14.415, 15.073, 55.775, 61.636, 64.973, 83.909, 116.253, 117.570, 128.079, 129.237, 130.311, 131.346, 137.211, 159.794, 166.783. ESI-MS (m/z $\text{M}+\text{H}^+$ = 304.78, $\text{M}+\text{Na}^+$ = 327.01)

Synthesis of **5.9**



Synthesis of **H**

Ethyl iodide (6.9 mL, 86.6 mmol) was added dropwise to a solution of 2-carboxybenzaldehyde (10 g, 66.6 mmol) and potassium carbonate (27.6 g, 200 mmol) in DMF. The solution was stirred for 12 h at room temperature. Saturated sodium carbonate was added to the solution and washed 3 times with DCM. The organic layers were pooled and dried over sodium sulfate. The solvent was removed under reduced pressure. Compound **I** was isolated by silica chromatography plug using as eluent a 70:30 mixture of DCM:hexanes. The isolated crude yield was 71%.

Synthesis of **I**

A solution of compound **H** (8.4 g, 47 mmol), triethyl orthoformate (25 mL, 155 mmol), EtOH (5.4 mL, 94 mmol), and TsOH (100 mg, 0.5 mmol), was refluxed for 3 h. The excess triethyl orthoformate and EtOH were removed under pressure. Saturated sodium carbonate was added to the solution and washed 3 times with DCM. The organic layers were pooled and dried over sodium sulfate. The solvent was removed under reduced pressure. Compound **I** was isolated by silica chromatography plug using as eluent a 65:33:2 mixture of DCM:hexanes:TEA. The yield was 67%. Characterization of (**I**) ^1H NMR (CDCl_3 , 400 MHz) 1.212 (t, 6H), 1.376 (t, 3H), 3.556 (m, 2H), 3.659 (m, 2H), 4.360 (m, 2H), 6.177 (s, 1H), 7.341 (t, 1h), 7.462 (t, 1H), 7.763 (m, 2H) ^{13}C NMR (CDCl_3 , 100 MHz) 14.163, 15.162, 60.951, 62.426, 99.086, 126.703, 127.963, 129.526, 130.411, 131.266, 139.494, 167.900 ESI-MS (m/z $\text{M}+\text{Na}^+$ = 275.09)

Synthesis of **J**

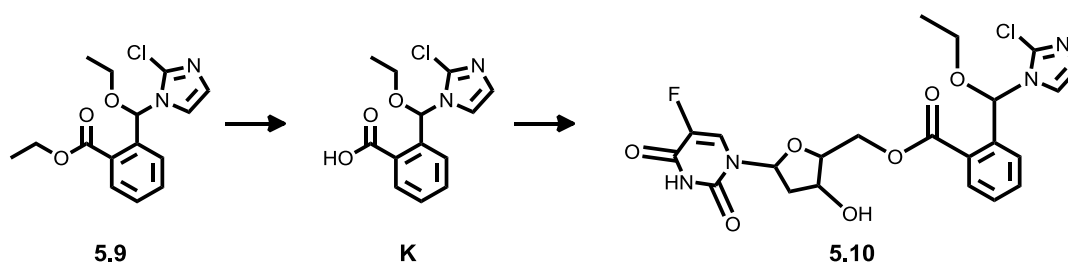
Compound **I** (514 mg, 2.0 mmol) and thionyl chloride (175 μL , 2.4 mmol) were combined without additional solvent and refluxed for one hour at 65 $^\circ\text{C}$ under N_2 . The excess thionyl chloride was removed under reduced pressure. Compound **J** was used without further purification.

Synthesis of **5.9**

In a separate dry flask, NaH (65 mg, 2.7 mmol) was added to a solution of 2-chloro-imidazole (137 mg, 1.7 mmol) dissolved in dry THF. The solution was allowed to stir for one hour at 23 $^\circ\text{C}$, and then the crude mixture of **J** was added dropwise to the 2-chloro-imidazole/NaH solution. The combined solution was stirred for 12 h at 23 $^\circ\text{C}$. Saturated sodium carbonate was added to the solution and washed 3 times with DCM. The organic layers were pooled and dried over sodium

sulfate. The solvent was removed under reduced pressure. Compound **5.9** was isolated by silica chromatography using as eluent a 20:78:2 mixture of EtoAc:hexanes:TEA. The isolated yield of compound **5.9** was 60% over the two steps. Characterization of (**5.9**) ^1H NMR (CDCl_3 , 400 MHz) δ 1.250 (t, 3H), 1.348 (t, 3H), 3.642-3.719 (m, 2H), 4.320 (m, 2H), 6.826 (m, 1H), 6.957 (m, 1H), 7.209 (s, 1H), 7.399 (d, 1H), 7.448 (t, 1H), 7.535 (t, 1H), 7.888-7.910 (dd, 1H). C^{13} NMR (CDCl_3 , 100 MHz) δ 14.41, 15.10, 61.65, 65.81, 83.92, 119.02, 126.76, 128.66, 129.31, 130.12, 130.81, 132.24, 132.53, 137.62, 167.09 ESI-MS (m/z $\text{M}+\text{H}^+$ = 308.64, $\text{M}+\text{Na}^+$ = 330.92)

Synthesis of **5.10**



Synthesis of **K**

Compound **5.9** (179 mg, 0.58 mmol) and 1M LiOH (0.64 μL , 0.64 mmol) was stirred in a solution of THF/ H_2O for 5 h. The solvent was removed under reduced pressure. The solid was washed with DCM 3 times and filtered. The filtrate was then washed 3 times with 20:80 MeOH:DCM and filtered. The product was dried under reduced pressure and compound **K** was used in the next step. Crude yield: 90% Compound **K** Characterization ^1H NMR (CD_3OD , 400MHz) δ 1.264 (t, 3H), 3.616-3.744 (m, 2H), 6.896 (m, 1H), 6.988 (m, 1H), 7.377-7.435 (m, 5H), 7.663 (t, 1H) ^{13}C NMR (CD_3OD , 100MHz) 14.785, 65.943, 85.152, 120.303, 126.159,

127.831, 129.207, 129.347, 129.462, 132.789, 135.236, 140.398, 175.446. ESI-MS (m/z, M-H⁻ = 278.82)

Synthesis of **5.10**

Compound **K**, (0.32 mmol), 2M6NBA (0.3mmol), TEA (89 μ L), DMAP (0.1 mmol), and 5-Fluoro-2'-deoxyuridine (0.15 mmol) were combined in a solution of THF and put into a microwave reactor for 4 h at 100 °C. The THF was removed under reduced pressure and the compound isolated by silica chromatography using as eluent a 5:93:2 mixture of MeOH, DCM, and triethylamine. 6% yield. To further purify, a 0.5 mm reverse phase plate was used with 4:6 acetone:water as eluent. Characterization of **5.10** ¹H NMR (CD₃OD, 400MHz) δ 1.20 (t, 3H), 2.12-2.37 (m, 2H), 3.57-3.70 (m, 2H), 4.11-4.17 (m, 1H), 4.35-4.59 (m, 3H), 6.20-6.24 (m, 1H), 6.90 (s, 1H), 6.96 (m, 1H), 7.19-7.23 (d, 1H), 7.39-7.41 (d, 1H), 7.53-7.66 (m, 3H), 7.97 (t, 1H) ESI-MS (m/z, M-H⁻= 506.96, M+Cl⁻ = 542.83) HR-MS: (M+Na⁺=531.1056), Theoretical Mass: 531.1053

Hydrolysis studies of **5.1, 5.7, 5.8, 5.9, 5.10**

The compounds were dissolved in DMSO, at 1 mg/mL, 20 μ L of this solution is combined with 180 μ L of buffer (MES buffer with 30% DMSO for pH 5.5, and HEPES buffer with 30% DMSO for pH 7.4). The samples are incubated at 37 °C and time points are taken on an Agilent 1100 Series HPLC using an analytical reverse-phase column (SPHERI-5 Phenyl 5 micron, 250 x 4.6 mm). The eluent is a gradient from 0-70% MeOH and water, depending on the compound.

Cytotoxicity studies of (5.6, 5.7, 5.10, 2-carboxybenzaldehyde, and 2-chloroimidazole) on human ovarian carcinoma 2008 cells and human mammary gland carcinoma MCF-7 cells.

Human ovarian carcinoma 2008 cells and human mammary gland carcinoma MCF-7 cells were plated into each well of a 96 well plate (3000 cells/well and 7000 cells/well respectively) using RPMI-1640 media with 10% FBS, and DMEM with sodium pyruvate, non-essential amino acids, and 10% FBS respectively. The cells were incubated for 24 h at 37 °C with 5% CO₂. After the incubation period, cells were dosed with various concentrations of **5.6, 5.7, 5.10**, 2-carboxybenzaldehyde, and 2-chloro-imidazole. The cells were allowed to incubate with the molecules for 72 h. After incubation, cells were washed 3 times with 200 µL of PBS (Mediatech, 46-013CM) pH 7.4. Cells were then fixed with 200 µL of PBS and 50 µL of 50% trichloroacetic acid for one hour at 4 °C. After fixation, cells were washed 5 times with 200 µmol water and allowed to dry. A 0.4% sulforhodamine B (SRB, Sigma Aldrich, S1402) solution in 1% acetic acid (100 µmol) was added to the cells and incubated for 15 minutes at room temperature. The cells were washed 3 times with 200 µL 1% acetic acid and the 96 well plate was allowed to dry. Tris base solution (10 mM, 200 µL) was added to the wells for 15 minutes prior to measuring the absorbance at 515 nm.

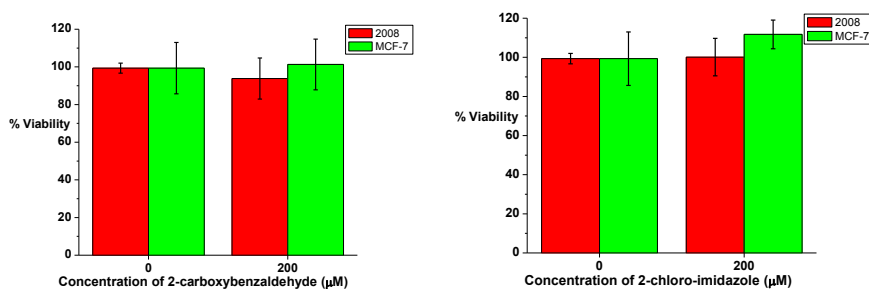


Figure 5.7 Cytotoxicity of 2-carboxybenzaldehyde and 2-chloro-imidazole.

Chapter 6

Studies towards the release of an amine containing drug from an *ortho-N*-ethoxybenzylimidazole platform

6.1 Introduction

In chapter 5, I demonstrated the release of an alcohol containing drug from an *ortho*-NEBI (*o*-NEBI) platform. In this chapter, I describe efforts made towards the release of an amine containing drug, namely doxorubicin, from the *o*-NEBI platform in an attempt to improve the potency of a DDS that consists of a NEBI linker carrying doxorubicin developed in chapter 4.

I showed in the chapter 5 that an EDG, meta to the ester in **5.7** influenced rate of hydrolysis of the *ortho*-formylbenzoyl ester. I hypothesized that EDGs and

EWGs in the para position to the ester would also influence the rates of *ortho*-formyl assisted hydrolysis of the esters. Increasing the rates of hydrolysis of an ester from *ortho*-formylbenzoyl esters would serve as a proof-of-concept to increase the rates of amide hydrolysis from a NEBI-based linker. Previous work reported by Bender *et. al.* showed that very slow release rates of amines from the *ortho*-formylbenzoyl amides were possible at pH 3.0.^{122, 126}

The ability to release amine-containing drugs from a DDS would increase the of potency amine-containing DDSs using the NEBI platform. While we were able to detect cytotoxicity of *N*-(4-formylbenzoyl)doxorubicin (**3.7**) in Chapter 3, **3.7** is much less potent ($IC_{50} = 5.8 \mu\text{M}$) than that of native doxorubicin ($IC_{50} = 1.6 \text{ nM}$, Figure 4.4). Addressing this decrease in potency was one of the biggest challenges in the development of the NEBI platform. In this chapter, I report studies that attempt to use the *o*-NEBI platform to release native doxorubicin through hydrolysis of the amide bond to address this issue.

6.2 Electronic effects of substitution on the rate *ortho*-formylbenzoyl ester hydrolysis

Compounds **6.1-6.3** were synthesized to determine the influence of electron donating and electron withdrawing substituents on ester hydrolysis of substituted *ortho*-formylbenzoyl esters, (Figure 6.1). Hydrolysis studies of these compounds showed that an electron donating methoxy group (R = OMe, **6.1**) did not change the rate of hydrolysis of the ester at pH 5.5 compared to the unsubstituted *ortho*-formylbenzoyl ester, **5.2**. Compound **6.2**, substituted with an electron withdrawing cyano group, increased the rate of ester hydrolysis to 25 h at pH 5.5 and 0.58 h at

pH 7.4. Substitution with a stronger electron withdrawing nitro substituent (**6.3**), exhibited further increased the rate of hydrolysis to a half-life of 3.8 h and 0.28 h at pH 5.5 and 7.4, respectively (Figure 6.1). The EWG apparently rendered the ester carbonyl in **6.2** and **6.3** more electron poor, thus making it more susceptible to attack by a neighboring formyl group and leading to accelerated hydrolysis.

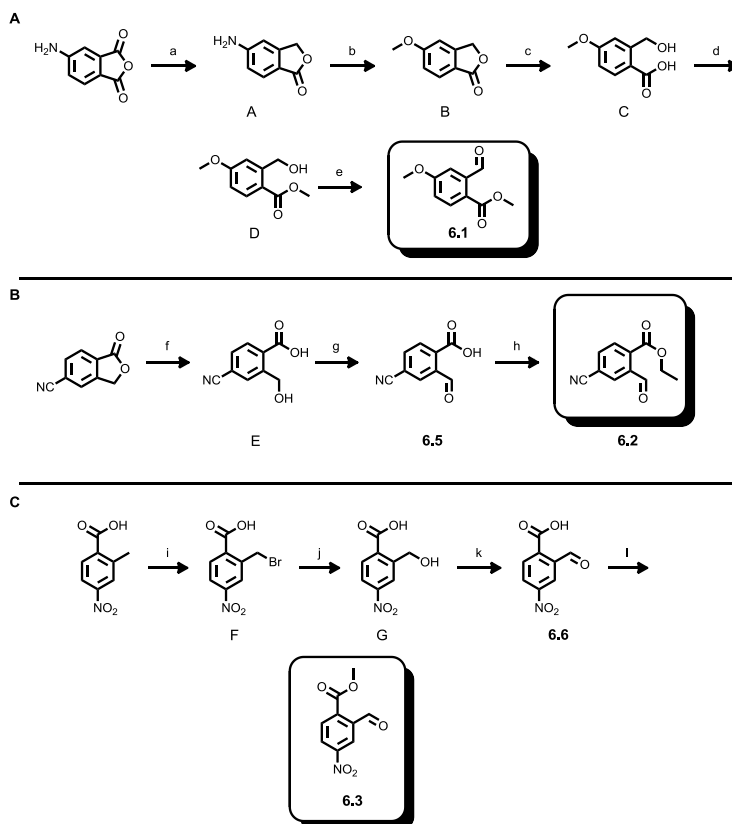
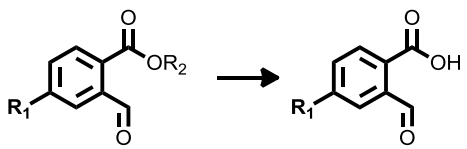


Figure 6.1 Schematic of the synthesis of **6.1**, **6.2** and **6.3**. A) Synthesis of **6.1**. Reagents: a) Zn, sodium hydroxide in water at 0 °C, 96% yield b) water and concentrated HCl, NaNO₂, MeOH c) potassium hydroxide, MeOH 60% yield, d) MeI, sodium carbonate, DMF, e) manganese oxide, THF, 55% yield. B) Synthesis of **6.2** f) LiOH, THF, water, 98% yield, g) manganese oxide, THF, reflux 32% yield, h) EtI, potassium carbonate, DMF, 92% yield. C) Synthesis of **6.3** i) 1,3-dibromo-5,5-dimethylhydantoin, DCM, j) LiOH, THF, water, 20% over two steps, k) manganese oxide, THF, 60 °C, 45% yield, l) MeI, potassium carbonate, DMF, 75% yield.

6.3 The presence of a nucleophile on the rate *ortho*-formylbenzoyl ester hydrolysis

Previous reports by Bender *et. al* also found that the presence of nucleophiles could assist in the hydrolysis of *ortho*-formylbenzoyl esters.¹²² There are a variety of nucleophiles found in physiological conditions. To verify Bender *et. al.*'s reports, I measured the rate of hydrolysis of **5.3**, **6.1** and **6.2** in the presence of glutathione (2.5 mM, the average glutathione concentration in cells)¹²⁷, a thiol containing nucleophile found in the cell. The rates of ester hydrolysis increased in both **5.3** and **6.1** in the presence of glutathione to a half-life of 55 h and 105 h, respectively (Figure 6.2). While glutathione did increase the rate of hydrolysis of **5.2**, it was less effective in **6.1** and **6.2**. The rate of hydrolysis for **6.3** in the presence of glutathione in pH 5.5 was not measured.



Compound	$t_{1/2}$ of hydrolysis (hours)		
	pH 5.5 ^a	pH 5.5 ^b	pH 7.4 ^c
5.2	130	55	5.1
6.1	130	105	N/A
6.2	25	23	0.58
6.3	3.8	N/A	0.28

5.2 R₁ = H R₂ = OMe
 6.1 R₁ = OMe R₂ = OMe
 6.2 R₁ = CN R₂ = OEt
 6.3 R₁ = NO₂ R₂ = OMe
 5.3 R₁ = H
 6.4 R₁ = OMe
 6.5 R₁ = CN
 6.6 R₁ = NO₂

Figure 6.2 Hydrolysis of substituted *ortho*formylbenzoyl esters. ^a50 mM MES buffer with 30% DMSO. ^b50 mM MES buffer, with 2.5 mM glutathione and 30% DMSO. ^c50 mM HEPES buffer with 30% DMSO

6.4 Hydrolysis studies of substituted *N*-(2-formylbenzoyl)doxorubicin

Substituted *N*-(2-formylbenzoyl)doxorubicin derivatives were synthesized to determine if the increased rates of ester hydrolysis in **6.2** and **6.3** could translate to the hydrolysis of a *N*-(2-formylbenzoyl)amide. Doxorubicin derivatives **6.7**, **6.8** and **6.9** were synthesized through EDC coupling (Figure 6.3). Compounds **6.7**, **6.8** and **6.9** were monitored for hydrolysis at pH 5.5 and 7.4 through HPLC. Unfortunately, the HPLC traces did not reveal any hydrolysis or release of free doxorubicin from **6.7**, **6.8** and **6.9** over the course of 10 days at either pH. While hydrolysis may have occurred eventually, the rates would be too slow to be relevant for a DDS using the *o*-NEBI platform. We also did not observe any amide hydrolysis of **6.7** in the presence of 2.5 mM glutathione after 100 h at pH 5.5.

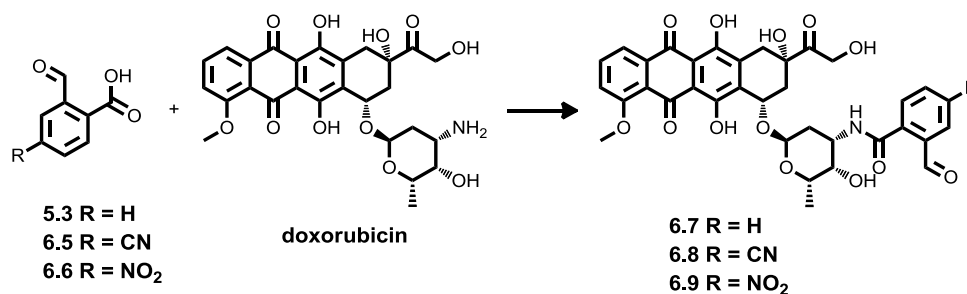


Figure 6.3 Synthesis of substituted *N*-(2-formylbenzoyl)doxorubicin. Reagents: EDC and DMAP.

6.5 Cytotoxicity studies of substituted *N*-(2-formylbenzoyl)doxorubicin

Although hydrolysis of **6.7-6.9** was not detected in cell free solutions, I considered that physiological conditions within the cell may lead to hydrolysis of the amide and release of native doxorubicin. While glutathione did not assist in amide hydrolysis in **6.7**, there are many other nucleophiles found in cells. I hypothesized that other nucleophiles found in physiological conditions may assist the hydrolysis of doxorubicin from **6.7-6.9**.

To determine if nucleophiles found in biological conditions could influence the rate of hydrolysis and increase the potency of substituted *N*-(2-formylbenzoyl)doxorubicin, cytotoxicity studies were performed on compounds **6.7-6.9**. I compared the IC_{50} of compounds **6.7-6.9** to the stable *N*-(4-formylbenzoyl)doxorubicin (**3.7**), and native doxorubicin. Cytotoxicity studies revealed that these doxorubicin derivatives (**6.7-6.9**) exhibit a slightly lower IC_{50} when compared to **3.7** (IC_{50} 5.8 μ M), but was still not as potent as native doxorubicin (IC_{50} 1.6 nM, Figure 6.4). While it is possible that hydrolysis of the amide is occurring in the cell, the hydrolysis is apparently very slow. And no evidence supports this hypothesis. Also, if we were to compare the theoretical rates of hydrolysis of amides **6.7-6.9**, we would assume **6.9** would have the highest rate of hydrolysis, and therefore higher potency than the other compounds, but derivatives **6.7-6.9** all had IC_{50} values in the same order of magnitude. I thus, conclude that there was little to no release of native doxorubicin from substituted *N*-(2-formylbenzoyl)doxorubicin derivatives in cells.

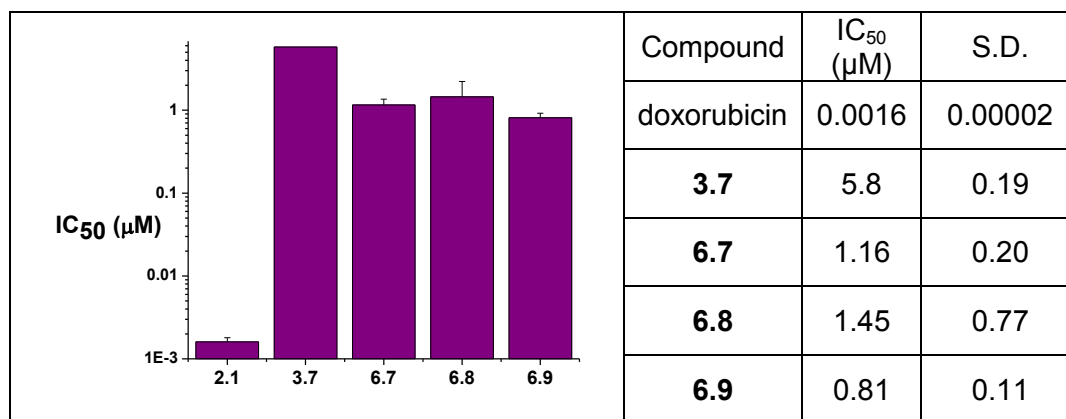


Figure 6.4 Cytotoxicity of doxorubicin and its derivatives.

6.6 Additional electronic effects on *o*-NEBI hydrolysis

Although we were unable to show the release native doxorubicin from this *o*-NEBI platform, we were able increase the rate of release of alcohols by substitution with an EWG in the para position to the ester. Such electronic effects may be useful for increasing the rate of alcohol containing drugs from a DDS comprised of an acid-sensitive *o*-NEBI linker. In Chapter 2, we showed that EDGs and EWGs in the para and ortho positions of the NEBI functional group had electronic effects that influenced the rate of hydrolysis. To fully characterize the effects of substitution on the rates of hydrolysis of the *o*-NEBI groups, I decided to determine the influence an EWG meta to the NEBI functional group would have on the rate of hydrolysis of the NEBI. In order to determine the effects of an EWG meta to the NEBI on the phenyl ring, I synthesized **6.10** (Figure 6.5) and measured the rate of hydrolysis.

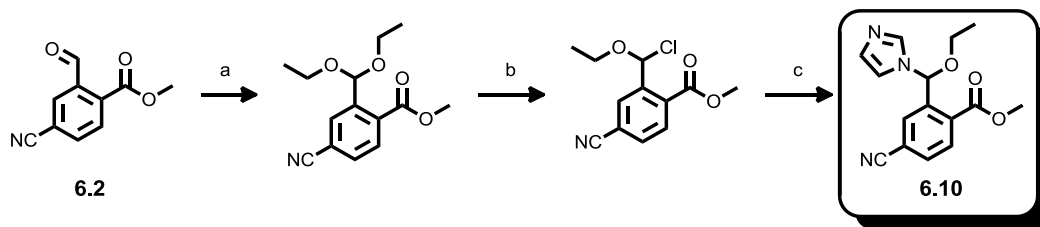


Figure 6.5 Synthetic scheme for 6.10. Reagents: a) ethylorthoformate, EtOH, and TsOH, 33% yield b) thionyl chloride c) imidazole, NaH, in THF, 64% yield over two steps.

Hydrolysis studies of the NEBI functional group was found to be very slow for compound **6.10**. At pH 5.5, the hydrolysis half life was 1000 h, and at 7.4 it was at approximately 3500 h. While these slow rates of hydrolysis are unfortunate, the tunable properties of the NEBI will allow for speeding up the first step through imidazole substitution as shown in Chapter 2 and 5.

6.7 Conclusions

In these studies, we found that EWGs could increase the rate of hydrolysis of the *ortho*-formylbenzoyl esters, but did not increase the rate of hydrolysis for substituted *N*-(2-formylbenzoyl)doxorubicin derivatives in a time frame that would be useful for the *o*-NEBI platform in a DDS. Cytotoxicity studies were used to investigate if nucleophiles found in physiological conditions could aid the hydrolysis for *N*-(2-formylbenzoyl)doxorubicin. There was no improvement in potency of substituted *N*-(2-formylbenzoyl)doxorubicin, compounds **6.7-6.9** when compared to *N*-(4-formylbenzoyl)doxorubicin. All of the data from the hydrolysis and cytotoxicity studies supports that there is not an appreciable amide hydrolysis that would be applicable to a DDS consisting of an *o*-NEBI linker.

While we were unable to show accelerated amide hydrolysis, we did find that the rate of ester hydrolysis can be increased through neighboring group assistance from *ortho*-formylbenzoyl esters. Substitution of *ortho*-formylbenzoyl esters led to an increase in ester hydrolysis rates, but also led to a decrease in the rate of NEBI hydrolysis. The rates of hydrolysis of the NEBI and the *ortho*-formylbenzoyl ester can likely be fine tuned in the future with a combination of substituents on the phenyl ring and on the imidazoles. Although these results may seem disappointing, the information gathered in these experiments were still vital in exploring and fully determining the properties of the *o*-NEBI platform.

Notes about this chapter

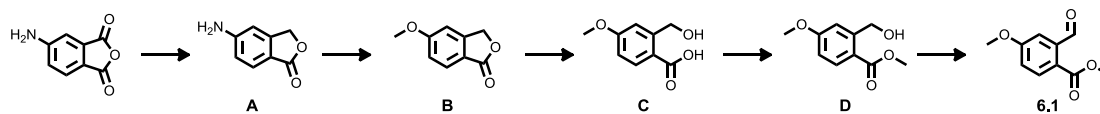
I would like to thank Barbara Breitenbücher for developing methods to synthesize compound **6.1** and Prof Jerry Yang for his guidance in this work.

6.8 Experimentals

All reagents were purchased from Sigma-Aldrich, Inc., TCI, or Alfa Aesar and used without further purification. NMR spectra were recorded on a Varian 400 (FT, 400 MHz, ¹H; 100 MHz, ¹³C) spectrometer. HR-MS (high-resolution mass spectra) were obtained in the Department of Chemistry & Biochemistry, University of California, San Diego. Kinetic analysis by reverse-phase high performance liquid chromatography (RP-HPLC) was performed with a Agilent 1100 Series HPLC using an analytical reverse-phase column (SPHERI-5 Phenyl 5 micron, 250 x 4.6 mm).

The synthesis of **5.2** was described in Chapter 5 and compound of **5.3** is commercially available.

Synthesis of 6.1



Synthesis of **A**

A solution of 4-Aminophthalimide (5.3 g) of was added to a solution of Zn (10.0 g) and NaOH (3.0 g) in water at 0 °C over the course of 15 minutes. The solution as refluxed at for 3 h and then filtered. Concentrated HCl was added to the solution until the pH was around 2.0. The solution was then boiled for 45 minutes. After the solution cooled, sodium carbonate was added until the pH was around 8. The product was allowed to precipitate overnight and then filtered out. 96% yield. Characterization of (**A**): $^1\text{H-NMR}$ (CD_3OD , 400 MHz) δ 5.184 (s, 2H), 6.652 (s, 1H), 6.727-6.752 (m, 1H), 7.518 (d, 1H, $J = 8.4$ MHz). ESI-MS (m/z , $\text{M}+\text{H}^+$) = 150.20 ($\text{M}+\text{Na}$) = 172.01.

Synthesis of **B**

A solution of **A** (4.68 g) in 50 mL of water and 50 mL of concentrated HCl was put in an ice bath. A solution of NaNO_2 (21.7 g) dissolved in water and MeOH was added slowly, keeping the temperature of the solution below 5 °C. MeOH (30 mLs) was added to the solution and refluxed for 2 h.¹²⁸ The MeOH was removed in under reduced pressure. Saturated ammonium chloride solution was added, and washed by EtOAc 3 times. The organic layers were pooled, dried with NaSO_4 and removed under reduced pressure. The product (**B**) was purified with column chromatography using eluent a 80:20 mixture of hexanes:EtOAc and 60:40 mixture

of hexanes:EtOAc. Characterization of (**B**): $^1\text{H-NMR}$ (CDCl_3 , 400 MHz) δ 3.901 (s, 3H), 5.249 (s, 2H), 6.917 (s, 1H), 7.028-7.050 (dd, 1H), 7.825 (d, 1H). ESI-MS (m/z , $\text{M}+\text{H}^+$) = 165.20, ($\text{M}+\text{NH}_4^+$) = 181.96.

Synthesis of **C**

A solution of **B** (1.1 g, 6.7 mmol) and KOH (470 mg, 8.37 mmol) in 7 mL of 85% aqueous MeOH was refluxed for 1.5 h. After removal of the solvent under reduced pressure, the crude mixture was taken up in 60 mL H_2O and extracted with 180 mL DCM. The aqueous layer was acidified with acetic acid, which resulted in the formation of crystals. These crystals were filtered and dried under reduced pressure. Product **C** (730 mg, 4 mmol, 60% yield) was isolated as colorless crystals. Characterization of (**C**): $^1\text{H-NMR}$ (CDCl_3 , 400 MHz) δ 3.891 (s, 3H), 4.812 (s, 2H), 5.302 (s, 1H), 6.873-6.991 (m, 1H), 6.997-7.013 (m, 1H), 8.093-8.124 (m, 1H). ESI-MS (m/z , $\text{M}+\text{H}^+$) = 182.97

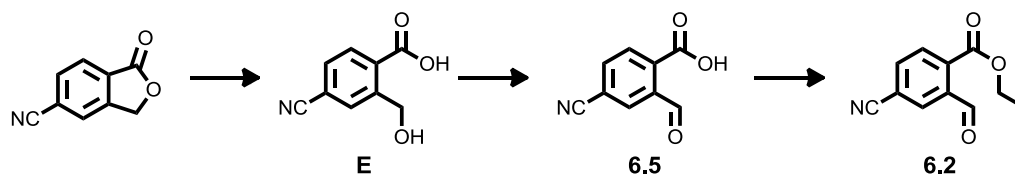
Synthesis of **D**

To a solution of **C** (15.5 mmol) and sodium carbonate in DMF was added methyl iodide (17.1 mmol). The solution was allowed to stir overnight. Sodium bicarbonate was added to the solution and extracted with EtOAc three times. The organic layer was pooled and dried over sodium sulfate. The organic layer was then dried under reduced pressure. Crude product **D** was used without further purification. 80% yield Characterization of (**D**): $^1\text{H-NMR}$ (CDCl_3 , 400 MHz) δ 3.859 (s, 3H), 3.893 (s, 3H), 4.757 (s, 2H), 6.830 (dd, 1H), 6.962 (d, 1H), 7.9983 (d, 1H) ESI-MS (m/z , $\text{M}+\text{H}^+$) = 196.91, ($\text{M}+\text{Na}^+$) = 219.02

Synthesis of **6.1**:

A solution of **D** (3.0 g, 1.3 mmol) and manganese oxide (7.8 g) was stirred in DCM for overnight. The solution was filtered and purified with column chromatography using as eluent 3:7 EtOAc:hexanes. 55% yield. Characterization of (**6.1**): $^1\text{H-NMR}$ (CDCl_3 , 400 MHz) δ 3.897 (s, 3H), 3.938 (s, 3H), 7.119 (dd, 1H), 7.406 (d, 1H), 7.984 (d, 1H), 10.700 (s, 1H) HR-ESI-FT-MS (m/z) calcd = 194.0574; found = 194.0576.

Synthesis of **6.2** and **6.5**



Synthesis of **E**

A 1M solution of LiOH (38 mL) was added to a solution of 5-cyanophthalide (5.0 g) in 1:1 of THF:H₂O and stirred over night. The solution was acidified by 3M HCl and extracted with EtOAc 3 times. The organic layer was pooled and dried with Na₂SO₄ and removed under reduced pressure. The product was used without further purification. 98% yield. Characterization of (**E**): $^1\text{H-NMR}$ (CD_3OD , 400 MHz) δ 4.975 (s, 2H), 7.725 (d, 1H), 8.036 (s, 1H), 8.055-8.075 (m, 2H) $^{13}\text{C-NMR}$ (CDCl_3 , 100 MHz) δ 61.435, 115.457, 118.015, 130.204, 130.432, 131.219, 132.588, 145.494, 167.620 ESI-MS (m/z , M-H⁻) = 176.00.

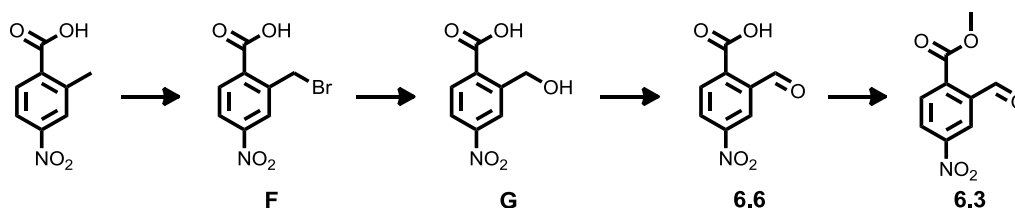
Synthesis of **6.5**

A solution of **E** (3.7 g) and manganese oxide (27.0 g) in THF was refluxed overnight. The reaction was filtered and purified using silica chromatography with 2:3:95 Acetic Acid:MeOH:DCM mixture as eluent. 32% yield. Characterization of (**6.5**): $^1\text{H-NMR}$ (CD_3OD , 400 MHz) 7.994 (d, 2H), 8.067 (s, 1H) δ ESI-MS (m/z , M-H^-) = 173.95

Synthesis of **6.2**

Potassium carbonate (2.0 g) and ethyl iodide (573 μL) was added to a solution of **6.5** (895 mg) in DMF and allowed to stir overnight. The product was extracted with DCM from saturated sodium bicarbonate. The product (**6.2**) was purified using silica chromatography with 20:80 EtOAc:hexanes mixture as eluent. Yield: 92%. Characterization of (**6.2**): $^1\text{H-NMR}$ (CD_3OD , 400 MHz) δ 1.441 (t, 3H), 4.493 (m, 2H), 7.899 (d, 1H), 8.110 (d, 1H), 8.205 (s, 1H), 10.599 (s, 1H) ^{13}C (CD_3OD , 100MHz) 14.388, 63.032, 115.649, 117.156, 131.1367, 132.394, 135.797, 135.937, 137.709, 164.494, 189.955. ESI-MS (m/z , M+H^+) = 203.95

Synthesis of **6.3** and **6.6**.



Synthesis of **F**

A solution of 2-methyl-4-nitrobenzoic acid (1.0 g) and 1,3-dibromo-5,5-dimethylhydantoin (1.0 g) was stirred in dry DCM at 10-20 $^{\circ}\text{C}$ until everything was

dissolved. The reaction was then transferred outside into the sunlight and stirred for 3 h. The DCM in solution was removed under reduced pressure. The crude (**F**) reaction was taken to the next step without purification.

Synthesis of **G**

A solution of 1M LiOH (6 mL) and THF/water was added to crude **F** and stirred for 48 h. The THF was removed under reduced pressure. A solution of 3N HCl was added to the solution until acidic, and then extracted 3 times with EtOAc. The product (**G**) was purified using silica chromatography, with 2:5:93 acetic acid:MeOH:DCM mixture as eluent. Yield: 20% over two steps. Characterization of (**G**): $^1\text{H-NMR}$ (CD_3OD , 400 MHz) δ 4.84 (s, 2H), 7.94, (m, 2H), 8.35 (s, 1H). ESI-MS (m/z , M-H^-) = 195.99

Synthesis of **6.6**

A solution of **G** (200 mg, 1 mmol) was stirred with manganese oxide (10.7 mmol) overnight in dry THF. The solution was heated at 60 °C for one hour. Compound **6.6** was purified with silica chromatography using 4:96 MeOH:DCM as an eluent. Yield: 45%. Characterization of (**6.6**): $^1\text{H-NMR}$ (CD_3OD , 400 MHz) δ 7.94 (d, 1H), 8.08 (d, 1H) 8.50 (s, 1H). ESI-MS (m/z , M-H^-) = 193.99

Synthesis of **6.3**

A solution of **6.6** (0.1 mmol), potassium carbonate (0.3 mmol), and methyl iodide (0.2 mmol) was stirred in dry DMF overnight. The DMF was removed under reduced pressure. The reaction was purified using silica chromatography, using 1:1 hexanes:DCM as an eluent. Yield: 75%. Characterization of (**6.3**): $^1\text{H-NMR}$

(CDCl₃, 400 MHz) δ 4.04 (s, 3H), 8.18 (d, 1H), 8.47 (d, 1H), 8.76 (s, 1H), 10.68 (s, 1H) ESI-MS (m/z , M-H⁻) = 208.14

Synthesis of 6.7

A solution of 2-carboxybenzaldehyde (2.58 mg), doxorubicin (3.7 mg), EDC (3.3 mg), and DMAP (1 crystal) was stirred in DMF overnight. Compound **6.7** was purified using silica chromatography with 2:7:91 TEA:MeOH:DCM mixture as eluent. Yield: 8%. Characterization of (**6.7**): ¹H-NMR (CD₃OD, 400 MHz) δ 1.32 (d, 3H), 1.44-1.46 (d, 1H), 2.15 -2.20 (m, 1H), 2.38-2.42 (m, 1H), 2.97-3.09 (m, 1H), 3.25-3.29 (m, 1H), 3.66 (m, 1H), 4.10 (3H, s), 4.38 (d, 2H), 4.78 (m, 2H), 5.37-5.38 (d, 1H), 5.37 – 5.38 (d, 1H), 7.40-7.42 (d, 1H), 7.52-7.64 (m, 3H), 7.76-7.82 (m, 2H), 8.03-8.06 (m, 1H). ESI-MS (m/z , M+Na⁺): 698.20 HR-MS M+Na⁺ = 698.1847

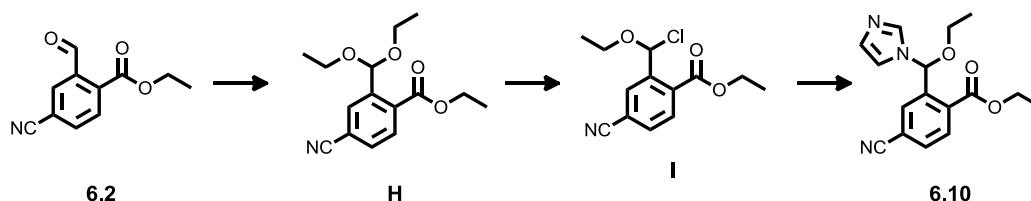
Synthesis of 6.8

A solution of **6.4** (8.0 mg), doxorubicin (13.2 mg), EDC (8.7 mg), and DMAP (1 crystal) was stirred in DMF overnight. Compound **6.8** was purified using silica chromatography with 2:7:91 TEA:MeOH:DCM mixture as eluent. Yield: 14%. Characterization of (**6.8**): ¹H-NMR (CDCl₃, 400 MHz) δ 1.32 (d, 3H), 1.74-1.77 (m, 1H), 1.97-2.00 (m, 1H), 2.14-2.24 (m, 1H), 2.36-2.42 (m, 1H), 3.26-3.38 (m, 2H), 3.65 (s, 1H), 3.90 (s, 1H), 3.97 (s, 1H), 4.05 (s, 3H), 4.34 (m, 1H), 4.80 (d, 2H), 5.57-5.61 (m, 1H), 7.37 (d, 1H), 7.73-7.98 (m, 4H), 8.01 (m, 1H). ESI-MS (m/z , M+Na⁺) = 723.16

Synthesis of 6.9

A solution of **6.5** (19 mg), doxorubicin (5.3 mg), EDC (53 mg), and triethylamine (34 μ L) was stirred in DMF overnight. Compound **6.9** was purified using silica chromatography with 2:7:91 TEA:MeOH:DCM mixture as eluent. Yield: 52%. ESI-MS (m/z , $M-H^-$) = 699.14

Synthesis of 6.10



Synthesis of H

A solution of **6.2** (20 mmol), triethyl orthoformate (60 mmol), and TsOH (1.9 mmol) was refluxed in 10 mL of EtOH for 24 hrs. After removal of ethanol under reduced pressure, DCM was added and the organic layer was extracted with saturated sodium bicarbonate solution. The organic layer was dried over anhydrous Na_2SO_4 . After removal of diethyl ether under reduced pressure, the crude mixture was isolated by silica chromatography using as eluent of 80:20 hexanes:diethyl ether to give pure **H** (33 % yield). Characterization of (**H**): $^1\text{H-NMR}$ (CDCl_3 , 400 MHz) δ 1.23 (t, 6H), 1.40 (t, 3H), 3.52-3.67 (m, 4H), 4.37 – 4.42 (m, 2H), 6.11 (s, 1H), 7.64 (dd, 1H), 7.79 (d, 1H), 8.07 (d, 1H). $^{13}\text{C-NMR}$ (CDCl_3 , 100 MHz) δ 14.38, 1537, 62.04, 62.79, 98.24, 115.00, 118.36, 130.19, 131.17, 131.87, 134.98, 141.00, 166.92. HR-MS (m/z , $M+\text{Na}^+$) = 300.1208 Theoretical 200.1206

Synthesis of I

Compound **H** (0.9 mmol) and thionyl chloride (1 mmol) were combined without additional solvent and refluxed for 1 hour at 65 °C under N₂. The excess thionyl chloride was removed under reduced pressure and the crude mixture was used without further purification

Synthesis of **6.10**

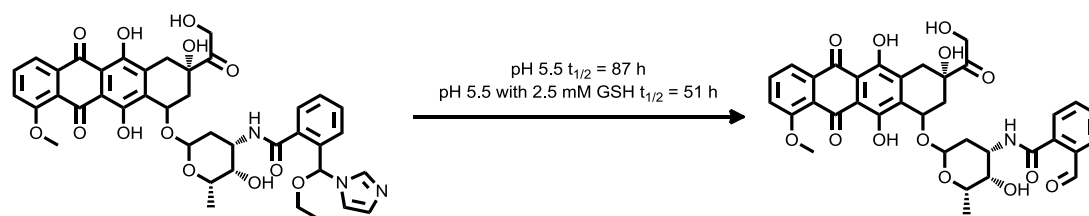
In a dry flask, NaH (2.7 mmol) was added to a solution of imidazole (1.8 mmol) dissolved in dry THF. The solution was allowed to stir for 1 hour at 23 °C, and then the crude mixture of **I** was added dropwise to the imidazole. The combined solution was stirred for 12 h at 23 °C. Saturated sodium bicarbonate was added to the solution and washed 3 times with DCM. The organic layers were pooled and dried over Na₂SO₄. The solvent was removed under reduced pressure. **6.10** was isolated by silica chromatography using as eluent a 2:58:40 mixture of TEA:EtOAc:hexanes. The isolated yield over two steps was 64%. Characterization of (**6.10**): ¹H-NMR (CDCl₃, 400 MHz) δ 1.22 (t, 3H), 1.30 (t, 3H), 3.48 (m, 1H), 3.56 (m, 1H), 4.29 (m, 2H), 6.87 (s, 1H), 7.02 (s, 1H), 7.11 (s, 1H), 7.65 (s, 1H), 7.68 (d, 1H), 7.92 (d, 1H), 8.01 (s, 1H) ¹³C-NMR (CDCl₃, 100 MHz) δ 14.28, 14.95, 62.39, 65.12, 82.69, 116.03, 117.28, 118.00, 129.94, 130.41, 131.24, 132.58, 132.96, 137.55, 140.46, 165.58. HR-MS = 299.1268, Theoretical = 299.1264

Hydrolysis and Cytotoxicity

Methods for hydrolysis and SRB cytotoxicity studies (with 2008 human ovarian carcinoma cells) followed those found in previous chapters (Chapters 3, 4).

Miscellaneous Data

Hydrolysis of Doxorubicin-o-NEBI



No amide hydrolysis was observed in this study after 100 hours.

Chapter 7

Towards the development of methods to site-specifically conjugate chemotherapeutic agents to trastuzumab via *o*-NEBI linkers

7.1 Introduction

This chapter focuses on developments made towards site-specific modifications of an antibody, trastuzumab, for future use in an antibody drug conjugate (ADC).¹²⁹ While there has been a lot of interest in antibodies as drug delivery carriers, most antibodies are labeled through solvent exposed lysines, or must be genetically engineered with cysteines available for modification.^{130, 131} In this chapter, we specifically modify the *N*-terminal amino acids on the heavy and light chains of trastuzumab for future conjugation to cytotoxic agents via a *o*-NEBI linker.

Trastuzumab is a monoclonal antibody, marketed by Genetech under the trade name Herceptin®, for treatment of breast cancer. Trastuzumab is known to bind to the HER2 receptor, which is over expressed in 25-30% of breast cancer patients.^{132, 133} The HER2 receptor dimerizes with other receptors in the same family (HER1, HER2, HER3, and HER4).¹³⁴ Binding of trastuzumab to the HER2 receptor prevents dimerization and interrupts signal transduction pathways in the cell, which can trigger apoptosis, lead to decreased angiogenesis, and antibody mediated cellular cytotoxicity.

While many antibodies have been explored for drug delivery, we choose trastuzumab because it is FDA approved, known to selectively bind the HER2 receptor, but, most importantly, it is known to undergo receptor mediated endocytosis.¹³⁵ Since we would like to create an ADC using trastuzumab as a carrier, it is imperative that the ADC reach the acidic endosomes and lysosomes in order for the NEBI to hydrolyze and release the cytotoxic agent.

In this chapter, I start using two mammary gland carcinoma cell lines for our studies. BT-474 and SK-BR-3 cells are known to over express the HER2 receptor.¹³³ For control purposes, we use human mammary gland carcinoma MCF-7 cells which do not over express the HER2 receptor. Our initial cytotoxicity studies with trastuzumab had no effect on MCF-7 cells, but lowered the cell survival to ~40% at 1 µg/mL concentrations in BT-474 and SK-BR-3 cells (Figure 7.1). The cytotoxicity data showed that we could not eliminate cell survival in BT-474 and SK-BR-3 cells using trastuzumab alone. This has been well documented by other labs who have also studied trastuzumab.¹³⁶ It is my hope that conjugation of a drug via

the NEBI will increase the potency of trastuzumab, and possibly further reduce cancer cell survival.

I modified the *N*-terminal amino acids using an innovative method developed by the Francis lab.^{137, 138} Treatment of proteins with pyridoxal 5-phosphate (PLP) gives an aldehyde or ketone to the *N*-terminal amino acid. The carbonyl formed in this reaction can undergo a reaction with an alkoxyamine to form an oxime. The oxime formation is considered a “click” reaction, and is advantageous because it is a bioorthogonal and high yielding reaction.

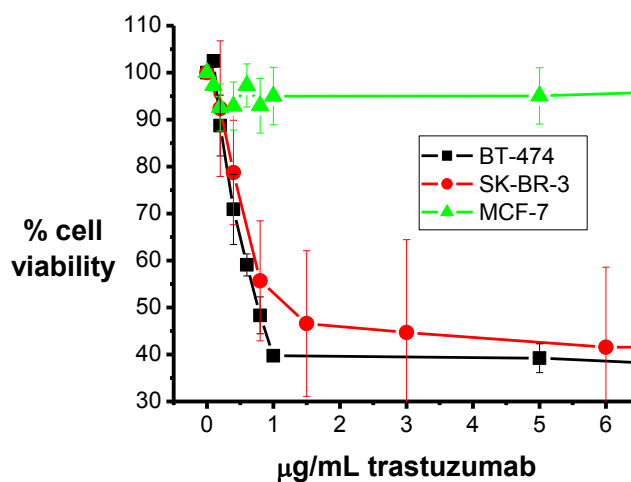


Figure 7.1 Cytotoxicity of trastuzumab on BT-474, SK-BR-3 and MCF-7 cells.

While we have not yet synthesized an ADC comprised of a NEBI linker and trastuzumab, we describe control experiments and the development of methods for future conjugation of trastuzumab to a drug via a NEBI linker. This chapter describes the extensive studies performed on trastuzumab in preparation of conjugation to the NEBI. I hope that new members of the lab can continue this work in the future by conjugating an *o*-NEBI bifunctional crosslinker with 5-fluoro-2'-deoxyuridine (5-FU) to create an ADC (Figure 7.2).

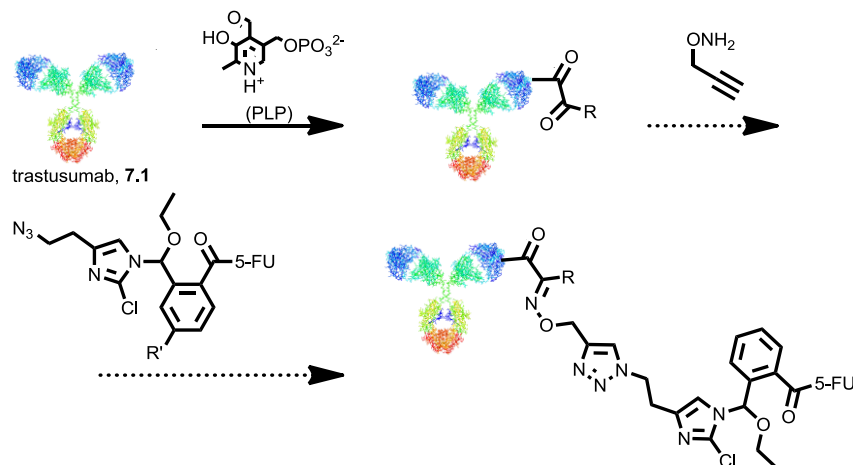


Figure 7.2 Proposed schematic for conjugation of 5-fluoro-2-deoxyuridine to trastuzumab.

7.2 Co-localization studies

To confirm that trastuzumab localized in the endosomes and lysosomes, trastuzumab (**7.1**) was labeled with fluorescein isothiocyanate to give fluorescein labeled trastuzumab (**7.2**). SK-BR-3 (Figure 7.3) cells, BT-474 cells (Figure 7.4), and MCF-7 cells were incubated with **7.2** and LysoTracker Blue (Invitrogen). The cells were imaged with a Delta Vision Deconvolution Microscope System. Figure 7.3A and Figure 7.4A show that **7.2** localized into the lysosomes of cells that overexpress the HER2 receptor. Analysis of co-localized images with the Pearson coefficient¹¹⁹ found that BT-474 cells (Figure 7.3C) had the highest correlation between fluorescein and LysoTracker Blue fluorescence with a Pearson coefficient of 0.6560. SK-BR-3 cells (Figure 7.4C) had a Pearson coefficient of 0.2599. The control study with MCF-7 cells had an expected lower Pearson coefficient of 0.1406 due to the lack of HER2 receptors on the cells. This MCF-7 cell co-localization data correlates well to the cytotoxicity data in Figure 7.1, which showed that trastuzumab had no effect on cell survival of MCF-7 cells.

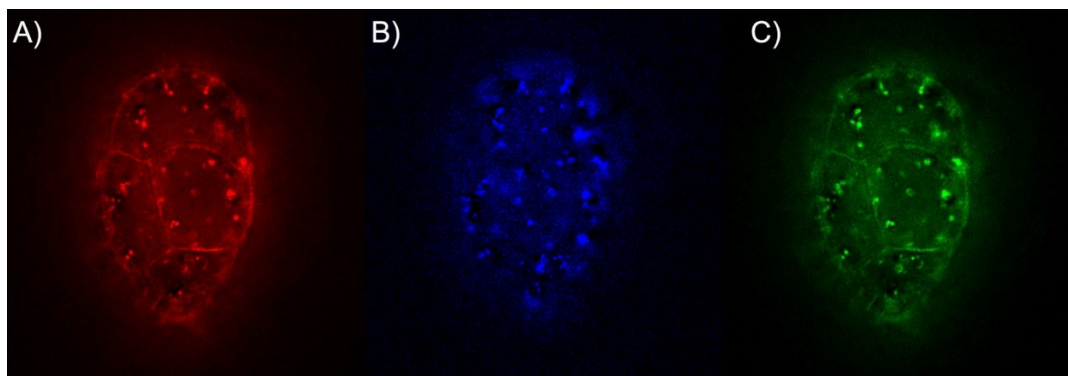


Figure 7.3 BT474 cells incubated with 7.2 and Lyotracker Blue. A) Fluorescence of 7.2. B) Fluorescence of Lyotracker Blue C) Colocalized image of A) and B) where there is fluorescence found from both channels. The correlation between fluorescein and lyotracker blue was found to be 0.6560 for this cell line.

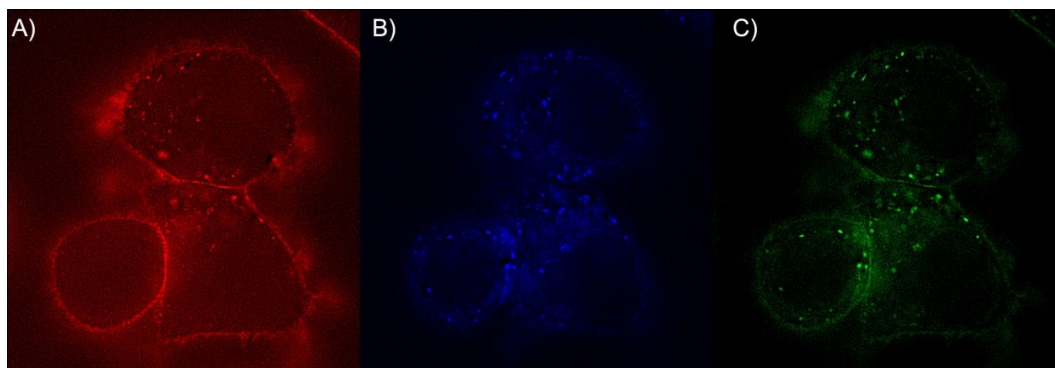


Figure 7.4 SK-BR-3 cells incubated with 7.2 and Lyotracker Blue. A) Fluorescence of 7.2. B) Fluorescence of Lyotracker Blue C) Colocalized image of A) and B) where there is fluorescence found from both channels. The correlation between fluorescein and lyotracker blue was found to be 0.2599 for this cell line.

7.3 Modification of trastuzumab

Transamination of the *N*-terminal amino acids of **7.1** was achieved by incubating **7.1** with PLP. A solution of **7.1** (100 μ L, 5 mg/mL, in 10mM sodium phosphate and 150 mM NaCl buffer at pH 7.4) was combined with PLP (100 μ L, 20 mM, in 25 mM sodium phosphate buffer at pH 6.5) at 37 $^{\circ}$ C (**7.3**), and 50 $^{\circ}$ C (**7.4**) for

20 h (Figure 7.5). Previous reports suggested that there was a higher *N*-terminal transamination at 50 °C than 37 °C. I did reactions at both temperatures to compare **7.3** to **7.4** to see if both would still be potent in cytotoxicity studies.

After the 20 h incubation, excess PLP was removed using a Zeba desalting column (Invitrogen). Modified trastuzumab, **7.3** and **7.4** were eluted using 10 mM phosphate buffer with 150 mM NaCl at pH 6.5.

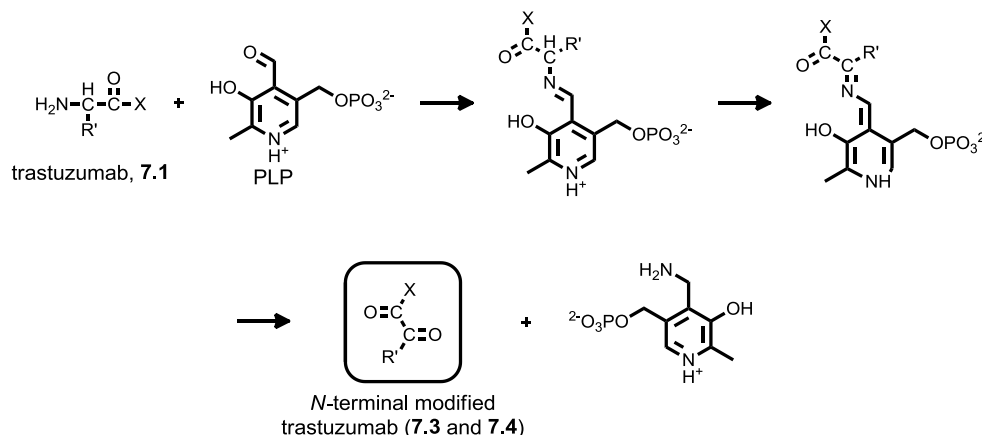


Figure 7.5 Schematic for modification of *N*-terminal amino acids with PLP, and formation of an oxime.

7.4 Verification of *N*-terminal transamination of trastuzumab

The transamination of the *N*-termini of **7.1** was verified through multiple methods. It was important to confirm the transamination would allow oxime formation, the location of transamination, and percent of modification. I first verified the formation of the ketone by labeling **7.3** and **7.4** with Alexa Fluor 488 hydroxylamine (Invitrogen, AF-488, Figure 7.6). A solution of **7.3** and **7.4** (20 μL , in 10 mM Phosphate buffer, 150 mM NaCl at pH 6.5) was incubated with AF-488 (1 μL , 2 mM in DMSO) for 18 h at room temperature. SDS-PAGE gel analysis showed

bands that correlated with the heavy and light chains of **7.3** and **7.4** to be fluorescently labeled. Control studies with **7.1** incubated with AF-488 showed no fluorescent labeling, which supports the formation of an oxime in **7.3** and **7.4** with AF-488. The control study verified that labeling of **7.1** required transamination, and it was not due to non-specific absorption of AF-488. These results are consistent with our hypothesis transamination of **7.3** and **7.4** were required for fluorescent labeling with AF-488 (Figure 7.6).

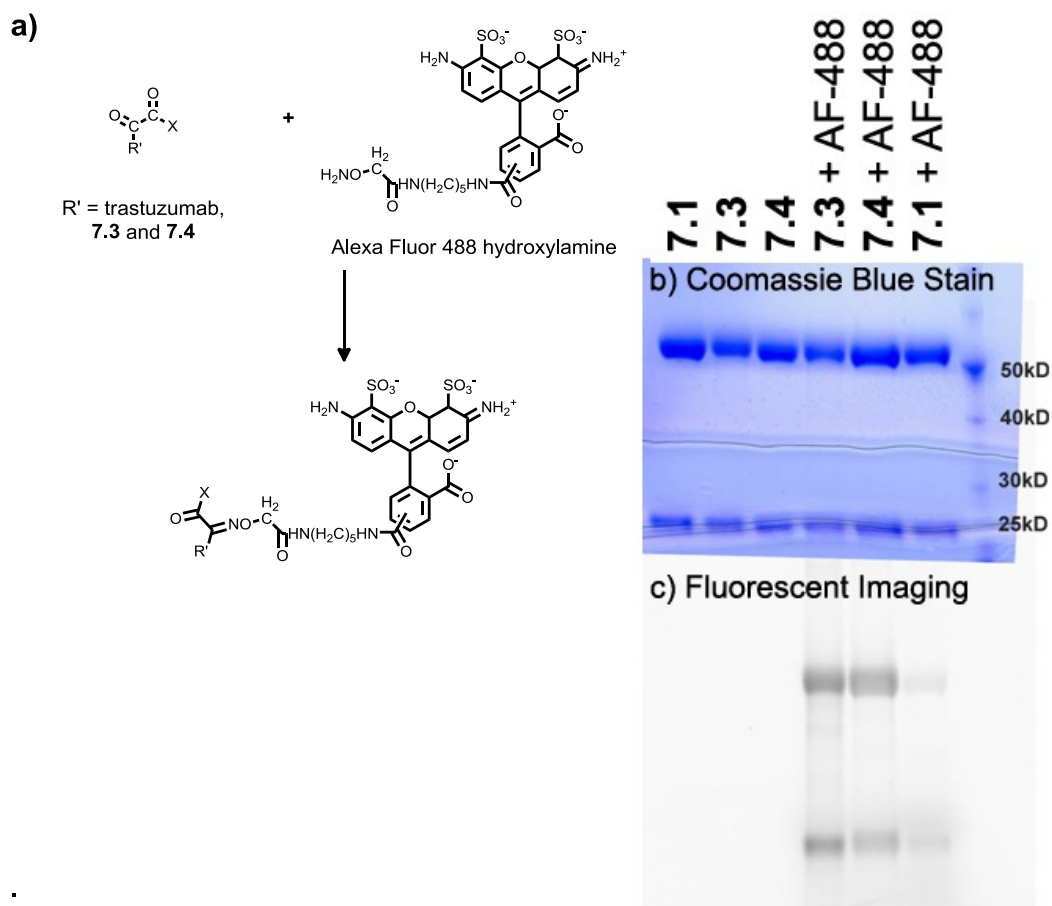


Figure 7.6 a) Schematic of labeling of **7.3** and **7.4** with AF-488 hydroxylamine. b) SDS-Page gel Coomassie Blue analysis of labeling of **7.1**, **7.3** and **7.4** with AF-488. c) Fluorescent image of SDS-PAGE gel.

While I was able to fluorescently label **7.3** and **7.4**, the location of AF-488 was not confirmed. To confirm the transamination occurred on the *N*-terminal amino acids of trastuzumab, I turned to MALDI MS. Initial studies of transamination of *N*-terminal amino acids performed by the Francis lab found that if the *N*-terminal amino acid was aspartic acid, there would also be a decarboxylation following the formation of the ketone (Figure 7.7).¹³⁸ Since the light chain of **7.1** contains an aspartic acid residue at the *N*-terminus, I confirmed the expected decarboxylation (similar to the decarboxylation of 3-ketoacids), as well as the formation of the ketone on the heavy chain through MALDI-TOF/MS.

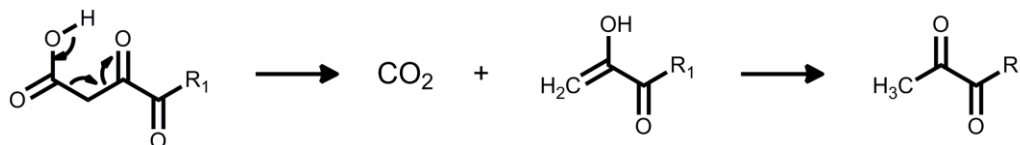


Figure 7.7 Proposed mechanism for decarboxylation

Samples of **7.1**, **7.3** and **7.4** were digested by trypsin, and the mass of the fragments were determined by MALDI-TOF/MS. The *N*-terminal light chain fragment, DIQMTQSPSSLSASVGDR, as expected from a trypsin digest of unmodified trastuzumab **7.1**, had a calculated mass of 1877.9 Da. The expected mass change due to transamination followed by decarboxylation was -44.6 Da, for a final mass of 1833.3 Da. The *N*-terminal heavy chain peptide fragment of **7.1**, EVQLVESGGLVQPGGSLR, had a calculated mass of 1881.0 Da. Transamination would change the mass by 1.0 dalton, giving a MW of 1880.0 Da. Analysis of the peptide sequence of trastuzumab showed that there would be no other trypsin fragments that would correlate to these masses.

When unmodified trastuzumab **7.1** was digested with trypsin MALDI-TOF/MS showed a $M+H^+$ peak for the light and heavy chain at 1879.9 and 1881.9 Da respectively (Figure 7.8A). Modified trastuzumab (**7.3** and **7.4**) showed an increase in intensity for 1880.95 Da, which correlates with transamination of the heavy chain $M+H^+$ (Figure 7.8B). There was also a diminished peak for the light chain $M+H^+$ (Figure 7.8B), and a new peak mass, $M+H = 1833.9$ Da, which correlates with the mass expected for the modified light chain $M+H^+$. This data supports that the modification occurred on the *N*-terminal amino acids of the light and heavy chains of trastuzumab. While I performed MALDI-TOF/MS on **7.4** as well, the data looks very similar to the data attained for **7.3**. Since this data is not quantitative, we did not include the data in the Figure 7.8.

In order to determine quantitatively the percent conversion of transamination of trastuzumab due to PLP modification, I turned to a LC-MS experiment. The data for the LC-MS experiment was gathered by Majid Ghassemiam at the Biomolecular/Proteomics Mass Spectrometry Facility. We analyzed only **7.1** and **7.4** to minimize costs. This LC-MS experiment was conducted to measure the conversion of *N*-terminal amino acids by comparing the intensity of unmodified *N*-terminal light and heavy chains against an internal standard.

Once again, samples of **7.1** and **7.4** were digested with trypsin. In this experiment, the charge on the fragments were 2^+ , giving m/z peaks that were half the expected mass of the fragments. The data for **7.1** and **7.4** was scanned for mass peaks that correlate with the unmodified heavy chain and light chain. The heavy chain had a retention time from ~29.3-31.2 min, while the light chain had a retention time of ~23.2-25.0 minutes. The number of counts for each peak was normalized

by an internal standard with the retention time of 41.2 minutes. The intensity of the light and heavy chain of **7.4** when normalized, show the amount of unmodified light and heavy chain remaining. This data showed that only 8% of the original unmodified heavy chain and 6% unmodified light chain remained after incubation of PLP with trastuzumab at 50 °C for 20 h. From this data, I calculated the conversion due to transamination to be 92% and 94% for the heavy and light chain, respectively (Figure 7.9).

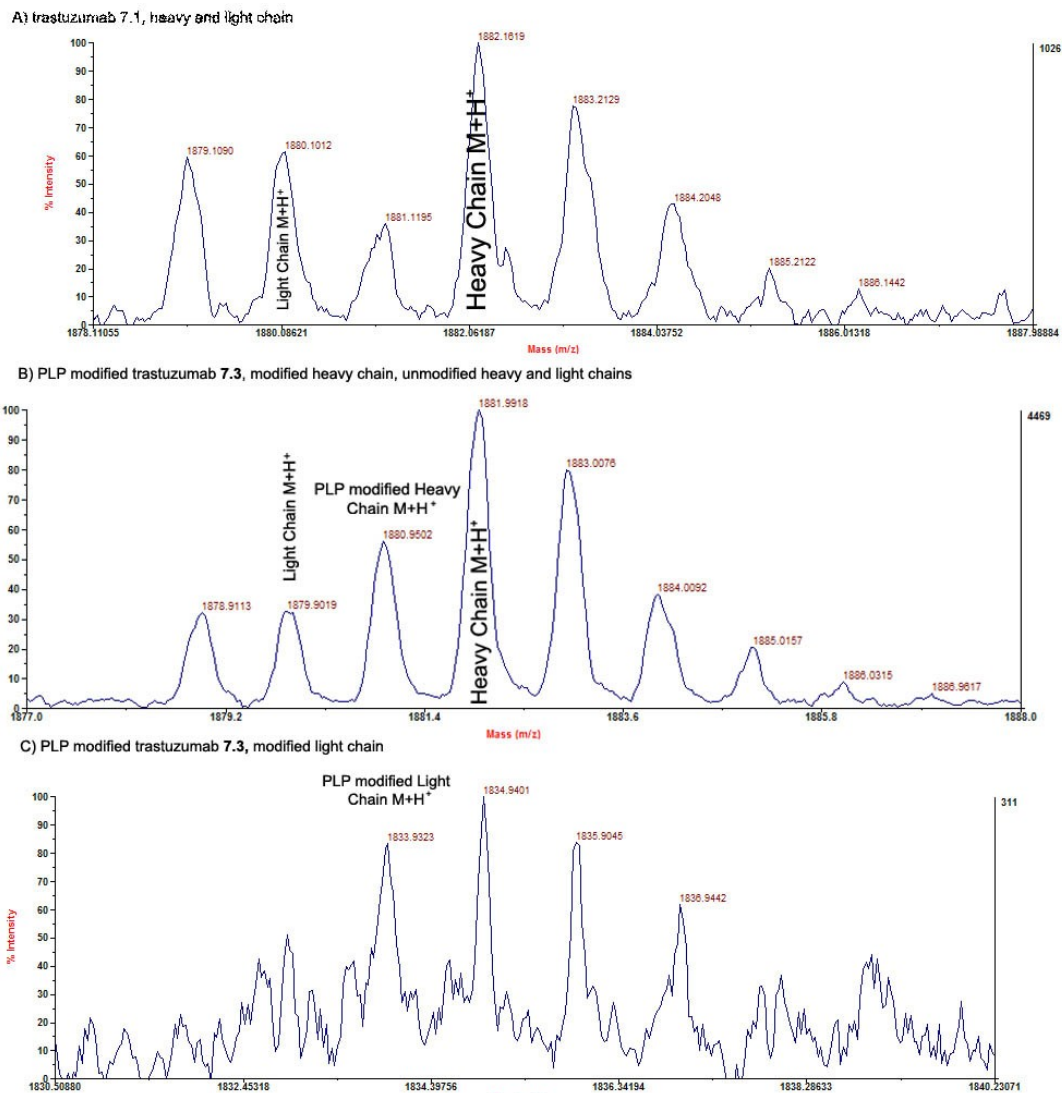


Figure 7.8 A) Sample 7.1, unmodified trastuzumab for control purposes. B) Sample 7.3, transaminated trastuzumab, with a increase peak at 1880.9 which correlates with a the M+H⁺ modified heavy chain. C) Sample 7.3, transaminated trastuzumab with a new peak at 1833.9 which correlates for the M+H⁺ of the modified light chain.

	Trastuzumab (7.1)		Transaminated trastuzumab (7.4)		Ratio of normalized intensity of unmodified chain	Percent modification
	Intensity	Normalized Intensity	Intensity	Normalized Intensity		
Heavy Chain	3.3E+05	5.8E-01	2582.9	4.83E-02	0.08	92
Light Chain	4.6E+05	8.2E-01	2768.8	5.18E-02	0.06	94
Internal Control	5.7E+05		5.4E+04			

Figure 7.9 LC-MS data comparing the intensity of mass peaks correlating to the heavy and light chain of 7.1 to 7.4. The peaks were normalized by an internal control, and the ratio provided the amount of unmodified heavy and light chain of 7.4. Assuming the lower intensity is due to conversion by PLP, we were able to calculate the percent modified by PLP.

7.5 Cytotoxicity Studies

Finally, I performed cytotoxicity studies on **7.3** and **7.4** to determine if transamination of trastuzumab had an effect on the potency of trastuzumab. The cytotoxicity data showed no significant difference in cell survival between the samples, and led us to conclude that transamination at 37 °C or 50 °C did not change the potency of **7.1** on SK-BR-3 cells (Figure 7.10).

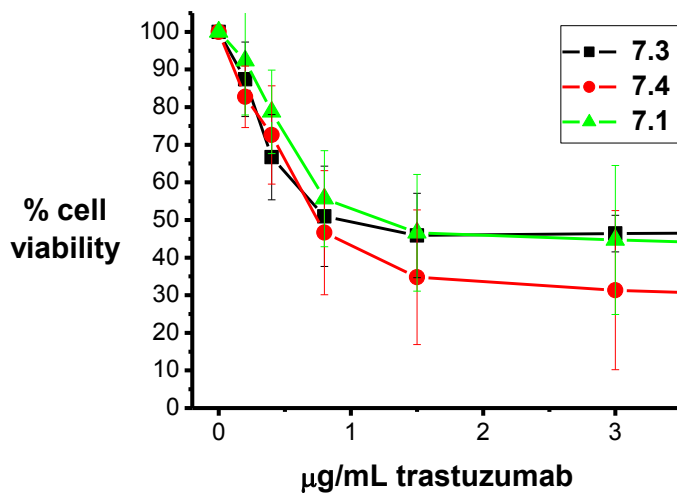


Figure 7.10 Cytotoxicity studies of 7.1, 7.3 and 7.4 on SK-BR-3 cells. Modification of trastuzumab with PLP showed no changes in cytotoxicity of trastuzumab.

7.6 Conclusions

Trastuzumab is an antibody that may be a good candidate as a drug delivery carrier because it binds specifically to the HER2 receptor, which is over expressed in 25-30% of breast cancer patients. While trastuzumab is known to undergo endocytosis, I confirmed this using by fluorescently labeling trastuzumab with fluorescein (7.2). Conjugate 7.2 was shown to enter the cells and localize in the endosomes and lysosomes. This verification is important, because an ADC comprised of a trastuzumab carrier and NEBI linker would require the acidic environment of the endosomes and lysosomes for hydrolysis and release of chemotherapeutics.

To specifically modify trastuzumab at the *N*-terminus, PLP was employed to transaminate the *N*-terminal amino acids found on the heavy and light chains of the antibody. AF-488 was used to verify that I could conjugate a hydroxylamine

containing compound to a modified trastuzumab. Labeling **7.3** and **7.4** with AF-488 was a proof-of-concept, supporting that the presence of a hydroxylamine on a NEBI bifunctional linker will most likely form an oxime with a transaminated trastuzumab (**7.3** and **7.4**) to label trastuzumab with alkyne functionalities. These alkynes will allow for covalent bonding of a NEBI carrying an alcohol containing drug via click chemistry.

Transamination of the *N*-terminal amino acids was confirmed by LC-MS methods. The percent conversion of transamination was high, with 92% and 94% conversion of heavy and light chains, respectively. This high conversion rate is important for conjugation of many NEBI linkers to deliver a higher payload of drugs when trastuzumab is used as a drug delivery carrier. In this case, with 92-94% conversion, we may be able to conjugate up to 3-4 drugs per ADC.

Lastly, to determine if the modifications on trastuzumab would influence the potency of trastuzumab, I performed a cytotoxicity study to compare native trastuzumab to the transaminated trastuzumab **7.3** and **7.4**. Cytotoxicity studies showed that there was no change in potency of **7.3** and **7.4** when compared to native trastuzumab. The data gathered in this chapter supports that trastuzumab is a good candidate for future as an drug delivery carrier for use in an ADC.

Notes of the chapter:

Many thanks to Kersi Pestonjamas from the UCSD Microscopy Facility for helping obtain fluorescent images. I would also like to thank Dr. Elizabeth Komives for training me to perform MALDI in Biomolecular/Proteomics Mass Spectrometry Facility. I would also like to thank Dr. Majid Ghassemiam for performing the LC-MS studies. Majid was also a lot of help when I required troubleshooting help for getting

my samples to fly in MALDI experiments. I would also like to thank Prof. Jerry Yang for his guidance, and for obtaining the grant from Genetech, which provided the trastuzumab used in this chapter.

7.7 Experimentals

FITC labeling of trastuzumab (7.2)

Trastuzumab (7.1, 2.6 mg/mL solution in PBS, pH 8.5, 1 mL) was combined with a solution of FITC (1 mg/mL solution in DMSO, 163 μ L). The 7.1/FITC mixture was incubated for 1 hour. The fluorescein labeled trastuzumab (7.2) was purified using a NAP 10 column, and eluted with phenol red free RPMI-1640 (Invitrogen) media.

Fluorescence Cellular Imaging Studies

Human mammary gland carcinoma BT-474, SK-BR-3, MCF-7 cells were plated with RPMI-1640, McCoys 5A, and DMEM phenol red free media supplemented with 10% FBS (Omega Scientific, FB-01) on 35 mm glass bottom dishes (MatTek Co., Ashland, MA) and incubated overnight. FITC-trastuzumab (7.2) was added to the cells to give a final concentration of 10 μ M of 7.2 and allowed to incubate for 24 h. LysoTracker Blue (Invitrogen, L7525) was added to the cells and incubated for 30 minutes. The remaining living cells were washed three times with phenol red free RPMI-1640 media without FBS and then immediately imaged with a Delta Vision Deconvolution Microscope System (Applied Precision, Issaquah, WA) equipped with a Nikon TE-200 inverted light microscope with infinity corrected lenses and with a mercury arc lamp as the illumination source. The co-localization

was determined using softWoRx image analysis software (Applied Precision, Issaquah, WA).

The intrinsic fluorescence of fluorescein (Abs/Em: 494/521 nm) was used to visualize the location of **7.2** and was observed by excitation with bandpass (bp) filtered light (Ex/bp: 490/20nm) and the emission monitored at Em/bp: 528/38 nm. The fluorescence of the LysoTracker Blue (Abs/Em: 373/422 nm) was detected using an Ex/bp: 360/40 nm excitation filter and an Em/bp: 457/50 nm emission filter.

In order to provide a quantifiable value for the co-localization of LysoTracker Blue and **7.2**, we determined the extent of overlap of the fluorescence of LysoTracker Blue and **7.2**. This imaging analysis afforded a Pearson's correlation coefficient.¹¹⁹

Trypsin Digestion and MALDI TOF/MS

5 μ L of sample (**7.1**, **7.3**, **7.4**) were combined with 15 μ L 70 mM Tris HCl with 9 mM urea and 5 mM DTT at pH 6.5. The solution heated at for 20 minutes at 95 °C and cooled. Iodoacetamide (1 μ L, 40 mM) was added to the solution and incubated for 30 minutes. Trypsin (20 μ L of 20 ng/ μ L) was added to the solution and incubated at 37 °C for 3 h. The samples were then lyophilized, and a Zip Tip was used to clean up and concentrate the samples for MALDI/TOF-MS, and LC-MS

Cytotoxicity studies of 7.1, 7.3 and 7.4 on MCF-7, BT-474 and SK-BR-3 cells

Human mammary gland carcinoma BT-474, SK-BR-3, MCF-7 cells were plated with RPMI-1640, McCoys 5A, and DMEM with 10% FBS respectively, on a 96 well plate (8000, 20,000, and 15,000 cells/well respectively). The cells were incubated for 24 h at 37 °C with 5% CO₂. After the incubation period, cells were

dosed with various concentrations of **7.1**, **7.3** and **7.4**. The cells were allowed to incubate with the antibodies for 72 h. After incubation, cells were washed 3 times with 200 μ L of PBS (Mediatech, 46-013CM) pH 7.4. Cells were then fixed with 200 μ L of PBS and 50 μ L of 50% trichloroacetic acid for one hour at 4 °C. After fixation, cells were washed 5 times with 200 μ L water and allowed to dry. A 0.4% sulforhodamine B (SRB, Sigma Aldrich, S1402) solution in 1% acetic acid (100 μ L) was added to the cells and incubated for 15 minutes at room temperature. The cells were washed 3 times with 1% acetic acid and the 96 well plate was allowed to dry. Tris base solution (10 mM, 200 μ L) was added to the wells for 15 minutes prior to measuring the absorbance at 515 nm.

REFERENCES

1. N. C. Institute, <http://www.cancer.gov/cancertopics/coping/chemo-side-effects>, Accessed May 9th, 2011.
2. V. P. Torchilin, *Nanoparticulates as Drug Carriers*, Imperial College Press, 2006.
3. A. Kale and V. Torchilin, *Polymer Science Series A*, 2009, **51**, 730-737.
4. G. S. Kwon and T. Okano, *Advanced Drug Delivery Reviews*, 1996, **21**, 107-116.
5. X. Qu, V. V. Khutoryanskiy, A. Stewart, S. Rahman, B. Papahadjopoulos-Sternberg, C. Dufes, D. McCarthy, C. G. Wilson, R. Lyons, K. C. Carter, A. Schatzlein and I. F. Uchegbu, *Biomacromolecules*, 2006, **7**, 3452-3459.
6. M. M. Yallapu, Jaggi M., Chauhan S.C., *Journal of Ovarian Research*, 2010, 19.
7. W. J. Gradishar, S. Tjulandin, N. Davidson, H. Shaw, N. Desai, P. Bhar, M. Hawkins and J. O'Shaughnessy, *Journal of Clinical Oncology*, 2005, **23**, 7794-7803.
8. K. Ulbrich and V. Subr, *Advanced Drug Delivery Reviews*, 2004, **56**, 1023-1050.
9. H. Maeda, J. Wu, T. Sawa, Y. Matsumura and K. Hori, *Journal of Controlled Release*, 2000, **65**, 271-284.
10. H. Maeda, *Bioconjugate Chemistry*, **21**, 797-802.
11. A. M. Wu and P. D. Senter, *Nat Biotech*, 2005, **23**, 1137-1146.
12. S. Chen, X. Zhao, J. Chen, J. Chen, L. Kuznetsova, S. S. Wong and I. Ojima, *Bioconjugate Chemistry*, **21**, 979-987.
13. R. Duncan, *Nat. Rev. Cancer*, 2006, **6**, 688.
14. L. Brannon-Peppas and J. O. Blanchette, *Advanced Drug Delivery Reviews*, 2004, **56**, 1649-1659.
15. E. Ruoslahti, *Nat Rev Cancer*, 2002, **2**, 83-90.
16. J. Sudimack and R. J. Lee, *Advanced Drug Delivery Reviews*, 2000, **41**, 147-162.

17. J. Gu, W.-P. Cheng, J. Liu, S.-Y. Lo, D. Smith, X. Qu and Z. Yang, *Biomacromolecules*, 2007, **9**, 255-262.
18. O. C. Farokhzad, J. Cheng, B. A. Teply, I. Sherifi, S. Jon, P. W. Kantoff, J. P. Richie and R. Langer, *Proceedings of the National Academy of Sciences*, 2006, **103**, 6315-6320.
19. A. N. Lukyanov and V. P. Torchilin, *Advanced Drug Delivery Reviews*, 2004, **56**, 1273-1289.
20. D. Schmaljohann, *Advanced Drug Delivery Reviews*, 2006, **58**, 1655-1670.
21. A. Lavasanifar, J. Samuel and G. S. Kwon, *Advanced Drug Delivery Reviews*, 2002, **54**, 169-190.
22. M. Shi, J. Lu and M. S. Shoichet, *Journal of Materials Chemistry*, 2009, **19**, 5485-5498.
23. C. Ding, J. Gu, X. Qu and Z. Yang, *Bioconjugate Chemistry*, 2009, **20**, 1163-1170.
24. O. Boussif, F. Lezoualc'h, M. A. Zanta, M. D. Mergny, D. Scherman, B. Demeneix and J. P. Behr, *Proceedings of the National Academy of Sciences*, 1995, **92**, 7297-7301.
25. U. Lungwitz, M. Breunig, T. Blunk and A. Göpferich, *European Journal of Pharmaceutics and Biopharmaceutics*, 2005, **60**, 247-266.
26. F. Kratz, Beyer, Ulrich, Schutte, Thomas Mark, *Critical Reviews in Therapeutic Drug Carrier Systems*, 1999, **16**.
27. K. R. West and S. Otto, *Current Drug Discovery Technologies*, 2005, **2**, 123-160.
28. G. Saito, J. A. Swanson and K.-D. Lee, *Advanced Drug Delivery Reviews*, 2003, **55**, 199-215.
29. E. Bílková, A. Imramovský, V. Buchta and M. Sedlák, *International Journal of Pharmaceutics*, **386**, 1-5.
30. J. Jagur-Grodzinski, *Polymers for Advanced Technologies*, 2009, **20**, 595-606.
31. E. M. Bachelder, T. T. Beaudette, K. E. Broaders, J. M. J. Freilichet, M. T. Albrecht, A. J. Mateczun, K. M. Ainslie, J. T. Pesce and A. M. Keane-Myers, *Molecular Pharmaceutics*, **7**, 826-835.

32. V. Knorr, L. Allmendinger, G. F. Walker, F. F. Paintner and E. Wagner, *Bioconjugate Chemistry*, 2007, **18**, 1218-1225.
33. R. Mosurkal, J. Kumar, V. S. Parmar and A. C. Watterson, *Journal of Macromolecular Science, Part A: Pure and Applied Chemistry*, 2007, **44**, 1289 - 1292.
34. H. Morinaga, H. Morikawa, Y. Wang, A. Sudo and T. Endo, *Macromolecules*, 2009, **42**, 2229-2235.
35. K. Engin, D. B. Leeper, J. R. Cater, A. J. Thistlethwaite, L. Tupchong and J. D. McFarlane, *International Journal of Hyperthermia*, 1995, **11**, 211-216.
36. A. S. E. Ojugo, P. M. J. McSheehy, D. J. O. McIntyre, C. McCoy, M. Stubbs, M. O. Leach, I. R. Judson and J. R. Griffiths, *NMR in Biomedicine*, 1999, **12**, 495-504.
37. R. van Sluis, Z. M. Bhujwalla, N. Raghunand, P. Ballesteros, J. Alvarez, S. Cerdán, J.-P. Galons and R. J. Gillies, *Magnetic Resonance in Medicine*, 1999, **41**, 743-750.
38. F. R. Maxfield and T. E. McGraw, *Nat Rev Mol Cell Biol*, 2004, **5**, 121-132.
39. I. Mellman, Fuchs, R., Helenius, A., *Ann. Rev. Biochem*, 1986, **55**, 663-700.
40. W. M. Hurwitz E., Pltha J, *J. Appl. Biochem.* , 1980, 25.
41. K. W. Mosure, A. J. Henderson, L. J. Klunk and J. O. Knipe, *Cancer Chemotherapy and Pharmacology*, 1997, **40**, 251-258.
42. A. A. Kale and V. P. Torchilin, *Bioconjugate Chemistry*, 2007, **18**, 363-370.
43. T. Kaneko, D. Willner, I. Monkovic, J. O. Knipe, G. R. Braslawsky, R. S. Greenfield and D. M. Vyas, *Bioconjugate Chemistry*, 1991, **2**, 133-141.
44. C. C. Lee, E. R. Gillies, M. E. Fox, S. J. Guillaudeu, J. M. J. Fréchet, E. E. Dy and F. C. Szoka, *Proceedings of the National Academy of Sciences*, 2006, **103**, 16649-16654.
45. H. S. Yoo, E. A. Lee and T. G. Park, *Journal of Controlled Release*, 2002, **82**, 17-27.
46. T. Etrych, J. Strohalm, L. Kovár, M. Kabesová, B. Ríhová and K. Ulbrich, *Journal of Controlled Release*, 2009, **140**, 18-26.

47. P. R. Hamann, L. M. Hinman, I. Hollander, C. F. Beyer, D. Lindh, R. Holcomb, W. Hallett, H.-R. Tsou, J. Upeslakis, D. Shochat, A. Mountain, D. A. Flowers and I. Bernstein, *Bioconjugate Chem.*, 2001, **13**, 47-58.
48. T. H. Fife and L. K. Jao, *The Journal of Organic Chemistry*, 1965, **30**, 1492-1495.
49. P. E. Soerensen, K. J. Pedersen, P. R. Pedersen, V. M. Kanagasabapathy and R. A. McClelland, *Journal of the American Chemical Society*, 1988, **110**, 5118-5123.
50. J. Harron, R. A. McClelland, C. Thankachan and T. T. Tidwell, *The Journal of Organic Chemistry*, 1981, **46**, 903-910.
51. R. Mosurkal, J. Kumar, V. S. Parmar and A. C. Watterson, *Journal of Macromolecular Science, Part A: Pure and Applied Chemistry*, 2007, **44**, 1289 - 1292.
52. E. R. Gillies, A. P. Goodwin and J. M. J. Frechet, *Bioconjugate Chemistry*, 2004, **15**, 1254-1263.
53. W. Chen, F. Meng, F. Li, S.-J. Ji and Z. Zhong, *Biomacromolecules*, 2009, **10**, 1727-1735.
54. E. M. Bachelder, T. T. Beaudette, K. E. Broaders, J. Dashe and J. M. J. Frechet, *Journal of the American Chemical Society*, 2008, **130**, 10494-10495.
55. A. P. Griset, J. Walpole, R. Liu, A. Gaffey, Y. L. Colson and M. W. Grinstaff, *Journal of the American Chemical Society*, 2009, **131**, 2469-2471.
56. X. Lin, Q. Zhang, J. R. Rice, D. R. Stewart, D. P. Nowotnik and S. B. Howell, *European Journal of Cancer*, 2004, **40**, 291-297.
57. K. Wang, Lu, J.F., and Li R.C., *Coord. Chem. Rev.* , 1996, 53.
58. N. Seetharamu, E. Kim, H. Hochster, F. Martin and F. Muggia, *Anticancer Research*, **30**, 541-545.
59. J. R. Rice, J. L. Gerberich, D. P. Nowotnik and S. B. Howell, *Clinical Cancer Research*, 2006, **12**, 2248-2254.
60. E. Wong and C. M. Giandomenico, *Chemical Reviews*, 1999, **99**, 2451-2466.
61. S. v. Zutphen and J. Reedijk, *Coordination Chemistry Reviews*, 2005, **249**, 2845-2853.

62. D. P. Nowotnik and E. Cvitkovic, *Advanced Drug Delivery Reviews*, 2009, **61**, 1214-1219.
63. P. Sood, K. B. Thurmond, J. E. Jacob, L. K. Waller, G. O. Silva, D. R. Stewart and D. P. Nowotnik, *Bioconjugate Chemistry*, 2006, **17**, 1270-1279.
64. W.-C. Shen and H. J. P. Ryser, *Biochemical and Biophysical Research Communications*, 1981, **102**, 1048-1054.
65. M. Wirth, A. Fuchs, M. Wolf, B. Ertl and F. Gabor, *Pharmaceutical Research*, 1998, **15**, 1031-1037.
66. A. Al-Shamkhani and R. Duncan, *International Journal of Pharmaceutics*, 1995, **122**, 107-119.
67. S. Zhu, M. Hong, L. Zhang, G. Tang, Y. Jiang and Y. Pei, *Pharmaceutical Research*, **27**, 161-174.
68. A. J. M. D'Souza and E. M. Topp, *Journal of Pharmaceutical Sciences*, 2004, **93**, 1962-1979.
69. F.-Q. Hu, L.-N. Liu, Y.-Z. Du and H. Yuan, *Biomaterials*, 2009, **30**, 6955-6963.
70. N. Lavignac, J. L. Nicholls, P. Ferruti and R. Duncan, *Macromolecular Bioscience*, 2009, **9**, 480-487.
71. W.-M. Choi, P. Kopeček, T. Minko and J. i. Kopeček, *Journal of Bioactive and Compatible Polymers*, 1999, **14**, 447-456.
72. A. J. Kirby and P. W. Lancaster, *Journal of the Chemical Society, Perkin Transactions 2*, 1972, 1206-1214.
73. E. Dinand, Zloh, M., Brocchini, S., *Australian Journal of Chemistry*, 2002, **55**, 467-474.
74. S. Fletcher, M. R. Jorgensen and A. D. Miller, *Organic Letters*, 2004, **6**, 4245-4248.
75. G. A. Lemieux and C. R. Bertozzi, *Trends in Biotechnology*, 1998, **16**, 506-513.
76. I. A. Müller, F. Kratz, M. Jung and A. Warnecke, *Tetrahedron Letters*, **51**, 4371-4374.
77. M. S. Shchepinov and V. A. Korshun, *Chemical Society Reviews*, 2003, **32**, 170-180.

78. V. F. Patel, J. N. Hardin, J. M. Mastro, K. L. Law, J. L. Zimmermann, W. J. Ehlhardt, J. M. Woodland and J. J. Starling, *Bioconjugate Chemistry*, 1996, **7**, 497-510.
79. V. V. Rostovtsev, L. G. Green, V. V. Fokin and K. B. Sharpless, *Angewandte Chemie International Edition*, 2002, **41**, 2596-2599.
80. M. Mondon, R. Delatouche, C. Bachmann, G. Frapper, C. Len and P. Bertrand, *European Journal of Organic Chemistry*, **2011**, 2111-2119.
81. C. C. Lee, E. R. Gillies, M. E. Fox, S. J. Guillaudeu, J. M. J. Fréchet, E. E. Dy and F. C. Szoka, *Proceedings of the National Academy of Sciences*, 2006, **103**, 16649-16654.
82. G. Pasut, F. Greco, A. Mero, R. Mendichi, C. Fante, R. J. Green and F. M. Veronese, *Journal of Medicinal Chemistry*, 2009, **52**, 6499-6502.
83. J. A. Boomer, M. M. Qualls, H. D. Inerowicz, R. H. Haynes, V. S. Patri, J.-M. Kim and D. H. Thompson, *Bioconjugate Chemistry*, 2008, **20**, 47-59.
84. M. C. Parrott, J. C. Luft, J. D. Byrne, J. H. Fain, M. E. Napier and J. M. DeSimone, *Journal of the American Chemical Society*, **132**, 17928-17932.
85. W. C. Floyd, G. K. Datta, S. Imamura, H. M. Kieler-Ferguson, K. Jerger, A. W. Patterson, M. E. Fox, F. C. Szoka, J. M. J. Fréchet and J. A. Ellman, *ChemMedChem*, **6**, 49-53.
86. X.-B. Xiong, Z. Ma, R. Lai and A. Lavasanifar, *Biomaterials*, **31**, 757-768.
87. R. Liu, Y. Zhang, X. Zhao, A. Agarwal, L. J. Mueller and P. Feng, *Journal of the American Chemical Society*, **132**, 1500-1501.
88. T. S. Manoharan and R. S. Brown, *The Journal of Organic Chemistry*, 1988, **53**, 1107-1110.
89. A. I. Meyers, T. Sohda and M. F. Loewe, *The Journal of Organic Chemistry*, 1986, **51**, 3108-3112.
90. F. A. Carroll, *Perspectives on Structure and Mechanism in Organic Chemistry*, Brooks/Cole Publishing Company, Pacific Grove., 1998.
91. K. A. Connors, *Chemical Kinetics: The Study of Reaction Rates in Solution*, Wiley-VCH, New York, (1990).
92. S. D. Kong, A. Luong, G. Manorek, S. B. Howell and J. Yang, *Bioconjugate Chemistry*, 2007, **18**, 293-296.

93. W. E. K. a. H. J. M. B. G. V. Iyengar, *The Elemental Composition of Human Tissue and Bodily Fluids*, Verlag Chemie, New York, 1978.
94. R. L. Momparler, M. Karon, S. E. Siegel and F. Avila, *Cancer Research*, 1976, **36**, 2891-2895.
95. J. William Lown, *Pharmacology & Therapeutics*, 1993, **60**, 185-214.
96. B. M. Mueller, W. A. Wrasidlo and R. A. Reisfeld, *Bioconjugate Chemistry*, 1990, **1**, 325-330.
97. M. Shi, K. Ho, A. Keating and M. S. Shoichet, *Advanced Functional Materials*, 2009, **19**, 1689-1696.
98. A. Malugin, P. Kopecková and J. Kopecek, *J. Control. Release*, 2007, **124**, 6-10.
99. V. Vichai and K. Kirtikara, *Nat. Protocols*, 2006, **1**, 1112-1116.
100. A. Luong, T. Issarapanichkit, S. D. Kong, R. Fong and J. Yang, *Organic & Biomolecular Chemistry*, 2010, **8**, 5105-5109.
101. B. Capon, Nimmo, K. , *J. Chem. Soc., Perkin Trans.*, 1975, **2**, 1113-1118.
102. K. Langer, S. Balthasar, V. Vogel, N. Dinauer, H. von Briesen and D. Schubert, *Int. J. Pharm.*, 2003, **257**, 169-180.
103. C. W. Tornøe, C. Christensen and M. Meldal, *The Journal of Organic Chemistry*, 2002, **67**, 3057-3064.
104. C. W. Tornøe, C. Christensen and M. Meldal, *The Journal of Organic Chemistry*, 2002, **67**, 3057-3064.
105. T. R. Chan, R. Hilgraf, K. B. Sharpless and V. V. Fokin, *Organic Letters*, 2004, **6**, 2853-2855.
106. A. E. Speers and B. F. Cravatt, *Chem. Biol.*, 2004, **11**, 535-546.
107. J. M. Walker, *The Protein Protocols Handbook*, Humana press, 2002.
108. K. Langer, S. Balthasar, V. Vogel, N. Dinauer, H. von Briesen and D. Schubert, *Int. J. Pharm.* , 2003, **257**, 169-180.
109. D. J. Taatjes, G. Gaudiano, K. Resing and T. H. Koch, *J. Med. Chem.*, 1996, **39**, 4135.

110. D. J. Taatjes, G. Gaudiano, K. Resing and T. H. Koch, *J. Med. Chem.*, 1997, **40**, 1276-1286.
111. R. C. Larock, *Comprehensive Organic Transformations*, John Wiley & Sons, 1999.
112. D. Yu, P. Peng, S. S. Dharap, Y. Wang, M. Mehlig, P. Chandna, H. Zhao, D. Filpula, K. Yang, V. Borowski, G. Borchard, Z. Zhang and T. Minko, *J. Control. Release*, 2005, **110**, 90-102.
113. Z. Xie, H. Guan, X. Chen, C. Lu, L. Chen, X. Hu, Q. Shi and X. Jing, *J. Control. Release*, 2007, **117**, 210-216.
114. A. Malugin, P. Kopeckova and J. Kopecek, *J. Control. Release*, 2007, **124**, 6-10.
115. M. K. Dhaon, R. K. Olsen and K. Ramasamy, *J. Org. Chem.*, 2002, **47**, 1962-1965.
116. I. M. Shiina, Ryo, *Heterocycles*, 2008, **76**, 1313-1328.
117. Lundquist and J. C. Pelletier, *Org. Lett.*, 2001, **3**, 781-783.
118. S. D. Kong, A. Luong, G. Manorek, S. B. Howell and J. Yang, *Bioconjugate Chem.*, 2007, **18**, 293-296.
119. S. Bolte and F. P. Cordelieres, *J. Cat Microsc*, 2006, **224**, 213-232.
120. D. J. Taatjes, G. Gaudiano, K. Resing and T. H. Koch, *J. Med. Chem.*, 1996, **39**, 4135-4138.
121. M. L. Bender and M. S. Silver, *Journal of the American Chemical Society*, 1962, **84**, 4589-4590.
122. M. L. Bender, J. A. Reinstein, M. S. Silver and R. Mikulak, *Journal of the American Chemical Society*, 1965, **87**, 4545-4553.
123. H. Nakagawa, N. Maeda, T. Tsuzuki, T. Suzuki, A. Hirayama, E. Miyahara and K. Wada, *Japanese Journal of Clinical Oncology*, 2001, **31**, 251-258.
124. A. A. Rashin, J. R. Rabinowitz and J. R. Banfelder, *Journal of the American Chemical Society*, 1990, **112**, 4133-4137.
125. I. A. Topol, G. J. Tawa, S. K. Burt and A. A. Rashin, *The Journal of Physical Chemistry A*, 1997, **101**, 10075-10081.

126. M. L. Bender, Y.-L. Chow and F. Chloupek, *Journal of the American Chemical Society*, 1958, **80**, 5380-5384.
127. C. Neumann, Boubakari, R. Grünert and P. J. Bednarski, *Analytical Biochemistry*, 2003, **320**, 170-178.
128. L. F. Levy and H. Stephen, *Journal of the Chemical Society (Resumed)*, 1931, 79-82.
129. S. C. Alley, D. R. Benjamin, S. C. Jeffrey, N. M. Okeley, D. L. Meyer, R. J. Sanderson and P. D. Senter, *Bioconjugate Chemistry*, 2008, **19**, 759-765.
130. J. Wu, T. Akaike and H. Maeda, *Cancer Res.*, 1998, **58**, 159.
131. M. Harris, *The Lancet Oncology*, 2004, **5**, 292-302.
132. D. J. Slamon, B. Leyland-Jones, S. Shak, H. Fuchs, V. Paton, A. Bajamonde, T. Fleming, W. Eiermann, J. Wolter, M. Pegram, J. Baselga and L. Norton, 2001, pp. 783-792.
133. J. Baselga, L. Norton, J. Albanell, Y.-M. Kim and J. Mendelsohn, *Cancer Research*, 1998, **58**, 2825-2831.
134. C. A. Hudis, *New England Journal of Medicine*, 2007, **357**, 39-51.
135. J. W. Park, D. B. Kirpotin, K. Hong, R. Shalaby, Y. Shao, U. B. Nielsen, J. D. Marks, D. Papahadjopoulos and C. C. Benz, *Journal of Controlled Release*, 2001, **74**, 95-113.
136. G. D. Lewis Phillips, G. Li, D. L. Dugger, L. M. Crocker, K. L. Parsons, E. Mai, W. A. Blattler, J. M. Lambert, R. V. J. Chari, R. J. Lutz, W. L. T. Wong, F. S. Jacobson, H. Koeppen, R. H. Schwall, S. R. Kenkare-Mitra, S. D. Spencer and M. X. Sliwkowski, *Cancer Research*, 2008, **68**, 9280-9290.
137. R. A. Scheck and M. B. Francis, *ACS Chemical Biology*, 2007, **2**, 247-251.
138. R. A. Scheck, M. T. Dedeo, A. T. Iavarone and M. B. Francis, *Journal of the American Chemical Society*, 2008, **130**, 11762-11770.